AD_____

Award Number: DAMD17-98-1-8574

TITLE: Androgen Regulation of p27 in the Normal and Neoplastic Prostate

PRINCIPAL INVESTIGATOR: Massimo Loda, M.D.

CONTRACTING ORGANIZATION: Dana Farber Cancer Institute
Boston, Massachusetts 02115

REPORT DATE: March 2001

TYPE OF REPORT: Final

PREPARED FOR: U.S. Army Medical Research and Materiel Command
Fort Detrick, Maryland 21702-5012

DISTRIBUTION STATEMENT: Approved for Public Release;
Distribution Unlimited

REPORT DOCUMENTATION PAGE

Form Approved
OMB No. 074-0188

1. AGENCY USE ONLY (Leave blank)	2. REPORT DATE	3. REPORT TYPE AND DATES COVERED
	March 2001	Final (1 Sep 98 - 28 Feb 01)

4. TITLE AND SUBTITLE
Androgen Regulation of p27 in the Normal and Neoplastic Prostate

5. FUNDING NUMBERS
DAMD17-98-1-8574

6. AUTHOR(S)
Massimo Loda, M.D.

7. PERFORMING ORGANIZATION NAME(S) AND ADDRESS(ES)
Dana Farber Cancer Institute
Boston, Massachusetts 02115

E-Mail: E-Mail: massimo_loda@dfci.harvard.edu

8. PERFORMING ORGANIZATION REPORT NUMBER

9. SPONSORING / MONITORING AGENCY NAME(S) AND ADDRESS(ES)
U.S. Army Medical Research and Materiel Command
Fort Detrick, Maryland 21702-5012

10. SPONSORING / MONITORING AGENCY REPORT NUMBER

11. SUPPLEMENTARY NOTES
This report contains colored photos

12a. DISTRIBUTION / AVAILABILITY STATEMENT
Approved for Public Release; Distribution Unlimited

12b. DISTRIBUTION CODE

13. Abstract ***(Maximum 200 Words)*** *(abstract should contain no proprietary or confidential information)*

The cyclin dependent kinase inhibitor (CKI) p27 is a negative regulator of the cell cycle and a potential tumor suppressor gene. p27 deficient mice develop pituitary tumors and display increased body size suggesting a growth-inhibitory function in vivo. In addition, our preliminary data at the time the grant was submitted suggested that its expression in the prostate was regulated by androgens. The original aims of this proposal included 1) to determine whether p27 is regulated by androgens in the prostate utilizing a well established animal model; 2) to study the expression of p27 in both androgen dependent and independent human prostate cancer; 3) to assess the expression of novel isopeptidases involved in the regulation of the ubiquitin-proteasome pathway and identify those enzymes with a strong association with p27 and its degradation. Using the rat castration-regeneration model we found that expression of p27 is regulated primarily by ubiquitin-mediated degradation. Castration blocks the elevated p27 degradation characteristic of intact rat prostates, leading to increased expression of p27. During testosterone-induced regeneration, p27 degradation inversely correlates with p27 expression. These findings have been published (Waltregny et al, Mol Endocrinol 2001, 15:765-782). We also found a significant difference in the expression of p27 in Ad and AI tumors (Cai, Y.C. et al Lab Invest, 80, 545A, 2000 and manuscript in preparation). Finally, the isopeptidase KIA-190 (UBPO) was founf to be overexpressed in 54% of prostate cancers but no correlation with p27 expression was found.

14. Subject Terms (keywords previously assigned to proposal abstract or terms which apply to this award)
p27, androgen regulation, prostate cancer, animal model, ubiquitin-Mediated degradation

15. NUMBER OF PAGES
56

16. PRICE CODE

17. SECURITY CLASSIFICATION OF REPORT	18. SECURITY CLASSIFICATION OF THIS PAGE	19. SECURITY CLASSIFICATION OF ABSTRACT	20. LIMITATION OF ABSTRACT
Unclassified	Unclassified	Unclassified	Unlimited

Table of Contents

Introduction

The cyclin dependent kinase inhibitor (CKI) p27 is a negative regulator of the cell cycle and a potential tumor suppressor gene. p27 deficient mice develop pituitary tumors and display increased body size suggesting a growth-inhibitory function in vivo. In contrast to traditional anti-oncogenes like the CKI p16, no homozygous deletions/mutations of the p27 gene have been found in cell lines or in human tumors. p27 levels slowly decrease as cells are stimulated to enter the cell cycle, primarily as a result of an accelerated degradation of the protein regulated post-translationally by ubiquitination and subsequent degradation. p27 is expressed in resting cells in a variety of tissues. Interestingly, our preliminary data suggest that its expression in the prostate may be regulated by androgens. In addition, we have recently determined that p27 loss is associated with poor prognosis in prostate cancer. The mechanism whereby it is inactivated appears to involve its targeted degradation by tumor cells, which requires the ubiquitin-proteasome pathway. Selective degradation of proteins through ubiquitination, however, is a reversible process. Isopeptidases (de-ubiquitinating enzymes) remove, rather than add, ubiquitin thus stabilizing their protein substrates. This novel family of enzymes has numerous members which share only a few conserved catalytic motifs, raising the exciting possibility of a high degree of substrate specificity. The aim of this proposal is 1) to determine whether p27 is regulated by androgens in normal and neoplastic prostate utilizing a well established animal model; 2) to study the expression of p27 in both androgen dependent and independent human prostate cancer; 3) to assess the expression of novel isopeptidases involved in the regulation of the ubiquitin-proteasome pathway and identify those enzymes with a strong association with p27 and its degradation; 4) to address to what extent isopeptidases modify proliferation and/or G1 arrest in cultured prostate cancer cells. Concomitant use of androgens to induce p27 and modification of p27 degradation through isopeptidases represents a novel approach aimed at prostate cancers that have become resistant to androgen ablation.

Body

Research accomplishments based on the approved Statement of Work

- **Specific Aim 1**

To determine whether testosterone regulates the expression of p27 in normal and neoplastic prostate.

The goal of this specific aim was to use the androgen-stimulated castrated Noble rat prostate rat model to investigate whether androgens regulate the levels of p27 in the regenerating gland.

Two weeks after castration, 3-months-old rats (7 rats/condition) were treated by I.M. testosterone (T) injections (6.6 mg/kg) and sacrificed at 12, 24, 48, 72, and 96 hours. Controls included 7 intact and 7 castrated untreated rats. Prior to sacrifice, rats were injected I.P. with BrdU. The prostate lobes (ventral and dorso-lateral) of each animal were harvested separately and processed for use in various assays (immunoblots, degradation and kinase assays, immunoprecipitations, quantitative real-time PCR, immunohistochemistry). Western blot experiments showed that (1) p27 protein levels are markedly higher in the prostate of castrated untreated rats than in that of intact animals, (2) a transient drop in p27 levels is observed after 12-24 hours of treatment followed by 3) an increase of p27 levels at 48-72 hours.

The mechanisms of regulation of p27 protein expression by androgens were investigated at both the transcriptional and the post-translational levels. Relative quantitative real-time PCR experiments using specific primers and probes for p27 show no modulation of p27 transcripts levels either between intact and castrated untreated rats or following T administration to castrated rats. Using *in vitro* degradation assays of recombinant histidine-tagged p27, we were able to show that p27 degradation activity by the prostate homogenates is inversely correlated with p27 protein levels. Furthermore, this degradation activity is specific for p27 since degradation of another Cki, p21 (whose protein levels are highly induced by T (not shown), is virtually unaffected by androgen replenishment (Waltregny et al). In addition, since this degradation activity is completely abolished by flutamide, it is under androgen control (Waltregny et al).

Immunohistochemical experiments yielded the following results: (1) p27 staining is detected in very few prostate epithelial cells in intact rats and BrdU labeling index is very low, (2) a strong nuclear staining is observed in most basal cells in the prostate of castrated untreated animals and BrdU staining is completely absent, (3) following T administration to castrated rats, p27 as well as BrdU are virtually undetectable at 12-24 hours, (4) at 48-72 hours, concomitantly to a marked increase in the number of BrdU+ cells, p27 is highly expressed in the majority of luminal cells. Double

immunofluorescence staining experiments for BrdU and p27 demonstrated that proliferating cells (BrdU+) are devoid of any p27 labeling and *vice versa* (shown below).

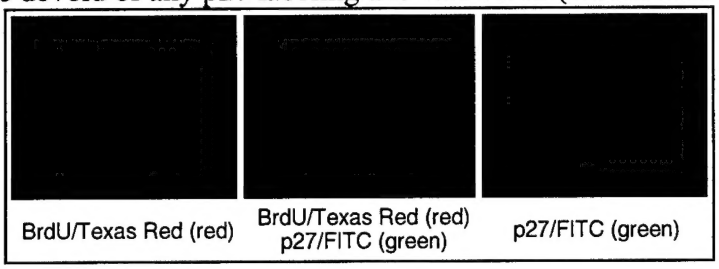

In summary, we have established that changes in p27 expression which result from castration and testosterone-induced regeneration of the rat prostate are secondary to changes in p27-specific degradation rather than to transcriptional control. Furthermore, p27 expression is differentially modulated by androgens in the different cellular components of the prostate epithelium (basal *vs* luminal; proliferating *vs* proliferating). This model will be extensively utilized in this proposal to study the androgen-controlled regulation of p27 and its mediators.

Waltregny D, Leav I, Signoretti S, Soung P, Lin D, Merk F, Adams JY, Bhattacharya N, Cirenei N, **Loda M.** Androgen-driven prostate epithelial cell proliferation and differentiation *in vivo* involve the regulation of p27. ***Mol Endocrinol*** 2001, 15:765-782 (see appendix).

- **Specific Aim 2**

To study expression of p27 in androgen-dependent (AD) and androgen independent (AI) human prostate cancer

p27 expression was examined by automated immunohistochemistry in radical prostatectomies from untreated patients (n= 88; named Androgen Dependent or AD) as well as patients previously treated for at least 3 months by androgen ablation (n= 63; named Androgen Independent or AI). No correlation was found between p27 and Gleason score (p=0.13), stage (p=0.66), pre-op PSA (p=0.4) or post-op PSA (p=0.69). 50% of cases expressed p27 (>50% of cells) in AD *vs* 34% in AI (p=0.043). A Table with the results is shown below:

	Untreated (n=88)	Treated (n=68)	P value
p27 + (≥50%)	44 (50%)	23 (34%)	0.043
Gleason Score:			
4-6	28	30	0.23
7	34	21	0.16
8-10	19	17	0.82

Unknown (mets)	7	0	
Stage:			
I+II	40	32	0.91
III+IV	39	30	0.91
Unknown (TURP)	9	6	
Ki67 ≥1%	38/67 (57%)	22/56 (39%)	0.05

These data suggest, that androgen ablation may select for p27 negative tumors with more aggressive behavior. Results have been presented at the United States and Canadian Academy of Pathology, (Cai, Y.C., et al., *Down-regulation of p27 in adenocarcinoma of the prostate after androgen ablation.* Lab Invest, 2000. **80**: p. 545A). (See appendix). In order to achieve increased statistical power, we plan to test a significantly higher number of cases which are currently being cut and stained and will be assessed for the final manuscript.

- **Specific Aim 3**

Ubiquitin-proteasome dependent degradation of p27 in androgen-mediated proliferation: role of isopeptidases

The isopeptidase KIA-190

Kia-190 seemed to be an interesting candidate since in preliminary data (before we generated specific antibodies against it) it was found to be overexpressed in prostate cancers by in situ hybridization in a subset of cases. Furthermore, its expression was correlated with that of p27. When a large database of prostate cancers was examined (n=109) and the expression compared to that in colon and breast carcinomas, Kia-190 mRNA was overexpressed in 54%, 66% and 25% of prostate, colon and breast tumors, respectively compared to the corresponding normal tissues. This demonstrates differential expression of Kia-190 in tumor vs normal as well as in different epithelial tumors. A significant correlation was found between Kia-190 and disease stage (p=0.005) but not with Gleason score or post-op PSA.

Kia-190 by in situ hybridization

	Low	High
Prostate	50/109 (46%)	59/109(54%)
Colon	17/51 (33%)	34/51(66%)
Breast	23/31(74%)	8/31(26%)

Utilizing the antibodies we have generated, we have analyzed Kia-190 protein expression by immunohistochemistry in the same tumors. Results confirmed the initial observations made by in situ hybridization.

Kia-190 by immunohistochemistry

	T<N	T=N	T>N
Prostate	12/105 (11%)	37/105 (35%)	56/105 (53%)
Colon	0/38 (0%)	9/38(24%)	29/38(76%)

Interestingly, in normal tissues kia-190 is expressed in rapidly proliferating tissues such as colonic crypts and germinal centers.

Correlations bewteen Kia-190 and p27. There was no correlation between expression of Kia-190 and that of p27 in AD or AI cases ($p<0.3723$) at the protein level.

Dr. Draetta (European Institute of tumors in Milan, Italy) utilized Kia-190 as bait in a yeast two-hybrid screen. Kia-190 was found to interact *in vivo* and *in vitro* with G3BP, a protein associated in a growth regulated manner, with ras-GTPase activating protein. We have established a collaboration with Dr. Draetta and a manuscript which combines the data from his lab and ours is in preparation.

•Specific Aim 4:

To assess the role of isopeptidases in prostate cancer cell proliferation and G1 arrest in LNCaP cells.

Kia-190 protein expression was studied in a variety of human cell lines by Western blot (see below). Note absent levels of Kia-190 in (normal) PrEC prostate cells and overexpression in the three prostate carcinoma cell lines.

Induction of p27 by 48 hours of serum starvation was obtained in LNCaP, PC-3 and DU-145 cells. However, no concomitant change in the levels of Kia-190 protein levels was observed by Western blot (not shown).

We then transfected normal basal prostate (PrEC) cells with pCR3.1/Kia-190 sense and mutated (active site cys to ala) constructs as well as pSV40-T and pCDNA3/H-rasV12 as positive controls. Immunohistochemistry verified the successful transfection of cells. We also transfected NIH3T3 cells with pCR3.1/Kia-190 sense and mutated and pCDNA3/H-rasV12. We then checked for growth in soft agar. Only clones transfected with pCDNA3/H-rasV12 (with or without Kia-190) were able to grow in soft agar.

Catalytically inactive mutants of KIA-190 had no affect on cell cycle kinetics or growth in soft agar, when transfected in PrECs.

Although the work completed during the first three years of the award yielded important information on KIA-190, and its role in prostate cancer, a p27-specific isopeptidase was not identified. Thus, we have recently adopted a novel strategy which utilizes degenerate oligonucleotides directed at the conserved catalytic domain of de-ubiquitinating enzymes (Cys and His boxes) to clone isopeptidases which are more abundant in p27 rich (castrates) *vs* p27 poor (intact) rat prostates as well as in charcoal stripped (p27 rich) vs asynchronously growing (relatively p27 poor) LNCaP cells. Utilizing the degenerate PCR-RACE approach we have recently obtained the full length clone of two isopeptidases differentially expressed in intact versus castrate rat prostates. We have also cloned the human equivalets of these isopeptidases. One of these two is an androgen responsive gene and the other is novel (not in genebank). We are actively pursuing characterization of these genes.

Key Research accomplishments

- Utilizing an animal model of castration and testosterone-induced regeneration of the prostate we determined that removal of androgens stabilizes p27 by completely inhibiting it's steady state levels of degradation. This is a mechanism to preserve basal and possibly stem cells in the prostate in an androgen depleted milieu. These cells are then ready to regenerate and proliferate again once the appropriate hormonal environment is restored.
- In addition, this is the first time that the regulation of the cell cycle inhibitor p27 is precisely outlined in prostate epithelial cells (Waltregny at el, 2001).

- In collaboration with Dr. Reiter's group at UCLA, we were the first to report that loss of p27 expression is a negative prognostic marker in prostate carcinoma (Yang et al, 1998). Such a finding has now been confirmed by several other groups.

- We have established that p27 expression is decreased in tumors from patients previously treated with androgen ablation, compared with stage-matched untreated tumors. The implications of these findings are still unclear but they may signify that Total Androgen Ablation may select for tumor cells which lack p27 and are therefore more aggressive (Cai et la, 2000).

- The ubiquitin pathway is involved in the proteolytic turnover of many short-lived cellular regulatory proteins. Since selective degradation of substrates of this system requires the covalent attachment of a polyubiquitin chain to the substrates, degradation could be counteracted by de-ubiquitinating enzymes (or isopeptidases) which selectively remove the polyubiquitin chain. Unp is one of the human isopeptidase with still poorly understood biological functions which we have studied. We have recently shown that cellular Unp specifically interacts with the retinoblastoma gene product (pRb) (Desalle et al, in press).

Reportable outcomes

Manuscripts sponsored by the DAMD17-98-1-8574 proposal

Yang RM, Naitoh J, Murphy M, Wang H-J, Philipson J, deKernion JB, **Loda M**, Reiter RE. Low levels of p27 protein expression predict poor disease-free survival in patients with prostate cancer. ***J Urol*** 1998;159:941-5.

Waltregny D, Leav I, Signoretti S, Soung P, Lin D, Merk F, Adams JY, Bhattacharya N, Cirenei N, **Loda M.** Androgen-driven prostate epithelial cell proliferation and differentiation *in vivo* involve the regulation of p27. ***Mol Endocrinol*** 2001, 15:765-782

Cai, Y.C., McMenamin M., Magi-Galluzzi C., Macri E., Montironi R., **Loda M**. Down-regulation of p27 in adenocarcinoma of the prostate after androgen ablation. ***Lab Invest***, 2000. **80**: p. 545A

Leav I, Merk FB, Lee KF, **Loda M**, Mandoki M, McNeal JE, Ho S-M. Prolactin receptor expression in the developing human prostate and in hyperplastic, dysplastic and neoplastic lesions. ***Am J Pathol*** 1999; 154:863-870.

Mc Menamin ME, Soung P, Perera S, Kaplan I, **Loda M**, Sellers WR. Loss of PTEN expression in paraffin-embedded primary prostate cancer correlates with high Gleason score and advanced stage. ***Cancer Res*** 59, 4291-96, 1999

Reiter, R, Sato, I, Thomas, G, Qian, Zhennan G, Watabe, T, **Loda, M**, Jenkins, R. Co-amplification of prostate stem cell antigen (PSCA) and c-myc in locally advanced prostate cancer. ***Genes Chrom Cancer*** 2000 Jan;27(1):95-103

Gu Z, Thomas G, Yamashiro J, Shintaku IP, Dorey F, Raitano A, Witte ON, Said JW, **Loda M**, Reiter RE. Prostate stem cell antigen (PSCA) expression increases with high Gleason score, advanced stage and bone metastasis in prostate cancer. ***Oncogene*** 2000 Mar 2;19(10):1288-96

Signoretti S, Waltregny D, Dilks J, Isaac B, Lin D, Garraway L, Yang A, McKeon F, **Loda M**. p63 is a prostate basal cell marker and is required for prostate development. ***Am J Pathol*** 157: 1769-75, 2000

Signoretti S, Montironi R, Manola J, Altimari A, Tam C, Bubley G, Balk S, Thomas G, Kaplan I, Hlatky L, Hahnfeldt P, Kantoff P, **Loda M**. Her-2-neu expression increases with progression towards androgen independence in human prostate cancer. ***J Natl Cancer Inst*** 92: 1918-25, 2000

DeSalle LM, Latres E, Lin D, Graner E, Montagnoli A, Baker RT, Pagano M, **Loda M**. The de-ubiquitinating enzyme Unp interacts with the Retinoblastoma protein ***Oncogene*** (In press)

Conclusions

The findings of our study sponsored by the DOD proposal DAMD17-98-1-8574 set the stage for the assessment of p27 regulation in prostate cancer cells. We have begun to address this issue comparing levels of p27 in tumors from patients treated with androgen ablation and comparing them to untreated ones. We are currently assessing in human prostate cancer the role of skp2, the ubiquitin ligase responsible for the targeting and subsequent degradation of p27 in proliferating tumor cells. Skp2 may constitute an important therapeutic target in prostate cancer.

References

Yang RM, Naitoh J, Murphy M, Wang H-J, Philipson J, deKernion JB, Loda M, Reiter RE. *Low levels of p27 protein expression predict poor disease-free survival in patients with prostate cancer.* J Urol 1998;159:941-5.

Waltregny D, Leav I, Signoretti S, Soung P, Lin D, Merk F, Adams JY, Bhattacharya N, Cirenei N, Loda M. *Androgen-driven prostate epithelial cell proliferation and differentiation in vivo involve the regulation of p27.* Mol Endocrinol 2001, 15:765-782

Cai, Y.C., McMenamin M., Magi-Galluzzi C., Macri E., Montironi R., Loda M. *Down-regulation of p27 in adenocarcinoma of the prostate after androgen ablation.* Lab Invest, 2000. **80**: p. 545A

DeSalle LM, Latres E, Lin D, Graner E, Montagnoli A, Baker RT, Pagano M, Loda M. *The de-ubiquitinating enzyme Unp interacts with the Retinoblastoma protein* Oncogene (In press)

Sherr, C.J., *Cancer cell cycles.* Science, 1996. **274**(5293): p. 1672-7.

Elledge, S.J., *Cell cycle checkpoints: preventing an identity crisis.* Science, 1996. **274**(5293): p. 1664-72.

Sherr, C.J. and J.M. Roberts, *CDK inhibitors: positive and negative regulators of G1-phase progression.* Genes Dev, 1999. **13**(12): p. 1501-12.

Slingerland, J. and M. Pagano, *Regulation of the cdk inhibitor p27 and its deregulation in cancer.* J Cell Physiol, 2000. **183**(1): p. 10-7.

Nakayama, K., et al., *Mice lacking p27(Kip1) display increased body size, multiple organ hyperplasia, retinal dysplasia, and pituitary tumors.* Cell, 1996. **85**(5): p. 707-20.

Kiyokawa, H., et al., *Enhanced growth of mice lacking the cyclin-dependent kinase inhibitor function of p27(Kip1).* Cell, 1996. **85**(5): p. 721-32.

Fero, M.L., et al., *A syndrome of multiorgan hyperplasia with features of gigantism, tumorigenesis, and female sterility in p27(Kip1)-deficient mice.* Cell, 1996. **85**(5): p. 733-44.

Fero, M.L., et al., *The murine gene p27Kip1 is haplo-insufficient for tumour suppression.* Nature, 1998. **396**(6707): p. 177-80.

Pagano, M., et al., *Role of the ubiquitin-proteasome pathway in regulating abundance of the cyclin-dependent kinase inhibitor p27.* Science, 1995. **269**(5224): p. 682-5.

Loda, M., et al., *Increased proteasome-dependent degradation of the cyclin-dependent kinase inhibitor p27 in aggressive colorectal carcinomas.* Nat Med, 1997. **3**(2): p. 231-4.

Sutterluty, H., et al., *p45SKP2 promotes p27Kip1 degradation and induces S phase in quiescent cells.* Nat Cell Biol, 1999. **1**(4): p. 207-14.

Tsvetkov, L.M., et al., *p27(Kip1) ubiquitination and degradation is regulated by the SCF(Skp2) complex through phosphorylated Thr187 in p27.* Curr Biol, 1999. **9**(12): p. 661-4.

Wilkinson, K.D., *Regulation of ubiquitin-dependent processes by deubiquitinating enzymes.* Faseb J, 1997. **11**(14): p. 1245-56.

Wilkinson, K.D., *Ubiquitination and deubiquitination: targeting of proteins for degradation by the proteasome.* Semin Cell Dev Biol, 2000. **11**(3): p. 141-8.

Papa, F.R. and M. Hochstrasser, *The yeast DOA4 gene encodes a deubiquitinating enzyme related to a product of the human tre-2 oncogene.* Nature, 1993. **366**(6453): p. 313-9.

Amerik, A., et al., *In vivo disassembly of free polyubiquitin chains by yeast Ubp14 modulates rates of protein degradation by the proteasome.* Embo J, 1997. **16**(16): p. 4826-38.

Lam, Y.A., et al., *Editing of ubiquitin conjugates by an isopeptidase in the 26S proteasome.*

Nature, 1997. **385**(6618): p. 737-40.

Shaeffer, J.R. and R.E. Cohen, *Differential effects of ubiquitin aldehyde on ubiquitin and ATP- dependent protein degradation.* Biochemistry, 1996. **35**(33): p. 10886-93.

Huang, Y., R.T. Baker, and J.A. Fischer-Vize, *Control of cell fate by a deubiquitinating enzyme encoded by the fat facets gene.* Science, 1995. **270**(5243): p. 1828-31.

Baker, R.T., et al., *Identification, functional characterization, and chromosomal localization of USP15, a novel human ubiquitin-specific protease related to the UNP oncoprotein, and a systematic nomenclature for human ubiquitin-specific proteases.* Genomics, 1999. **59**(3): p. 264-74.

Gilchrist, C.A., D.A. Gray, and R.T. Baker, *A ubiquitin-specific protease that efficiently cleaves the ubiquitin- proline bond.* J Biol Chem, 1997. **272**(51): p. 32280-5.

Gupta, K., et al., *Unp, a mouse gene related to the tre oncogene.* Oncogene, 1993. **8**(8): p. 2307-10.

Gupta, K., M. Chevrette, and D.A. Gray, *The Unp proto-oncogene encodes a nuclear protein.* Oncogene, 1994. **9**(6): p. 1729-31.

Frederick, A., M. Rolfe, and M.I. Chiu, *The human UNP locus at 3p21.31 encodes two tissue-selective, cytoplasmic isoforms with deubiquitinating activity that have reduced expression in small cell lung carcinoma cell lines.* Oncogene, 1998. **16**(2): p. 153-65.

Gray, D.A., et al., *Elevated expression of Unph, a proto-oncogene at 3p21.3, in human lung tumors.* Oncogene, 1995. **10**(11): p. 2179-83.

Tobias, J.W. and A. Varshavsky, *Cloning and functional analysis of the ubiquitin-specific protease gene UBP1 of Saccharomyces cerevisiae.* J Biol Chem, 1991. **266**(18): p. 12021-8.

Naviglio, S., et al., *UBPY: a growth-regulated human ubiquitin isopeptidase.* Embo J, 1998. **17**(12): p. 3241-50.

Montagnoli, A., et al., *Ubiquitination of p27 is regulated by Cdk-dependent phosphorylation and trimeric complex formation.* Genes Dev, 1999. **13**(9): p. 1181-9.

Appendices

Yang RM, Naitoh J, Murphy M, Wang H-J, Philipson J, deKernion JB, **Loda M**, Reiter RE. Low levels of p27 protein expression predict poor disease-free survival in patients with prostate cancer. ***J Urol*** 1998;159:941-5.

Waltregny D, Leav I, Signoretti S, Soung P, Lin D, Merk F, Adams JY, Bhattacharya N, Cirenei N, **Loda M.** Androgen-driven prostate epithelial cell proliferation and differentiation *in vivo* involve the regulation of p27. ***Mol Endocrinol*** 2001, 15:765-782

Cai, Y.C., McMenamin M., Magi-Galluzzi C., Macri E., Montironi R., **Loda M**. Down-regulation of p27 in adenocarcinoma of the prostate after androgen ablation. ***Lab Invest***, 2000. **80**: p. 545A

Signoretti S, Waltregny D, Dilks J, Isaac B, Lin D, Garraway L, Yang A, McKeon F, **Loda M**. p63 is a prostate basal cell marker and is required for prostate development. ***Am J Pathol*** 157: 1769-75, 2000

Signoretti S, Montironi R, Manola J, Altimari A, Tam C, Bubley G, Balk S, Thomas G, Kaplan I, Hlatky L, Hahnfeldt P, Kantoff P, **Loda M**. Her-2-neu expression increases with progression towards androgen independence in human prostate cancer. ***J Natl Cancer Inst*** 92: 1918-25, 2000

Androgen-Driven Prostate Epithelial Cell Proliferation and Differentiation *in Vivo* Involve the Regulation of p27

David Waltregny, Irwin Leav, Sabina Signoretti, Peggy Soung, Douglas Lin, Frederick Merk, Jason Y. Adams, Nandita Bhattacharya, Nicola Cirenei, and Massimo Loda

Department of Adult Oncology (D.W., S.S., P.S., D.L., N.B., N.C., M.L.)
Dana-Farber Cancer Institute, and
Department of Pathology (S.S., M.L.)
Brigham and Women's Hospital
Harvard Medical School
Boston, Massachusetts 02115

Department of Pathology (I.L., F.M., J.Y.A.)
Medicine and Veterinary School
Tufts University
Boston, Massachusetts 02111

Androgens control both growth and differentiation of the normal prostate gland. However, the mechanisms by which androgens act upon the cell cycle machinery to regulate these two fundamental processes are largely unknown. The cyclin-dependent kinase (cdk) inhibitor p27 is a negative cell cycle regulator involved in differentiation-associated growth arrest. Here, we investigate the role and regulation of p27 in the testosterone proprionate (TP)-stimulated regeneration of the ventral prostate (VP) of castrated rats. Continuous TP administration to castrated rats triggered epithelial cell proliferation, which peaked at 72 h, and then declined despite further treatment. Castration-induced atrophy of the VP was associated with a significant increase in p27 expression as compared with the VP of intact animals. Twelve hours after the initiation of androgen treatment, total p27 levels as well as its fraction bound to cdk2, its main target, significantly dropped in the VP of castrated rats. Thereafter, concomitantly to the induction of epithelial cell proliferation, the glandular morphology of VP was progressively restored at 48–96 h of TP treatment. During this period of the regenerative process, whereas both proliferating basal and secretory epithelial cells did not express p27, the protein was selectively up-regulated in the nonproliferating secretory epithelial compartment. This up-regulation of p27 expression was coincident with an increase in its association with, and presumably inhibition of, cdk2.

At each time point of TP treatment, p27 abundance in the VP was inversely correlated with the level of its proteasome-dependent degradation activity measured *in vitro* in VP lysates, whereas only slight changes in the amount of p27 transcripts were detected. In addition, the antiandrogen flutamide blocked maximal TP-induced p27 degradation completely. Finally, the expression of skp2, the ubiquitin ligase that targets p27 for degradation, was seen to increase with androgen administration, preceding maximal proliferation and concomitantly to augmented p27 degradation activity.

Taken together, our data indicate that androgens mediate both proliferation and differentiation signals in normal prostate epithelial cells *in vivo*, through regulation of p27. (Molecular Endocrinology 15: 765–782, 2001)

0888-8809/01/$3.00/0
Molecular Endocrinology 15(5): 765–782

INTRODUCTION

Cell proliferation and differentiation are controlled by extracellular signals that impinge upon the cell cycle machinery and modulate the expression/activity of key cell cycle regulators. In the normal prostate gland, these two fundamental processes are regulated to a large extent by androgens (1). Like its human counterpart, the epithelial compartment of the rat prostate is composed of two types of cells: basal and secretory cells. Secretory cells compose approximately 85% of

the total cells in the ventral prostate (VP) of a sexually mature male rat. Basal cells are numerically less abundant, and their function is still poorly understood, although they are believed to be precursors of secretory cells (2, 3). After castration, the rat prostate rapidly involutes as a result of a major loss of secretory cells (60%–70% within 7 days of androgen deprivation), which chronically require physiological levels of androgens for their maintenance (3, 4). Testosterone stimulation can dramatically accelerate the proliferation rate of prostate epithelial cells in a sexually immature rat, yet once the organ has attained adult size additional androgen has little influence on proliferation (5). Likewise, sustained androgen administration to mature castrated rats can trigger the regrowth of the prostate gland, which will eventually return to its original size (5–7). This regenerative process is timely regulated since proliferation rates decline to the baseline levels found in intact animals despite further androgen treatment (6, 8). Concomitantly with their mitogenic activity, androgens induce histological and biochemical changes characteristic of glandular differentiation in the prostate of castrated rats (5–7, 9, 10). For example, testosterone replenishment in castrated rats results in the reconstitution of the normal secretory cell compartment simultaneous with a significant reduction in VP expression levels of basal cell-associated cytokeratins (7, 9). In addition, the mRNA levels of the C3 gene, which encodes for a major subunit of a prostate secretory protein (prostatic steroid-binding protein) exclusively expressed in secretory cells, are dramatically induced in the regenerating VP of castrated rats (11, 12).

The regulation of mammalian cell proliferation by growth-stimulatory and growth- inhibitory extracellular signals occurs during the first gap (G_1) phase of the cell cycle. The enzymes that regulate G_1 phase progression include the cyclin-dependent kinases cdk4 and cdk6, which can be activated through their association with D-type cyclins, and cdk2, which forms active complexes with cyclins E and A (for reviews, see Refs. 13–15). The activity of these cdk/cyclin complexes is negatively regulated by cyclin-dependent kinase inhibitors, which belong to two known families (16). The INK4A family comprises p16, p15, p18, and p19, which bind to and specifically inhibit cdk4 and cdk6. The CIP/KIP family includes p21, p27, and p57, which preferentially target cdk2 complexes (16–18).

The cdk inhibitor p27 was initially identified as an inhibitor of cdk2/cyclin E complex activity in transforming growth factor-β-treated or contact-inhibited mink lung epithelial cells (19), and it was found to induce cell cycle arrest when overexpressed in cultured cells (20, 21). p27 has since been shown to play a pivotal role in mediating G_1 arrest in some normal and neoplastic cells in response to a variety of antiproliferative signals, including growth in suspension (22), cAMP agonists (23), interferon-β (24) and -γ (25), interleukin-6 (26), and rapamycin (27). In contrast to p21, p27 expression is highest in quiescent cells (28, 29) and declines as cells are stimulated to reenter the cell cycle (27, 28). p27 abundance is regulated primarily at the posttranslational level. Once activated, cdk2/cyclin E complexes phosphorylate p27 at Threonine-187 (30–33), thereby signaling for its degradation by the ubiquitin-proteasome system through the ubiquitin-ligase SCF (Skp1/Cul1/F-box)-skp2 complex (34, 35). Hence, maximum degradation of p27 by the ubiquitin-proteasome pathway is detected in extracts prepared from cells in S-phase (36). Accumulation of p27, however, can also be regulated by other mechanisms, including transcriptional (26, 37–39) and translational control (40, 41).

Several lines of evidence from studies in p27 knockout mice indicate a direct involvement of p27 in differentiation-associated cell cycle arrest. Homozygous p27-deficient female mice display infertility with both impaired release of eggs during the estrus cycle and deficient implantation of embryos (42–44). In this instance, the absence of p27 prevents the coupling of differentiation with growth arrest in granulosa cells in response to LH (45, 46). Other studies using $p27^{-/-}$ mice have highlighted an important role for this protein in regulating the differentiation of oligodendrocytes (47) and osteoblasts (48). In addition, p27 expression increases during the differentiation of various normal and neoplastic cell types, both *in vivo* and *in vitro* (49). For example, treatment of LNCaP human prostate cancer cells with interleukin-6 (50) or the flavanoid antioxidant silibinin (51) results in increased p27 expression associated with G_1 arrest and neuroendocrine differentiation.

Prior data have suggested that androgens regulate the expression of p27 in both normal and neoplastic prostate epithelial cells, and that p27 levels may mediate the androgen-driven proliferative and differentiation signals in such cells (7, 52–55). However, the mechanisms by which androgens modulate the expression of p27 are unknown. Testosterone-induced regeneration of the castrated rat VP follows a highly reproducible time course, thus making this system an excellent model for scrutinizing the androgen-mediated regulation of proteins involved in the cell cycle. In this study, we have used this model to investigate the regulation of p27 by testosterone proprionate (TP). We herein provide convincing evidence that in this system 1) p27 plays an important role in the control of TP-stimulated proliferation and differentiation of normal prostate epithelial cells and 2) TP regulates the expression of p27 mainly through modulation of its specific degradation by the ubiquitin-proteasome proteolytic system.

RESULTS

Epithelial Cell Proliferation in the VP of Castrated Rats after Androgen Treatment

As expected, TP administration (6.6 mg/kg, once daily) to the castrated rats caused a dramatic re-

growth of their VP, which returned to a size almost comparable to that of age-matched noncastrated rats after 4 days of treatment (data not shown). *In situ*, proliferating epithelial cells were recognized by immunohistochemical detection of BrdU. Figure 1A shows representative examples of anti-BrdU immunostaining of VP epithelial cells at each time point of TP treatment as well as those from intact animals. Virtually no detectable anti-BrdU nuclear staining was identified in epithelial cells from untreated castrated or intact rats. The induction of cell proliferation became apparent 48 h after the initiation of TP treatment, and BrdU incorporation was detected in both basal and secretory cell subsets (Fig. 1A, *inset*). The proportion of DNA-synthesizing basal and secretory cells reached a peak at 72 h (11.7% ± 0.2%), and then declined in both cell types despite further androgen administration (Fig. 1B). Interestingly, at peak proliferation, the percentage of BrdU-positive basal cells (22.9% ± 0.6%) was almost 2.5 times higher than the percentage of BrdU-positive secretory cells (9.2% ± 0.5%) (paired *t* test, $P < 0.0001$).

Expression of G_1-Related cdks, Cyclins, and cdk Inhibitors in the VP of Androgen-Replenished Castrated Rats

To understand the relationship between androgen stimulus and the proliferation/differentiation response of regenerating VPs, we next investigated the temporal changes in expression levels of p27 and other key regulators involved in the G_1 phase progression of the cell cycle. Changes in androgen receptor (AR) expression were also examined. Western blot analysis of AR, cdk2, cdk4, cdk6, cyclin D1, cyclin E, p21, and p27 expression was performed by using total VP protein lysates from rats killed at each time point of androgen treatment (Fig. 2).

Although the AR protein was expressed as early as 12 h after the initiation of TP treatment, the levels of cdks and their associated cyclins remained unchanged at this time point. The expression levels of these cell cycle proteins gradually increased at 24 h of treatment and peaked during the next 3 days. p21 protein was virtually undetectable in the VP of untreated castrated rats and during the first 24 h of TP replenishment. Thereafter, its expression gradually increased. The highest level of p21 expression was detected in the VP of intact rats.

p27 expression levels followed more complex temporal changes. The protein levels were highest in the VP of untreated castrated rats. TP administration induced an early (12 h) substantial decrease in the amount of p27 protein. Subsequently, p27 levels increased and peaked at 72 h (concomitantly with maximal proliferation rate) and decreased again at 96 h of treatment. The protein abundance was lowest in the VP of intact animals.

In Situ Expression of p27 in the Regenerating VP of Castrated Rats

Since our Western blot experiments were performed with the use of total protein extracts, it was possible that the changes in p27 expression levels detected with this technique may not reflect those that take place in the epithelial cells. Thus, to rule out this potential bias as well as to assess p27 expression in the two subsets of VP epithelial cells, we used immunohistochemistry. Figure 3A shows representative examples of anti-p27 immunostaining in VP glands during the first 96 h of TP administration to castrated rats as well as in the VP of intact animals. p27 expression was scored separately in the basal and secretory cells according to the percentage of positive cells (Fig. 3B).

p27 immunoreactivity in the epithelial cells was mainly nuclear (Fig. 3A). Overall, temporal changes in p27 expression levels were similar in basal and secretory cell compartments and strictly paralleled those detected by Western blot in the corresponding total protein extracts (compare Fig. 3B and Fig. 2). The percentages of p27-expressing epithelial cells were high in the VP of untreated castrated rats and, after 12 and 24 h of TP treatment, fell significantly in both secretory (unpaired *t* test, $P = 0.03$) and basal cells (unpaired *t* test, $P = 0.05$). Subsequently, p27 expression levels increased in both cell types and peaked at 72 h of treatment. However, this increase in p27 levels was significant only in the secretory cell subset (unpaired *t* test, $P = 0.2$ and $P < 0.0001$ for basal and secretory cells, respectively). p27 levels then slightly dropped in both subsets of cells at 96 h of treatment (unpaired *t* test, $P = 0.62$ and $P = 0.47$ for secretory and basal cells, respectively). The lowest level of p27 expression was found in the VP epithelial cells of intact animals.

In the VP of untreated castrated rats, a significantly higher percentage of p27-positive cells was observed in the basal compartment (64.7% ± 12.8%) than in the secretory one (45.6% ± 9.3%) (paired *t* test, $P = 0.005$) (Fig. 3B). After 24 h of TP treatment, the level of p27 expression was similar in both cell types (paired *t* test, $P = 0.38$). Subsequently, at 48–96 h of treatment, p27 expression levels were significantly higher in secretory than in basal cells (paired *t* test, $P < 0.05$). Also, a significant difference in the percentages of basal (4.6% ± 2%) and secretory (7% ± 2.8%) p27-positive cells was observed in the VP of intact animals (paired *t* test, $P < 0.05$).

Thus, both our immunohistochemical and immunoblot data unexpectedly indicated that the expression levels of the cell cycle inhibitor were high in the regenerating VP at peak proliferation (72 h). To understand this paradox, we performed double immunofluorescence experiments for BrdU and p27 using VP tissue sections from animals killed at 72 h of TP treatment. Remarkably, all epithelial cells in S-phase (BrdU-positive) exhibited no detectable p27 expression (Fig.

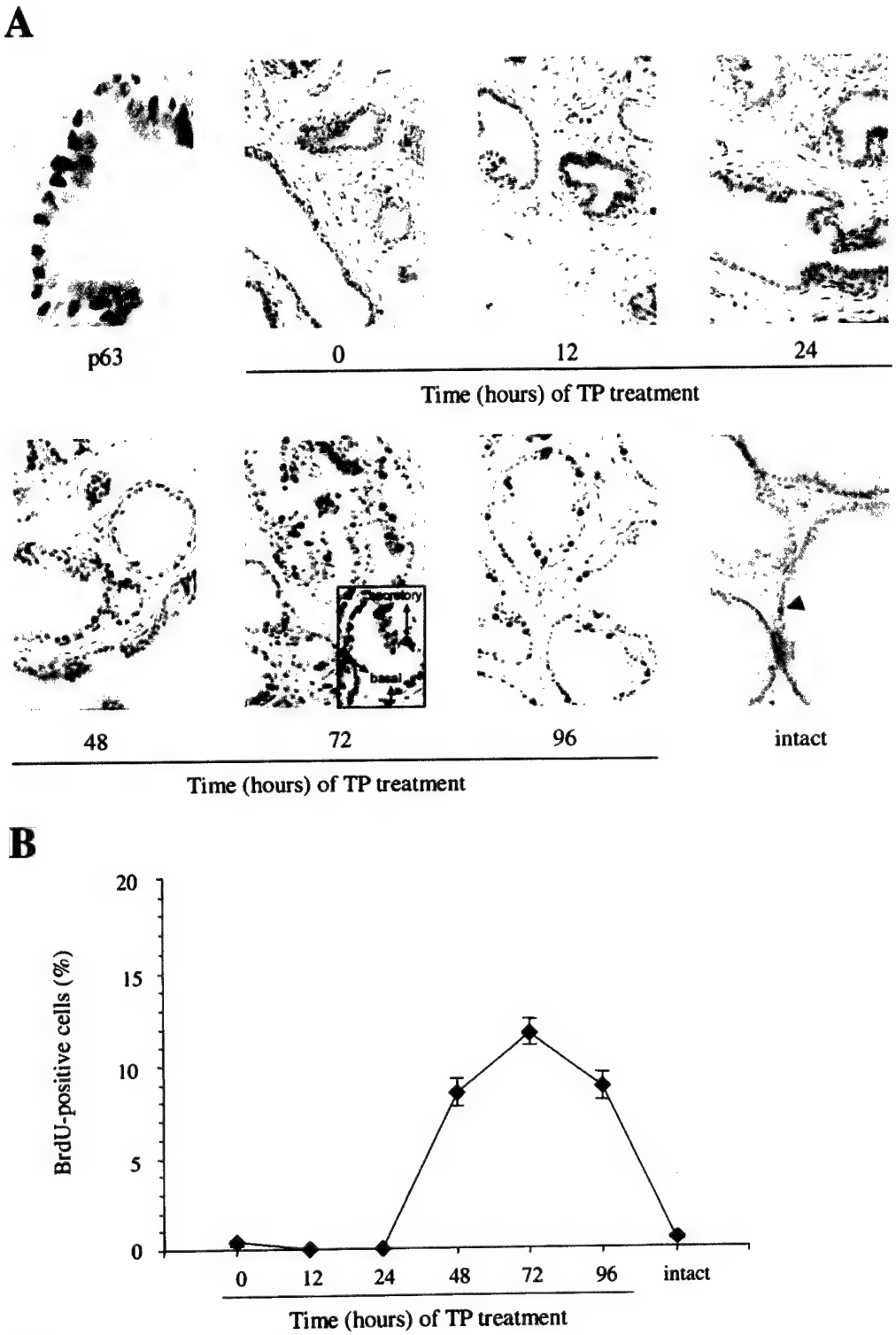

Fig. 1. Epithelial Cell Proliferation in the VP of Castrated Rats Treated by TP

A, Castrated rats were treated by TP (6.6 mg/kg, once daily) for 4 days. At 0, 12, 24, 48, and 96 h after the initiation of the treatment, rats (seven per time point) were injected with BrdU (10 mM) and killed 30 min later. Seven untreated noncastrated age-matched male rats were also included as control animals. Tissue sections were cut from each paraffin-embedded VP sample, immunostained with either anti-p63 monoclonal antibody or anti-BrdU monoclonal antibody, and counterstained with methyl green and hematoxylin, respectively as described in *Materials and Methods*. For recognition of basal *vs.* secretory cells, immunohistochemistry for p63 is shown in the *first panel*. p63 positive basal cells show nuclear immunoreactivity. Representative examples of BrdU immunodetection are shown for each group of seven rats. Positive staining was completely abolished when the primary antibody was omitted from the staining procedure (data not shown). Original magnification: ×200. *Inset,* Detection

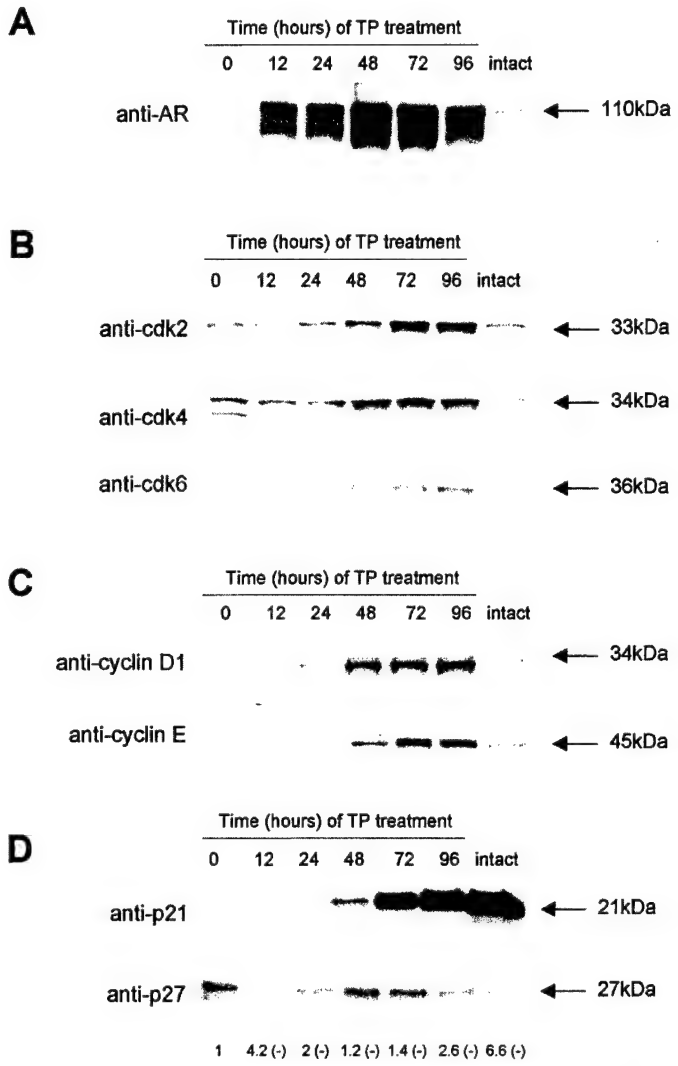

Fig. 2. Expression of G_1 Phase-Related Cyclin-Dependent Kinases, Cyclins, and Cyclin-Dependent Kinase Inhibitors in the VP of Testosterone-Treated Castrated Rats

Castrated rats (7 per time point) were killed 0, 12, 24, 48, 72, and 96 h after the beginning of androgen replenishment (6.6 mg/kg TP, once daily). The VP of each animal was harvested. VP specimens from seven age-matched intact animals were also used. Tissue sample duplicates for each group of seven rats were obtained by pooling separately the VP specimens from three and four animals. Total proteins were extracted from the pooled samples. Protein lysates (100 μg per sample) were subjected to Western blot analysis of AR, cdk2, cdk4, cdk6, cyclin D1, cyclin E, p21, and p27 expression, as described in *Materials and Methods*. Ponceau S staining of the membranes showed equal protein sample loading and transferring (data not shown). Each Western blot experiment was performed at least twice with both sets of pooled samples and consistent results were observed. Fold increases (+) or decreases (−) in p27 protein levels quantified by the ImageQuant program are indicated *under* the Western blot.

4, A–C). Thus, during the proliferation phase, two main subsets of epithelial cells could be distinguished: cells in S phase (BrdU positive/p27 negative) and cells likely to be arrested in G_1 phase (BrdU negative/p27 positive). In addition, a small proportion of basal and secretory cells were double negative for both antibodies.

Association of p27 with cdk2/Cyclin Complexes in the Regenerating VP of Castrated Rats

To further substantiate our results, we determined whether the increased levels of p27 expression detected at 72 h of TP replenishment would translate into

of anti-BrdU immunoreactivity in the nucleus of both secretory and basal cells. *Arrow*, Identification of a BrdU-positive epithelial cell. B, Epithelial cell proliferation rates in the VP of castrated rats treated by TP. The percentage of proliferating epithelial cells in the VP of each animal was calculated by dividing the number of BrdU-positive epithelial cells by the total number of epithelial cells counted (~1,000 cells). Assessment of the percentage of BrdU-positive epithelial cells was also done in the VP of seven intact rats. Values are expressed as the mean ± SE (*error bar*) for each group of seven animals.

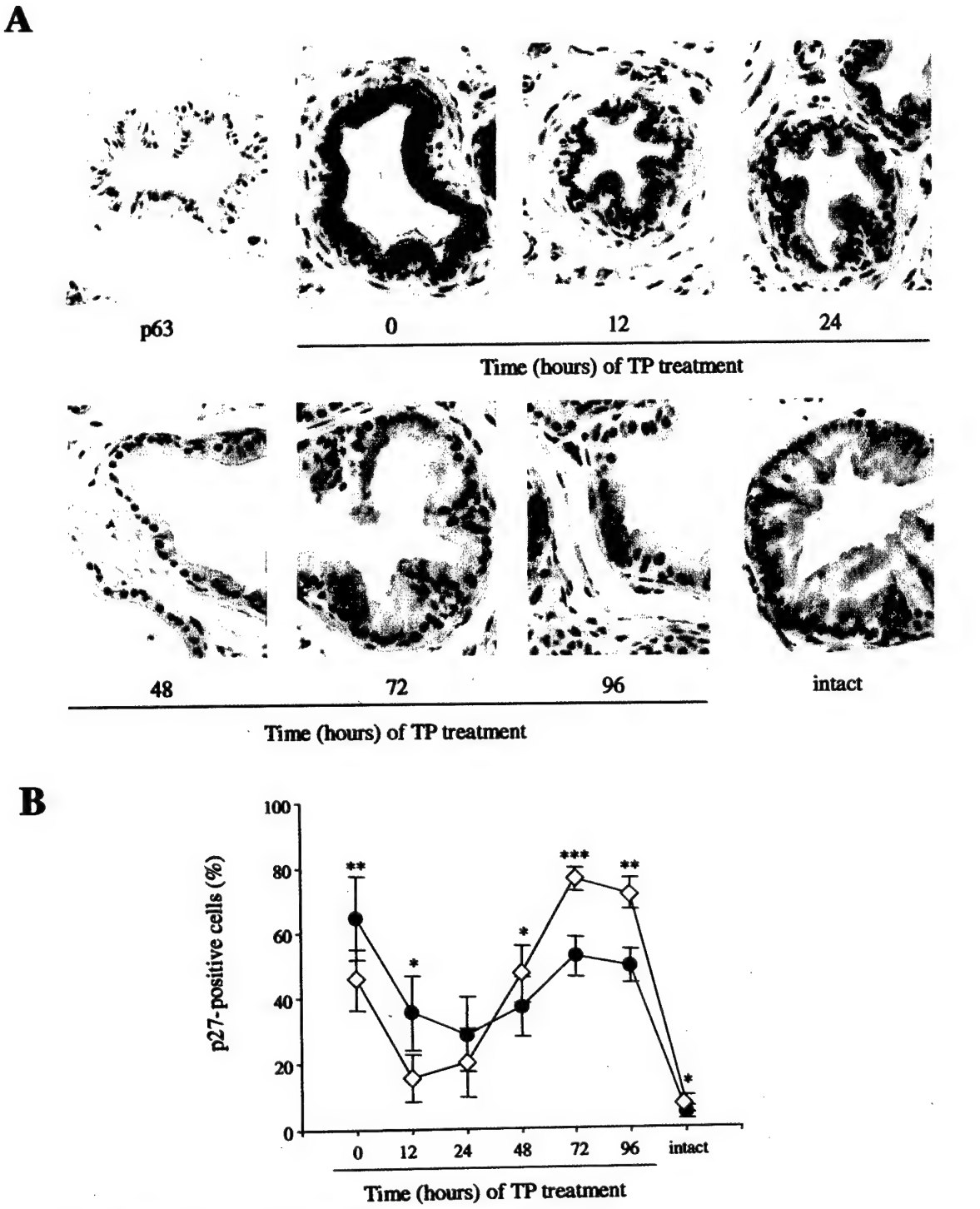

Fig. 3. *In Situ* Expression of p27 in the Regenerating VP of Castrated Rats

A, Immunodetection of p27 in the VP of castrated rats treated by TP. After treatment by TP (6.6 mg/kg, once daily) for the indicated times, castrated rats (7 per time point) were killed and the VP from each animal was harvested. Seven intact age-matched male rats were also used. Tissue sections from each paraffin-embedded VP were cut, immunostained with either anti-p63 monoclonal antibody or anti-p27 monoclonal antibody, and counterstained with methyl green and hematoxylin, respectively, as described in *Materials and Methods*. For recognition of basal *vs.* secretory cells, immunohistochemistry for p63 is shown in the first panel. p63-positive basal cells show nuclear immunoreactivity. Representative examples of p27 staining are shown for each group of seven animals. Substitution of the primary antibody with PBS did not yield any specific staining for either antibody (data not shown). Original magnification: ×400. B, Levels of p27 expression in the VP of castrated rats treated by TP, as determined by immunohistochemistry. Scoring of p27 immunostaining in the VP of each rat was done according to the percentage of epithelial cells (~500 cells counted) exhibiting nuclear anti-p27 reactivity. p27 scoring was also done in the VP of

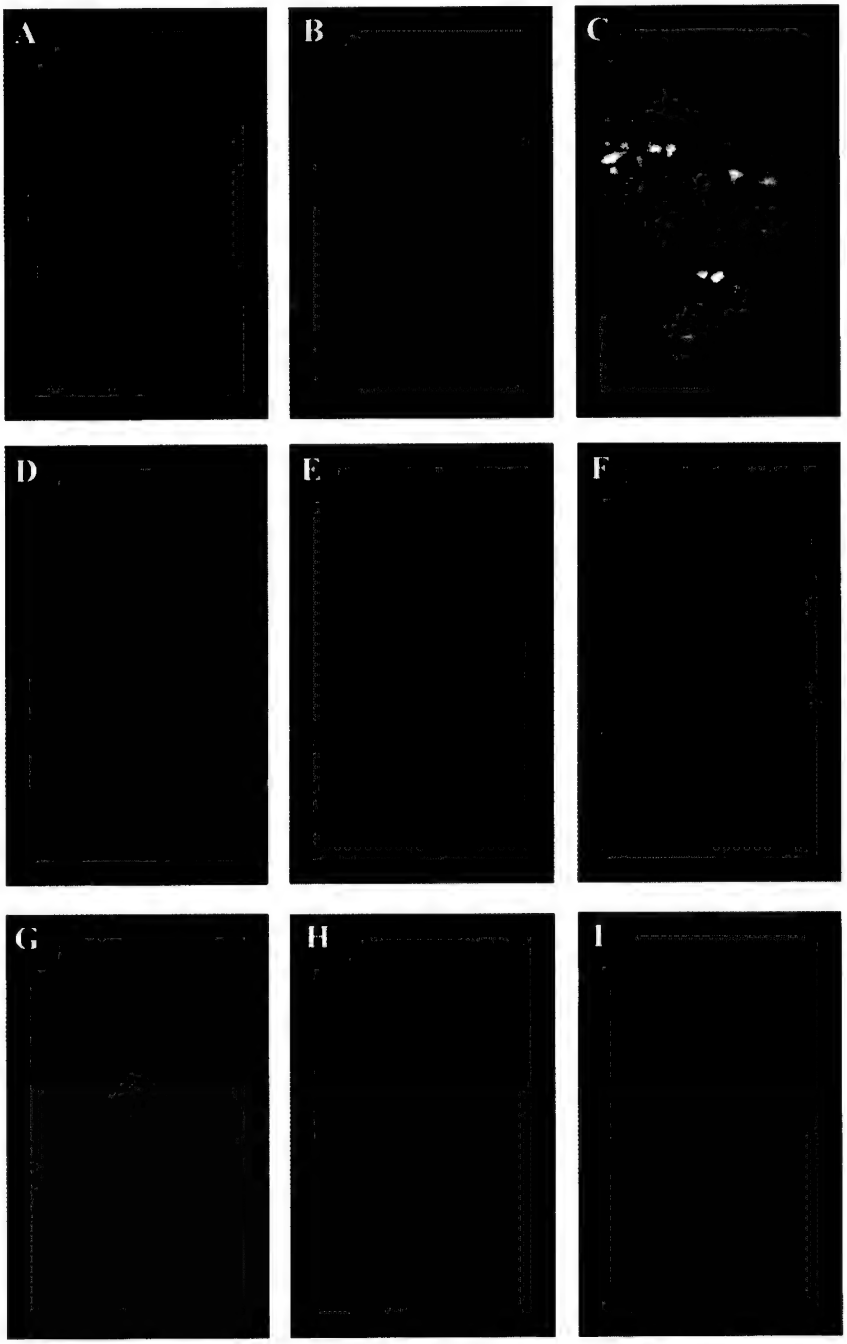

Fig. 4. Absence of p27 Expression in Proliferating Epithelial Cells from the Regenerating VP of Castrated Rats

Double immunofluorescence staining for p27 and BrdU was performed in paraffin-embedded VP specimens from seven castrated rats that had been killed after 3 days of continuous TP treatment (6.6 mg/kg, once daily). Tissue sections from each VP were immunostained with an anti-p27 antibody, and detection was performed utilizing FITC-conjugated streptavidin (*green* staining). Subsequently, the same sections were immunostained with anti-BrdU monoclonal antibody, and detection was done using Texas red-conjugated streptavidin (*red* staining). Substitution of the primary antibodies with PBS did not yield any specific staining (data not shown). Photomicrographs of double immunofluorescence staining for p27 and BrdU in representative prostate glands were taken under an UV microscope using appropriate filters for detecting FITC/p27 (A, ×200; D, ×400; G, ×1,000), Texas red/BrdU (B, ×200; E, ×400; H, ×1,000), and both FITC/p27 and Texas Red/BrdU (C, ×200; F, ×400; I, ×1,000).

seven intact rats. p27 scores were determined in the basal (*closed circles*) and secretory cell (*open diamonds*) subsets separately. All scoring values are expressed as the mean ± SE (*error bar*) for each group of seven rats. The paired *t* test was used to assess whether there were significant differences in p27 expression levels between basal and secretory cells at each treatment time point. Statistically significant differences are indicated as *asterisks* (*, $P < 0.05$; **, $P < 0.01$; ***, $P < 0.005$).

an increased association of p27 with cdk2. We performed coimmunoprecipitation experiments in which cdk2 was pulled down from the VP protein lysates at the different time points of TP treatment with the use of an anti-cdk2 antibody. The immunoprecipitates were subjected to SDS-PAGE and transferred to nitrocellulose membranes that were blotted with an anti-p27 antibody (Fig. 5A).

Temporal changes in the association of p27 with cdk2 matched those in endogenous p27 protein expression (compare Fig. 5A and Fig. 2). Indeed, as compared with the VP of untreated castrated rats, the amount of cdk2/p27 complexes was substantially decreased and almost undetectable in the VP of castrated rats treated by TP for 12 or 24 h. The abundance of p27 bound to cdk2 increased significantly at 48 h of TP treatment, peaked at 72 h, and then declined at 96 h despite further TP treatment. The lowest amount of cdk2- bound p27 was found in the VP of intact animals. These coimmunoprecipitation experiments were performed using high amounts of protein lysates and low amounts of anti-cdk2 antibody to saturate anti-cdk2 antibodies with cdk2 in each condition. Thus, since the abundance of immunoprecipitated cdk2 was similar in all samples (Fig. 5B), the increased association of p27 with cdk2 at 48–96 h of TP treatment was not merely due to an increased amount of cdk2 protein in the lysates.

Evidence for Androgen Regulation of p27 Expression by Degradation via the Ubiquitin-Proteasome Pathway

We next searched for the mechanisms responsible for the regulation of p27 expression by TP. We first tested for levels of p27 ubiquitin-proteasome-mediated degradation activity in the different VP lysates by using a previously described assay (36, 56, 57) in which puri-

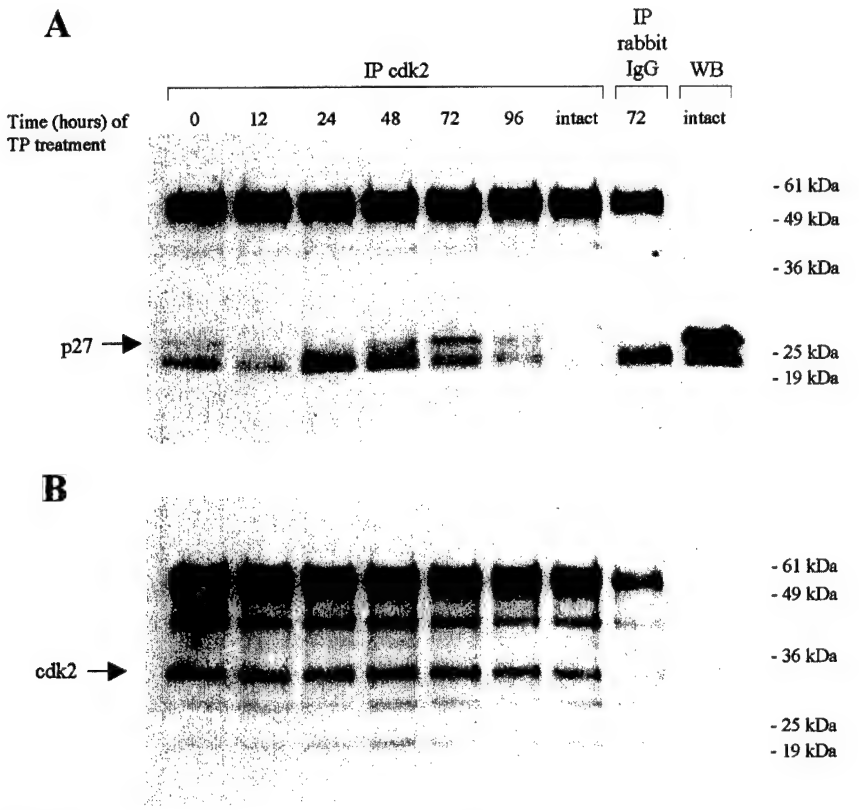

Fig. 5. Association of p27 with cdk2 in the Regenerating Prostate of Castrated Rats

After treatment by TP (6.6 mg/kg, once daily) for the indicated times, castrated rats (7 per time point) were killed, and the VP from each animal was harvested. The VP from seven intact age-matched male rats was also collected. The VP specimens from each group of seven rats were randomly pooled in duplicates containing three and four VP specimens, each. Total proteins were extracted and used in cdk2/p27 coimmunoprecipitation experiments. A, Protein lysates (500 μg per sample) were immunoprecipitated with 1.5 μg of anti-cdk2 antibody, as detailed in *Materials and Methods*. The immunoprecipitates were subjected to SDS-PAGE and transferred to nitrocellulose membranes, which were blotted with an anti-p27 antibody. Immunoprecipitates of VP lysates (500 μg) from rats treated by TP for 72 h with 1.5 μg of rabbit IgG were used as negative controls. One hundred micrograms of nonimmunoprecipitated intact VP protein lysates were also used in the Western blotting procedure. Coimmunoprecipitation experiments were performed with both sets of pooled samples and yielded reproducible results. B, p27-probed membranes were subsequently stripped and reprobed with an anti-cdk2 antibody to examine the amount of immunoprecipitated cdk2 in the different samples.

fied recombinant his_6-tagged p27 serves as a substrate to the lysates. Kinetic profiles of p27 degradation obtained by using the samples from each time point of TP treatment clearly showed that VP protein lysates were able to degrade exogenous p27 and that this ability to degrade the protein was modulated in time, as prostates were replenished with TP (Fig. 6A). p27 was degraded in a proteasome-dependent manner since the addition of a specific proteasome inhibitor (MG-132) to the VP protein lysates (which contained the nonproteosomal protease inhibitors phenylmethylsulfonylfluoride , aprotinin, and leupeptin) completely nullified p27 degradation (Fig. 6C).

To measure p27 degradation activity levels in the different samples and to correlate these levels with the expression levels of the endogenous protein in the corresponding samples, the relative amounts of undegraded his_6-p27 after 0 and 4 h of incubation in the presence of the lysates were analyzed by Western blotting and quantified by densitometry. p27 abundance was inversely correlated with the level of degradation activity for the protein during the course of TP treatment (Fig. 7A). Importantly, the highest level of p27 degradation activity was observed in the intact VP, while castration abolished this activity almost completely.

Some degradation of p21, which is also a target of the ubiquitin-proteasome pathway (58–61), was noted in all the samples tested (Fig. 6B). However, in contrast to p27, the levels of p21 degradation activity remained stable (Fig. 7A).

We then determined whether Flutamide (F) blocked TP-induced degradation of p27 as further proof that degradation of p27 was under androgen control and that this effect was AR-mediated. As shown in Fig. 8, *top panel*, F completely blocked degradation induced by TP in castrate rats. A Western blot of VP lysates probed with probasin antibody (*bottom panel*), a marker of testosterone activity in mouse and rat prostate (56), showed that castration abolished its expression. Probasin expression was partially restored by 24 h of TP treatment, and the TP-induced probasin expression was almost completely blocked by F.

Expression of p27 transcripts during the Androgen-Induced Regeneration of Castrated Rat VP

We also investigated whether p27 and p21 mRNA levels were modulated in the regenerating VP of castrated rats using Taqman Real-Time RT-PCR (PE Applied Biosystems, Foster City, CA). After inducing a drop in the level of p27 transcripts at 12 h of treatment (2.6-fold decrease), sustained TP administration resulted in a slight but consistent increase in p27 mRNA levels, which peaked at 96 h of treatment (2.3-fold induction) (Fig. 7B). The highest level of p27 transcripts was detected in the VP from intact rats. On the other hand, p21 mRNA levels were gradually and substantially up-regulated, with maximal levels attained at 96 h of TP treatment (5.7-fold induction). Also, the level of p21 transcripts was almost 3 times higher in the VP of intact rats than that in the VP of untreated castrated animals. Thus, our results strongly suggest that testosterone regulates p27 expression mainly through its ubiquitin-proteasome-mediated degradation while it transcriptionally induces p21 expression in the regenerating rat prostate.

Expression of skp2, the Ubiquitin Ligase for p27, in the Regenerating Rat Prostate

To further elucidate the mechanism(s) by which the proteasome-mediated degradation of p27 is restored by readministration of TP to castrate animals, we assessed expression of skp2, the p27 targeting F-box protein in the ubiquitin ligase for p27, at the various time points of the treatment. Whereas no change was noted between VP lysates from intact and those from castrate rats, a substantial increase in skp2 levels, which preceded times of peak proliferative rates and paralleled p27 degradation activity, was observed starting as early as 12 h after TP administration and consistently decreasing thereafter (Fig. 9). These results suggest that, when androgen-driven proliferation is induced, increased skp2 may be responsible for the enhanced degradation of p27.

DISCUSSION

In the present study, we have used a castration-regeneration rat prostate model for investigating the *in vivo* regulation of p27 expression by androgens. In agreement with other reports, our results demonstrate that sustained TP administration to castrated rats stimulates VP epithelial cell proliferation, whose rate peaks at 72 h of androgen replenishment and then declines despite further treatment (1, 3, 5, 62–64).

Using Western blot experiments, we show that the castration-induced atrophy of the VP is associated with a significant up-regulation of p27 expression as compared with the VP of intact animals. In addition, TP administration to castrated rats induces an early (12 h) and substantial drop in p27 levels while the expression levels of several G_1-associated cdks and cyclins remains unchanged. This significant decrease in p27 expression levels is also detected by immunohistochemistry in both basal and secretory cells. Furthermore, the amount of p27 bound to cdk2, its main target, declines markedly in the early phase of TP replenishment, suggesting a release in the inhibition of cdk2 activity. Together, these results thus indicate that the initial down-regulation of p27 in the androgen-induced regeneration of VP in castrated rats may represent a primary cell cycle event, thereby allowing VP epithelial cells to proliferate.

Unexpectedly, the level of p27 expression detected by Western blot peaks at the same time as the rate of

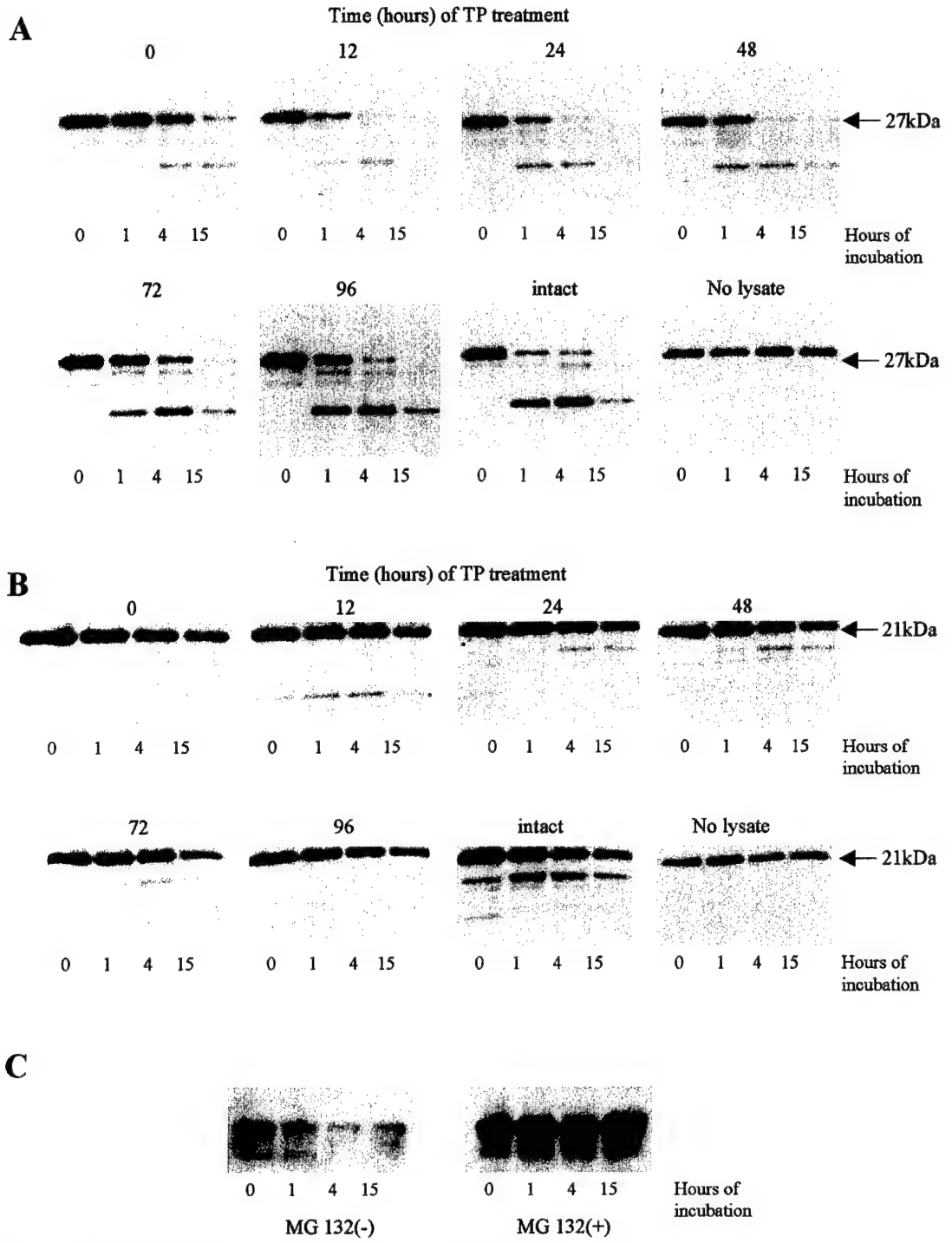

Fig. 6. Kinetics of p27 and p21 Degradation in the Regenerating VP of Castrated Rats

After treatment by TP (6.6 mg/kg, im, once daily) for the indicated times, castrated rats (7 per time point) were killed and the VP from each animal was harvested. The VP from seven intact age-matched male rats was also collected. The VP specimens from each group of seven rats were randomly pooled in duplicates containing three and four VP specimens each. Total proteins were isolated from each pooled sample. Purified human recombinant his_6-tagged p27 (A) and p21 (B) proteins (300 ng) were incubated for the indicated times at 37 C in the presence of a degradation mix containing 100 μg of each VP protein lysate, as described in *Materials and Methods*. The degradation of the his_6-tagged proteins by the lysates was analyzed by immunoblotting with an antihistidine antibody. Each degradation assay was performed at least twice with both sets of pooled samples and consistent results were observed. Control experiments included the omission of the lysates from the degradation mix. No specific signal was obtained when the tagged proteins were not added to the degradation mix (data not shown). C, Protein lysates (100 μg) from the VP of intact animals were assayed for his_6-p27 degradation activity in the presence or absence of the proteasome inhibitor MG-132 (100 μM) in the degradation mixture.

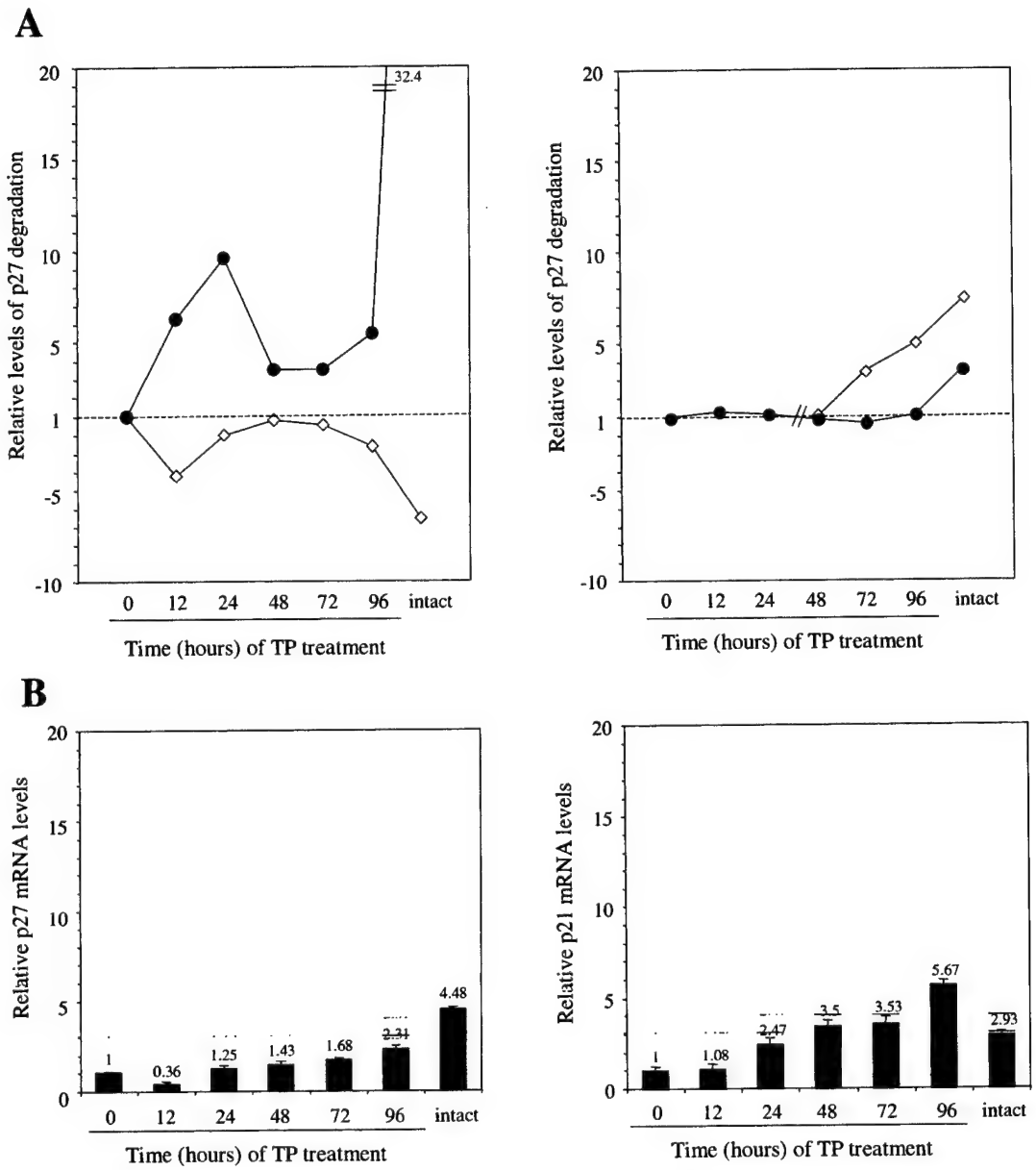

Fig. 7. Androgen Regulation of p27 and p21 Expression in the Regenerating Prostate of Castrated Rats

After treatment by TP (6.6 mg/kg, once daily) for the indicated times, castrated rats (7 per time point) were killed and the VP from each animal was harvested. The VP from seven intact age-matched male rats was also harvested. The VP specimens from each group of seven rats were randomly pooled in duplicates containing three and four VP specimens each. A, The degradation activity of the VP lysates for his_6-tagged p21 and p27 proteins was analyzed by immunoblotting with an antihistidine antibody, as described in *Materials and Methods*. Quantification of degradation activity for the exogenous proteins was done by densitometric analysis of the bands at ±22 kDa and ±28 kDa corresponding to undegraded his_6-tagged p21 and p27 proteins, respectively. Relative degradation activity of the samples at each time point after TP injections (*closed circles*) was calculated by dividing the densitometric value of the band obtained with the sample without incubation (0 h) by the one obtained with the sample incubated for 4 h in the degradation mix. Relative levels of p27 and p21 degradation activity were compared with the endogenous levels of p27 and p21 proteins (*open diamonds*) in the VP at each time point (see Fig. 2). All values are normalized to those found in the VP of untreated castrated rats. B, Total RNA was extracted from each VP tissue duplicate. One microgram of total RNA per sample was reverse-transcribed and a one-twentieth of each RT reaction was subjected to Taqman Real-Time PCR amplification, as described in *Materials and Methods*. The specific rat p27 and p21 primers and probes used in the PCR reactions are shown in Table 1. The housekeeping GAPDH gene was used as endogenous control. The relative amounts of p27 and p21 transcripts in each sample were determined using the standard curve method and were normalized to GAPDH mRNA expression levels. All values represent the mean of triplicates and are normalized to those found in the VP of untreated castrated rats. *Error bars* stand for SDS. Taqman PCR experiments were performed with both sets of pooled samples, and consistent results were observed. PCR reactions with samples in which the reverse transcriptase or the target RNA was omitted from the RT reaction did not yield any significant amplification (data not shown).

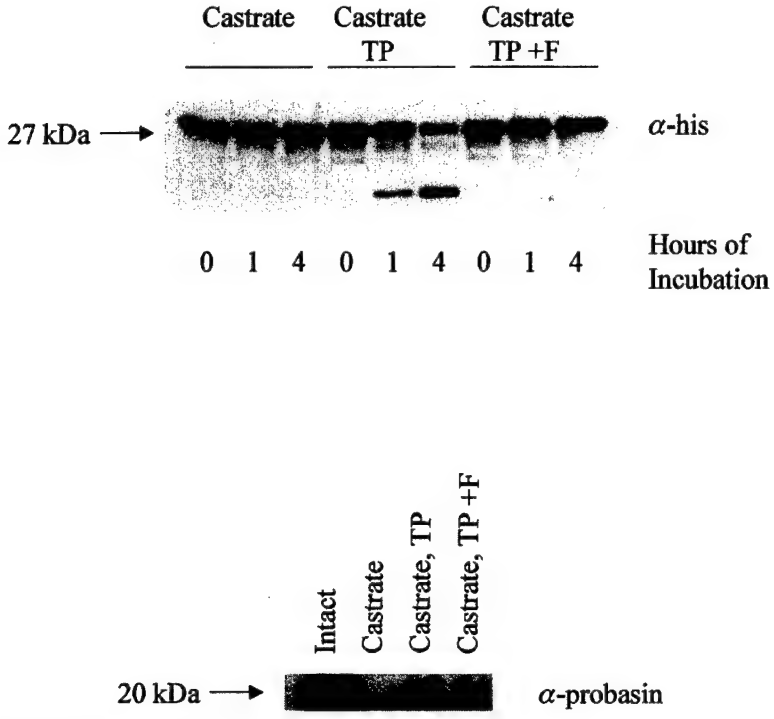

Fig. 8. Effects of Flutamide (F) on TP-Mediated Degradation of p27

Fourteen days after surgical castration, rats were injected sc with 10 mg of F , twice a day, for 48 h. At 24 h from the initial F injection, rats were injected with 6.6 mg/kg of TP im, once a day, for 24 h. The animals were then killed. Castrated rats injected with TP only and killed 24 h after injection served as controls. The VPs of castrates (first three lanes, *top panel*), castrates treated with TP alone (middle three lanes, *top panel*) or castrates treated with both F and TP (last three lanes, *top panel*) were harvested, degradation assays for p27 were performed, and immunoblots were probed with antihistidine (α-his) antibodies as described. Zero-, 1-, and 4-h time points are shown for all treatment groups. Antiprobasin Western blot performed on lysates of castrates, TP-treated castrates, and TP- and F-treated castrates is shown in the *lower panel*.

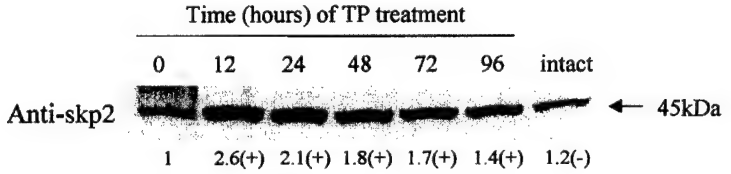

Fig. 9. Expression of skp2 in the VP of Testosterone-Treated Castrated Rats

Castrated rats (7 per time point) were killed 0, 12, 24, 48, 72, and 96 h after the beginning of androgen replenishment (6.6 mg/kg TP, once daily). The VP of each animal was harvested. VP specimens from seven age-matched intact animals were also used. Tissue sample duplicates for each group of seven rats were obtained by pooling separately the VP specimens from three and four animals. Total proteins were extracted from the pooled samples. Protein lysates (100 μg per sample) were subjected to Western blot analysis of skp2 expression, as described in *Materials and Methods*. Ponceau S staining of the membranes showed equal protein sample loading and transferring (data not shown). Each Western blot experiment was performed at least twice with both sets of pooled samples and consistent results were observed. Fold increases (+) or decreases (−) in skp2 protein levels quantified by the ImageQuant program are indicated under the Western blot.

epithelial cell proliferation and the levels of G_1-related cdks and cyclins are maximal. Indeed, this observation is in apparent contradiction with the fact that p27 expression is known to be down-regulated in proliferating cells (36). Findings from our immunohistochemical experiments have helped clarify this paradoxical observation. First, the levels of p27 in prostate epithelial cells parallel those detected by Western blot in the corresponding total protein extracts during the course of TP treatment, indicating that the changes in p27 expression detected in the crude homogenates are representative of those occurring in the VP epithelial compartment. Second, when the rate of cell proliferation reaches its maximum, the majority of epithelial cells express p27 whereas a minority of them proliferate. Third, the detection of BrdU and the expression of p27 in epithelial cells are mutually exclusive. In addition, the increased levels of p27 expression detected

at peak TP-induced proliferation are coincident with an increased association of p27 with, and presumably inhibition of, cdk2. Since cells expressing p27 are BrdU-negative, our results indicate that in this model, p27 may play a significant role in controlling the regrowth and restoring the glandular structure of the VP by limiting the proliferation of epithelial cells and favoring their postmitotic differentiation. Further evidence is provided by our observation that, concomitant with the androgen-stimulated enhancement of cell proliferation and progressive reconstitution of VP morphology, p27 expression is significantly induced only in nonproliferating secretory cells. It is also noteworthy that, in the VP of intact rats, the percentage of p27-positive cells is also significantly higher in the secretory compartment than in the basal one. This is in keeping with the wide expression of p27 in human prostate secretory cells as compared with the more restricted expression of this protein in basal cells (65) and the lack of its expression in the putative, transiently proliferating intermediate cell compartment (52). Altogether, our results thus add weight to the body of data indicating an important role for p27 in the switch from proliferation to differentiation of precursor/progenitor cells from different lineages (41–48, 66).

In the VP of untreated castrated rats, p27 expression levels are significantly higher in basal than in secretory cells. We have observed a similar although more striking pattern of selective distribution of p27 expression in the VP gland of rats that had been castrated for 4 months. In those rats, a high level of anti-p27 nuclear reactivity is detected in virtually all basal cells while residual secretory cells are consistently devoid of any staining (M. Loda, I. Leav, and D. Waltregny, unpublished data). Since basal cells do not suffer a substantial loss in number after castration (3), it is tempting to hypothesize that the sustained, high expression of p27 observed in basal cells after castration may be related to the suggested role of this protein in the prevention of cell death. Recent studies on $p27^{-/-}$ mice have revealed an antiapoptotic role of p27 in growth factor-deprived mesangial cells and fibroblasts (67). p27 also protects cells from cyclohexamide-induced apoptosis (71) and has been shown to inhibit apoptosis after inflammatory injuries in renal glomerular and tubular cells (68). In a human leukemia cell line, overexpression of p27 confers resistance to induction of apoptosis by several cytotoxic agents (69). Thus, although our hypothesis that p27 overexpression may safeguard basal cells from androgen deprivation-induced apoptosis remains at this time highly speculative, it certainly deserves further investigation.

It is known that p27 expression can be regulated at multiple levels (49), but the relative contribution of transcriptional, translational, or proteolytic control to p27 regulation in various physiological and pathological contexts in the prostate gland remains largely unknown. Our results provide the first demonstration that androgens regulate p27 expression in an animal model. Using lysates from VPs at the various time points, we determined that p27 is regulated primarily by ubiquitin-proteasome-mediated degradation. In fact, a maximal level of p27 degradation activity is observed in the VP of intact animals, whereas castration abrogates this activity almost completely. Progressive restoration of p27 degradation activity is obtained with TP replenishment and blocked by the antiandrogen flutamide. In contrast to the p21 gene, to date, no androgen response element has been found in the cloned portion of the p27 gene promoter (70). Our results reveal that TP treatment slightly modulates p27 transcription in the VP of castrated rats. However, in view of the kinetics and magnitude of changes in p27 mRNA expression, androgen-mediated p27 transcriptional regulation, alone, is insufficient to explain the levels of p27 protein expression detected during the course of the treatment. Furthermore, since the highest level of p27 transcripts is found in the VP of intact rats while the protein level is the lowest, we conclude that in the VP of sexually mature rats TP induces a high p27 protein turnover by augmenting its proteasome-mediated degradation.

The specific mechanism by which androgens regulate p27 degradation is unknown. It has been recently shown that the F-box protein skp2 is the targeting subunit of the ubiquitin ligase complex specific for p27 (34, 35, 71). Skp2 levels are highest in S-phase when p27 degradation is also maximal (34, 35, 71–73). We therefore assessed levels of this protein in the various experimental conditions. We provide evidence that the amount of skp2 parallels the level of p27 degradation activity in the regenerating (proliferating) prostate and, importantly, its increased expression precedes peak proliferation. Although the mechanism regulating p27 degradation activity in the nonproliferative state, *i.e.* the intact prostate, remains unknown, our data suggest that skp2 is induced by testosterone and may mediate this process when prostate epithelial cells are stimulated to proliferate.

The regulation of p27 proteasome-mediated proteolytic activity in the regenerating prostate may be specific for this protein. Indeed, the levels of p21 degradation activity, another target of the ubiquitin-proteasome pathway (58–61), remain unchanged during the course of TP treatment and thus cannot account for the gradual increase in expression levels of this protein observed during TP treatment. In fact, it has been shown that the p21 gene can be transcriptionally activated by androgens *in vitro* through binding of AR with an androgen response element present in its proximal promoter (74). In this report, we substantiate these findings in an *in vivo* model by demonstrating that the levels of p21 transcripts are significantly up-regulated by androgens.

In summary, the results from the present study convincingly suggest that p27 plays an important role in the control of testosterone-stimulated proliferation and differentiation of normal prostate epithelial cells. In addition, these results support the hypothesis that the

regulation of p27 levels by androgens in these cells is dependent on the AR and achieved through modulation of its specific degradation by the ubiquitin-proteasome proteolytic system.

MATERIALS AND METHODS

Animals and Tissues

All animals were maintained in accordance with the NIH Guide for the Care and Use of Laboratory Animals, and the specific protocol used in this study was approved by the Dana-Farber Cancer Institute Animal Care and Use Committee. Twelve week-old male Noble rats were purchased from Charles River Laboratories, Inc. (Wilmington, MA). Fourteen days after surgical castration, rats were injected im with 6.6 mg/kg TP (Sigma, St. Louis, MO) in tocopherol-stripped corn oil (ICN Biomedicals, Inc., Aurora, OH), once a day, for 4 days. At 0, 12, 24, 48, 72, and 96 h after the beginning of TP injections, animals (seven rats per time point) were injected ip with 5 ml of PBS containing 10 mM BrdU (Roche Molecular Biochemicals, Mannheim, Germany) and killed 30 min later by CO_2 asphyxiation. The ventral prostate (VP) was then harvested, freed of fat, and two-thirds of each VP were immediately flash-frozen in liquid nitrogen and then stored at −80 C for subsequent RNA and protein isolation. The remaining third of each VP was fixed in 10% phosphate buffered formalin overnight, dehydrated in graded alcohols, and paraffin embedded for immunohistochemical procedures. Seven noncastrated untreated age-matched male rats were also included as control animals.

Castrated rats were also injected sc with 10 mg of the anti-androgen flutamide (F) (Sigma, St. Louis, MO), twice a day, for 48 h. At 24 h from the initial F injection, rats were injected im with 6.6 mg/kg of TP (Sigma), once a day, for 24 h. The animals were then killed and the VPs were harvested and processed as described above. Castrated rats injected with TP only and killed 24 h after injection served as controls.

Every 20 mg of flutamide was dissolved in 75 μl of methanol, 75 μl of butanol, and 850 μl of tocopherol-stripped corn oil (ICN Biomedicals, Inc., Aurora, OH).

Protein and RNA Extraction

The frozen VP specimens from each group of seven rats were randomly pooled in two separate sample duplicates containing three and four VP specimens, each. All the experiments described in this study were performed with both sets of pooled samples and yielded reproducible results (data not shown). The pooled frozen VP samples were homogenized by pulverization using a Mikro-Dismembrator S (B. Braun Biotech Intl. GmbH, Melsungen, Germany) to generate a tissue powder that was immediately processed for protein and RNA extraction. Total RNA was extracted from 10–20 mg of each tissue homogenate by using the RNeasy mini kit (QIAGEN, Valencia, CA), according to the manufacturer's protocol. The remaining tissue powder was lysed in 3.5 vol/wt of lysis buffer [10% sucrose, 1% Nonidet P-40, 20 mM Tris (pH 8.0), 137 mM NaCl, 10% glycerol, 2 mM EDTA, 10 mM NaF, 1 mM Na_3VO_4] containing phenylmethylsulfonyl fluoride (1 mM), soybean trypsin inhibitor (10 μg/ml), leupeptin (1 μg/ml), and aprotinin (1 μg/ml). Protein lysates were placed in ice for 30 min, vortexed every 10 min, and then cleared by centrifugation at 12,000 × *g* for 20 min at 4 C. The supernatants were retrieved and frozen at −80 C until use in immunoblot, coimmunoprecipitation, and degradation assays. The protein concentration was measured using the Bio-Rad protein assay kit (Bio-Rad Laboratories, Inc. Hercules, CA).

Western Blot Analysis

Protein lysates (100 μg from each sample) were resolved by size on 12% or 16% SDS-polyacrylamide gels and transferred onto nitrocellulose membranes (Protran, Schleicher & Schuell, Inc., Keene, NH), which were stained with Ponceau S (Sigma) to examine the equal protein sample loading and transferring (data not shown). The membranes were blocked with 5% nonfat dry milk in Tris-buffered saline [20 mM Tris base (pH 7.6), 150 mM NaCl] containing 0.1% Tween-20 (TBS-T), and probed with the following antibodies: anti-cdk2 (M2) (0.4 μg/ml), anti-cdk4 (C-22) (0.4 μg/ml), anti-cdk6 (C-21) (0.4 μg/ml), anticyclin E (M-20) (0.4 μg/ml), anti-p21 (C-19) (0.4 μg/ml), anti-skp2 (H-435) (0.4 μg/ml) (Santa Cruz Biotechnology, Inc., Santa Cruz, CA), anti-AR (PG-21) (1.5 μg/ml) (Upstate Biotechnology, Inc., Lake Placid, NY), anticyclin D1 (CC12) (0.8 μg/ml) (Calbiochem, Cambridge, MA), anti-p27 (0.1 μg/ml) (Transduction Laboratories, Inc., Lexington, KY) and antiprobasin (1:3,000) (56) (kind gift of Dr. Norman Greenberg, Baylor College of Medicine, Houston, TX) antibodies. After washing in TBS-T, membranes were incubated with horseradish peroxidase (HRP)-conjugated secondary antibodies (Bio-Rad Laboratories, Inc. Hercules, CA) and developed using an enhanced chemiluminescence detection system (ECL detection kit; Amersham Pharmacia Biotech, Arlington Heights, IL) according to the instructions of the manufacturer. Membranes were exposed to X-Omat AR film (Eastman Kodak Co., Rochester, NY). The immunoblots were quantitated by densitometric analysis using ImageQuant software (Molecular Dynamics, Inc., Sunnyvale, CA).

Coimmunoprecipitation Assay

To study the association of p27 with cdk2/cyclin complexes, lysates containing 500 μg of total proteins normalized to a 1 ml volume in lysis buffer were precleared by incubation with 100 μl of a 1:1 (vol/vol) slurry of protein A-sepharose beads (Sigma) for 45 min on a rotator at 4 C. Protein complexes were immunoprecipitated from the precleared lysates by addition of 1.5 μg of anti-cdk2 antibodies overnight at 4 C with constant rotation, followed by the addition of 50 μl of a 50% slurry of beads for 45 min at 4 C with mild agitation. After three washes with 1 ml cold lysis buffer, pelleted beads were quenched in 20 μl of 2× Laemmli sample buffer and boiled. The mixtures were spun down at 10,000 × *g* for 30 sec and 20 μl of each supernatant were retrieved and analyzed by immunoblot using anti-p27 antibody as described above. The filters were subsequently stripped and reprobed with an anti-cdk2 antibody to examine the amount of immunoprecipitated cdk2 in the different samples tested. Immunoprecipitations with 1.5 μg of rabbit IgG (Vector Laboratories, Inc. Burlingame, CA) instead of anti-cdk2 antibodies were used as negative control experiments.

Degradation Assay

Degradation assay experiments were performed as previously described (36, 57, 75) with minor modifications. Three hundred nanograms of human hexahistidine(his_6)-tagged p27 and p21 proteins (bacterially expressed and purified as in Ref. 36) were incubated at 37 C for 0, 1, 4, and 15 h in 60 μl of degradation mix containing 100 μg of protein homogenates, 50 mM Tris-HCl, pH 8.0, 5 mM $MgCl_2$, 1 mM dithiothreitol, 2 mM ATP, 60 μg/ml creatine phosphokinase, 10 mM creatine phosphate, and 5 μM ubiquitin. The reactions were carried out in a PCR instrument and stopped at the different time points by addition of 2× Laemmli sample buffer. The degradation of his_6-tagged p27 and p21 proteins by the rat VP protein lysates was analyzed by immunoblotting with an antihistidine monoclonal antibody (0.1 μg/ml) (QIAGEN, Valencia, CA), as detailed above. To ensure that endogenous p27 present in the VP lysates was not significantly competing

for proteasome degradation with his_6-tagged p27, we had previously checked by Western blot using an anti-p27 antibody that the amount of exogenous p27 added to the degradation mixtures was in large excess to that of endogenous p27 (data not shown). Control degradation experiments included the omission of the his_6-tagged protein as well as the omission of the lysate from the degradation mix. To demonstrate that p27 degradation activity was dependent on the proteasome proteolytic activity of the lysates, degradation assays were performed, in which either the proteasome inhibitor MG-132 (carbobenzoxyl-L-leucyl-L-leucyl-L-leucinal, Calbiochem-Novabiochem Corp., La Jolla, CA) dissolved in dimethylsulfoxide (DMSO) (100 μM final concentration) or DMSO alone was added to the degradation mixture. Quantification of degradation activity was done by densitometric analysis of the bands of slowest electrophoretic migration, *in extenso* the bands at ±22 kDa and ±28 kDa corresponding to undegraded his_6-tagged p21 and p27 proteins, respectively. Relative degradation activity of the samples at each time point after TP injections was then calculated by dividing the densitometric assessment of the band intensity obtained without incubation (0 h) by the one obtained after 4 h of incubation in the degradation mix.

Real-Time RT-PCR (Taqman RT-PCR)

Reverse Transcription. For cDNA synthesis, 1 μg of total RNA was reverse-transcribed in a 20 μl reaction mixture containing 250 μM of each deoxynucleoside triphosphate (dNTP), 20 U of RNase inhibitor, 50 U of MuLV Reverse Transcriptase (RT), 2.5 μM random hexamers, and 1× buffer (1.5 mM $MgCl_2$) (all reagents purchased from PE Applied Biosystems, Foster City, CA). The reaction mix was incubated at 42 C for 45 min and then denatured at 99 C for 5 min. Reactions not containing the RT or omitting the target RNA were used as controls.

Primers and Probes. Specific primers and probes for rat p27 and p21 genes (Table 1) were designed from sequences available in the GenBank database, using the Primer Express 1.0 Software (PE Applied Biosystems). The housekeeping glyceraldehyde-3-phosphate dehydrogenase (GAPDH) gene (Taqman rodent GAPDH control reagents kit, PE Applied Biosystems, Foster City, CA) was used as endogenous control to normalize the amount of p27 and p21 transcripts in each reaction. The choice of this reference gene was guided by results from a previous study showing that GAPDH mRNA levels were not significantly altered in the regenerating prostate of castrated rats treated by TP (12). All sets of primers and probe were selected to work under identical cycling conditions. cDNA amplification products with the different primer pairs had been previously checked to yield a single band of the expected size after electrophoretic migration in a 2% agarose gel stained with ethidium bromide (data not shown). Probes were synthesized by PE Applied Biosystems.

Table 1. Sequences of Primers and Probes Used for Taqman PCR Experiments

Oligonucleotide Name	Sequence
p27 Amplicon size: 128 bp	
p27 Forward primer	CCACAGTGCCAGCATTCG
p27 Reverse primer	TGGGTTAGCGGAGCAGTGT
p27 Hybridization probe	AATCTTCTGCCGCAGGTCGCTTCC
p21 Amplicon size: 124 bp	
p21 Forward primer	AGCAGTTGAGCCGCGATT
p21 Reverse primer	CGAACACGCTCCCAGACG
p21 Hybridization probe	CTTTGACTTCGCCACTGAGACGCCA

The rat p27 gene contains an intron (our unpublished data, GenBank Accession no. AF213701). Discrimination between cDNA and genomic DNA was enhanced by use of intron-spanning primers for p27. In addition, the hybridization probes for p27 also spanned an intron to minimize annealing to genomic DNA. No intronic sequence has been reported for the rat p21 gene.

Real-Time PCR. Taqman PCR was performed on the cDNA samples using an ABI PRISM 7700 Sequence Detector (PE Applied Biosystems). The Taqman PCR Core Reagent kit (PE Applied Biosystems) was used according to the manufacturer's directions with the following modifications: dUTP was replaced by dTTP at the same concentration, and incubation with AmpErase was omitted. For each sample tested, PCR reaction was carried out in a 50 μl volume containing 1 μl of cDNA reaction (equivalent to 50 ng of template RNA) and 2.5 U of AmpliTaq Gold (PE Applied Biosystems). Oligonucleotide primers and fluorogenic probes were added to a final concentration of 100 nM each. After activation of AmpliTaq Gold for 10 min at 94 C, the amplification step consisted of 60 cycles of 94 C for 45 sec, 58 C for 45 sec, and 64 C for 1 min.

In each experiment, seven additional reactions with serial dilutions (500× magnitude) of intact VP cDNA as template were performed with each set of primers and probe in the same 96-well plate to generate standard curves relating the threshold cycle (C_T) to the log input amount of template. All samples were run in triplicate. The relative amounts of p27 and p21 transcripts in each sample were determined using the standard curve method and were normalized to GAPDH mRNA expression levels, as described in detail in ABI PRISM Sequence Detection System User Bulletin 2 (PE Applied Biosystems) and elsewhere (76).

Immunohistochemistry and Immunofluorescence

Antibodies and Immunodetection of p63, p27, and BrdU. Immunostaining experiments for p27 and BrdU were performed in all paraffin-embedded VP tissue specimens with anti-p63 (4A4, gift of Frank McKeon, Harvard Medical School), anti-p27 (Transduction Laboratories, Inc., Lexington, KY), and anti-BrdU monoclonal antibodies (Becton Dickinson and Co., Mansfield, MA), respectively. Double immunofluorescence staining for p27 and BrdU was performed in the paraffin-embedded VP specimens from seven castrated rats that had been killed at 72 h of TP treatment.

Five-micrometer sections were deparaffinized in xylene, and then rehydrated and subjected to microwaving in 10 mM citrate buffer, pH 6.0 (BioGenex Laboratories, Inc. San Ramon, CA) in a 750 W oven for 15 min. Slides were allowed to cool at room temperature for 30 min. Immunohistochemistry was performed by an automated processor (Optimax Plus 2.0 bc, BioGenex Laboratories, Inc. San Ramon, CA). After quenching of the endogenous peroxidase activity with 3% hydrogen peroxide in methanol for 10 min, slides were incubated for 10 min with a buffered casein solution (Power Block Reagent, BioGenex Laboratories, Inc.) to block the nonspecific binding sites. Antibodies (anti-p63, 1:50 dilution, anti-p27, 1:3,000 dilution; anti-BrdU, 1:100 dilution) were applied at room temperature for 2 h in the automated stainer. Detection steps were performed by the instrument utilizing the MultiLink-HRP kit (BioGenex Laboratories, Inc.). Standardized development times with the chromogenic substrate [3,3′-diaminobenzidine tetrahydrochloride (DAB) (for anti-p27 staining) ± nickel chloride (DAB-NC) (for anti-BrdU staining)] allowed accurate comparison of all samples. Sections were counterstained with hematoxylin, rehydrated, and mounted for microscopic examination.

For double immunofluorescence staining experiments, antigen retrieval and blocking steps were performed as described above. Anti-p27 antibody (dilution 1:100) was applied at room temperature for 1 h. Sections were then incubated with secondary biotinylated antibody (MultiLink, BioGenex

Laboratories, Inc.), followed by detection with fluorescein isothiocyanate (FITC)-conjugated streptavidin (Vector Laboratories, Inc. Burlingame, CA). Sections were then blocked with, successively, FITC-conjugated antimouse immunoglobulin antibody (Vector Laboratories, Inc.), a blocking solution (Power Block, BioGenex Laboratories, Inc.), avidin, and biotin (both from BioGenex Laboratories, Inc.), for 10 min each. Subsequently, anti-BrdU antibody (dilution 1:10) was applied for 1 h at room temperature. Then, sections were incubated with a secondary antibody (MultiLink, BioGenex Laboratories, Inc.) and detection was performed by addition of Texas red-conjugated streptavidin (Vector Laboratories, Inc.). Slides were mounted with an antifading fluorescent medium for microscopic examination and photomicrography under an BX50 microscope (Olympus Corp., Lake Success, NY) equipped with appropriate filters.

Substitution of the primary antibodies with PBS served as negative staining control. For p27, strong immunoreactivity in small lymphocytes, which invariably infiltrated the prostate stroma, was used as an internal positive control.

Evaluation of Immunohistochemical Staining. The percentage of BrdU-positive epithelial cells in each VP was calculated by dividing the number of epithelial cells with BrdU-positive nucleus by the total number of epithelial cells counted (~1000 cells). BrdU counts were done separately in basal cells and secretory cells from the VP of castrated rats treated by TP for 72 h. Scoring of p27 immunostaining was done according to the percentage of epithelial cells (~500 cells counted) exhibiting detectable nuclear anti-p27 reactivity, as previously described (57, 77). p27 scores were determined in the basal and secretory cell subsets separately in all VP specimens. The distinction between basal and secretory cells was done according to the location and morphology of the nucleus of these epithelial cells, as determined by microscopic examination of both hematoxylin-eosin-stained and anti-p27 immunostained sections. In addition, to confirm the morphological assessment of basal cells, immunohistochemistry for the prostate basal cell marker p63 was performed in serial sections from each VP, as previously detailed (78). All scoring values are expressed as the mean ± SE for each group of seven rats.

Statistical Analysis

The paired *t* test was used to assess whether there were significant differences in p27 expression (percentage of positive cells) between basal and secretory cells within the same VP specimen at each time point of TP treatment. The same test was performed to examine the statistical significance of differences in the percentages of BrdU-positive cells between the basal and secretory compartments in the VP of rats treated by TP for 72 h. The unpaired *t* test was used to determine whether there were significant differences in the percentages of p27-positive basal or secretory cells between rats treated by TP for different times. The tests were two-tailed and $P < 0.05$ was considered statistically significant. The analyses were performed with a statistics software package (Statview 4.02, Abacus Concepts Inc., Berkeley, CA).

Acknowledgments

The authors thank William Sellers, Myles Brown, and Michele Pagano for critical review of the manuscript and Jane Hayward for assistance with photography.

Received July 14, 2000. Re-revision received February 12, 2001. Accepted February 16, 2001.

Address requests for reprints to: Massimo Loda, M.D., Department of Adult Oncology, Dana Building 740B, Dana-Farber Cancer Institute, 44 Binney Street, Boston, Massachusetts 02115. E-mail: Massimo_Loda@dfci.harvard.edu.

This work was supported by Department of Defense Grant PC970273 and National Cancer Institute Grant 5RO1CA-81755–03 (to M.L.) and by the National Fund for Scientific Research (Belgium), and the Léon Frédérick Foundation (Liège, Belgium) (to D.W.).

REFERENCES

1. Cunha GR, Donjacour AA, Cooke PS, Mee S, Bigsby RM, Higgins SJ, Sugimura Y 1987 The endocrinology and developmental biology of the prostate. Endocr Rev 8:338–362
2. Evans GS, Chandler JA 1987 Cell proliferation studies in the rat prostate. I. The proliferative role of basal and secretory cells during normal growth. Prostate 10: 163–178
3. English HF, Santen RJ, Isaacs JT 1987 Response of glandular versus basal rat ventral prostatic epithelial cells to androgen withdrawal and replacement. Prostate 11: 229–242
4. Isaacs JT, Lundmo PI, Berges R, Martikainen P, Kyprianou N, English HF 1992 Androgen regulation of programmed death of normal and malignant prostatic cells. J Androl 13:457–464
5. Bruchovsky N, Lesser B, Van Dorne E, Craven S 1975 Hormonal effects on cell proliferation in rat prostate. Vitam Horm 33:61–102
6. Ho SM, Damassa D, Kwan PW, Seto HS, Leav I 1985 Androgen receptor levels and androgen contents in the prostate lobes of intact and testosterone-treated Noble rats. J Androl 6:279–290
7. Chen Y, Robles AI, Martinez LA, Liu F, Gimenez-Conti IB, Conti CJ 1996 Expression of G1 cyclins, cyclin-dependent kinases, and cyclin-dependent kinase inhibitors in androgen-induced prostate proliferation in castrated rats. Cell Growth Differ 7:1571–1578
8. Leav I, Merk FB, Kwan PW, Ho SM 1989 Androgen-supported estrogen-enhanced epithelial proliferation in the prostates of intact Noble rats. Prostate 15:23–40
9. Wang X, Hsieh JT 1994 Androgen repression of cytokeratin gene expression during rat prostate differentiation: evidence for an epithelial stem cell-associated marker. Chin Med Sci J 9:237–241
10. English HF, Drago JR, Santen RJ 1985 Cellular response to androgen depletion and repletion in the rat ventral prostate: autoradiography and morphometric analysis. Prostate 7:41–51
11. Katz AE, Benson MC, Wise GJ, Olsson CA, Bandyk MG, Sawczuk IS, Tomashefsky P, Buttyan R 1989 Gene activity during the early phase of androgen-stimulated rat prostate regrowth. Cancer Res 49:5889–5894
12. Epner DE, Partin AW, Schalken JA, Isaacs JT, Coffey DS 1993 Association of glyceraldehyde-3-phosphate dehydrogenase expression with cell motility and metastatic potential of rat prostatic adenocarcinoma. Cancer Res 53:1995–1997
13. Morgan DO 1997 Cyclin-dependent kinases: engines, clocks, and microprocessors. Annu Rev Dev Biol 13: 261–291
14. Sherr CJ 1996 Cancer cell cycles. Science 274:1672–1677
15. Elledge SJ 1996 Cell cycle checkpoints: preventing an identity crisis. Science 274:1664–1671
16. DelSal G, Loda M, Pagano M 1996 Cell cycle and cancer: critical events at the G1 restriction point. Crit Rev Oncog 7:127–142
17. Sherr CJ, Roberts JM 1999 CDK inhibitors: positive and negative regulators of G1-phase progression. Genes Dev 13:1501–1512
18. Hengst L, Reed SI 1998 Inhibitors of the Cip/Kip family. Curr Top Microbiol Immunol 227:25–41

19. Polyak K, Kato JY, Solomon MJ, Sherr CJ, Massague J, Roberts JM, Koff A. p27, a cyclin- 1994 Cdk inhibitor, links transforming growth factor-β and contact inhibition to cell cycle arrest. Genes Dev 8:9–22
20. Polyak K, Lee M-H, Erdjument-Bromage A, Koff A, Roberts JM, Tempst P, Massague J 1994 Cloning of p27, a cyclin-dependent kinase inhibitor and a potential mediator of extracellular antimitogenic signals. Cell 78:59–66
21. Toyoshima H, Hunter T 1994 p27, a novel inhibitor of G1 cyclin-Cdk protein kinase activity, is related to p21. Cell 78:67–74
22. Fang F, Orend G, Watanabe N, Hunter T, Ruoslahti E 1996 Dependence of cyclin E-CDK2 kinase activity on cell anchorage. Science 271:499–502
23. Kato J, Matsuoka M, Polyak K, Massague J, Sherr CJ 1994 Cyclic AMP-induced G1 phase arrest mediated by an inhibitor (p27) of cyclin-dependent kinase 4 activation. Cell 79:487–496
24. Kuniyasu H, Yasui W, Kitahara K, Naka K, Yokozaki H, Akama Y, Hamamoto T, Tahara H, Tahara E 1997 Growth inhibitory effect of interferon-β is associated with the induction of cyclin-dependent kinase inhibitor p27 in a human gastric carcinoma cell line. Cell Growth Differ 8:47–52
25. Harvat BL, Seth P, Jetten AM 1997 The role of p27 in γ-interferon-mediated growth arrest of mammary epithelial cells and related defects in mammary carcinoma cells. Oncogene 14:2111–2122
26. Kortylewski M, Heinrich PC, Mackiewicz A, Schniertshauer U, Klingmuller U, Nakajima K, Hirano T, Horn F, Behrmann I 1999 Interleukin-6 and oncostatin M-induced growth inhibition of human A375 melanoma cells is STAT-dependent and involves upregulation of the cyclin-dependent kinase inhibitor p27/KIP1. Oncogene 18:3742–3753
27. Nourse J, Firpo E, Flanagan WM, Coats S, Polyak K, Lee MH, Massague J, Crabtree GR, Roberts JM 1994 Interleukin-2-mediated elimination of the p27 cyclin-dependent kinase inhibitor prevented by rapamycin. Nature 372:570–573
28. Coats S, Flanagan WM, Nourse J, Roberts JM 1996 Requirement of p27 for restriction point control of the fibroblast cell cycle. Science 272:877–880
29. Rivard N, L'Alleimain G, Bartek J, Pouyssegur J 1996 Abrogation of p27 by cDNA antisense suppresses quiescence (G0 state) in fibroblasts. J Biol Chem 271: 18337–18341
30. Sheaff RJ, Groudine M, Gordon M, Roberts JM, Clurman BE 1997 Cyclin E-CDK2 is a regulator of p27. Genes Dev 11:1464–1478
31. Montagnoli A, Fiore F, Eytan E, Carrano AC, Draetta GF, Hershko A, Pagano M 1999 Ubiquitination of p27 is regulated by Cdk-dependent phosphorylation and trimeric complex formation. Genes Dev 13:1181–1189
32. Nguyen H, Gitig DM, Koff A 1999 Cell-free degradation of p27(kip1), a G1 cyclin-dependent kinase inhibitor, is dependent on CDK2 activity and the proteasome. Mol Cell Biol 19:1190–1201
33. Vlach J, Hennecke S, Amati B 1997 Phosphorylation-dependent degradation of the cyclin-dependent kinase inhibitor p27. EMBO J 16:5334–5344
34. Carrano AC, Eytan E, Hershko A, Pagano M 1999 SKP2 is required for ubiquitin-mediated degradation of the CDK inhibitor p27. Nat Cell Biol 1:193–199
35. Tsvetkov LM, Yeh KH, Lee SJ, Sun H, Zhang H 1999 p27(Kip1) ubiquitination and degradation is regulated by the SCF(Skp2) complex through phosphorylated Thr187 in p27. Curr Biol 9:661–664
36. Pagano M, Tam SW, Theodoras AM, Beer-Romero P, Del Sal G, Chau V, Yew PR, Draetta GF, Rolfe M 1995 Role of the ubiquitin-proteasome pathway in regulating abundance of the cyclin-dependent kinase inhibitor p27. Science 269:682–685
37. Medema RH, Kops GJ, Bos JL, Burgering BM 2000 AFX-like Forkhead transcription factors mediate cell-cycle regulation by Ras and PKB through p27. Nature 404:782–787
38. Menjo M, Kaneko Y, Ogata E, Ikeda K, Nakanishi M 1998 Critical role for p27 in cell cycle arrest after androgen depletion in mouse mammary carcinoma cells (SC-3). Oncogene 17:2619–2627
39. Cordon-Cardo C, Koff A, Drobnjak M, Capodieci P, Osman I, Millard SS, Gaudin PB, Fazzari M, Zhang ZF, Massague J, Scher HI 1998 Distinct altered patterns of p27 gene expression in benign prostatic hyperplasia and prostatic carcinoma. J Natl Cancer Inst 90:1284–1291
40. Millard SS, Yan JS, Nguyen H, Pagano M, Kiyokawa H, Koff A 1997 Enhanced ribosomal association of p27(Kip1) mRNA is a mechanism contributing to accumulation during growth arrest. J Biol Chem 272: 7093–7098
41. Hengst L, Reed SI 1996 Translational control of p27 accumulation during the cell cycle. Science 271: 1861–1864
42. Fero ML, Rivkin M, Tasch M, Porter P, Carow CE, Firpo E, Polyak K, Tsai LH, Broudy V, Perlmutter RM, Kaushansky K, Roberts JM 1996 A syndrome of multiorgan hyperplasia with features of gigantism, tumorigenesis, and female sterility in p27(Kip1)-deficient mice. Cell 85: 733–744
43. Kiyokawa H, Kineman RD, Manova-Todorova KO, Soares VC, Hoffman ES, Ono M, Khanam D, Hayday AC, Frohman LA, Koff A 1996 Enhanced growth of mice lacking the cyclin-dependent kinase inhibitor function of p27(Kip1). Cell 85:721–732
44. Nakayama K, Ishida N, Shirane M, Inomata A, Inoue T, Shishido N, Horii I, Loh DY 1996 Mice lacking p27(Kip1) display increased body size, multiple organ hyperplasia, retinal dysplasia, and pituitary tumors. Cell 85:707–720
45. Tong W, Kiyokawa H, Soots TJ, Park MS, Soares VC, Manova K, Pollard JW, Koff A 1998 The absence of p27, an inhibitor of G1 cyclin-dependent kinases, uncouples differentiation and growth arrest during the granulosa-luteal transition. Cell Growth Differ 9:787–794
46. Robker RL, Richards JS 1998 Hormone-induced proliferation and differentiation of granulosa cells: a coordinated balance of the cell cycle regulators cyclin D2 and p27. Mol Endocrinol 12:924–940
47. Casaccia-Bonnefil P, Tikoo R, Kiyokawa H, Friedrich V, Chao MV, Koff A 1997 Oligodendrocyte precursor differentiation is perturbed in the absence of the cyclin-dependent kinase inhibitor p27. Genes Dev 11: 2335–2346
48. Drissi H, Hushka D, Aslam F, Nguyen Q, Buffone E, Koff A, van Wijnen A, Lian JB, Stein JL, Stein GS 1999 The cell cycle regulator p27 contributes to growth and differentiation of osteoblasts. Cancer Res 59:3705–3711
49. Sgambato A, Cittadini A, Faraglia B, Weinstein IB 2000 Multiple functions of p27(Kip1) and its alterations in tumor cells: a review. J Cell Physiol 183:18–27
50. Mori S, Murakami-Mori K, Bonavida B 1999 Interleukin-6 induces G1 arrest through induction of p27(Kip1), a cyclin-dependent kinase inhibitor, and neuron-like morphology in LNCaP prostate tumor cells. Biochem Biophys Res Commun 257:609–614
51. Zi X, Agarwal R 1999 Silibinin decreases prostate-specific antigen with cell growth inhibition via G1 arrest, leading to differentiation of prostate carcinoma cells: implications for prostate cancer intervention. Proc Natl Acad Sci USA 96:7490–7495
52. De Marzo AM, Meeker AK, Epstein JI, Coffey DS 1998 Prostate stem cell compartments: expression of the cell cycle inhibitor p27 in normal, hyperplastic, and neoplastic cells. Am J Pathol 153:911–919
53. Tsihlias J, Zhang W, Bhattacharya N, Flanagan M, Klotz L, Slingerland J 2000 Involvement of p27 in G1 arrest by

high dose 5 α-dihydrotestosterone in LNCaP human prostate cancer cells. Oncogene 19:670–679
54. Kokontis JM, Hay N, Liao S 1998 Progression of LNCaP prostate tumor cells during androgen deprivation: hormone-independent growth, repression of proliferation by androgen, and role for p27 in androgen-induced cell cycle arrest. Mol Endocrinol 12:941–953
55. Agus DB, Cordon-Cardo C, Fox W, Drobnjak M, Koff A, Golde DW, Scher HI 1999 Prostate cancer cell cycle regulators: response to androgen withdrawal and development of androgen independence. J Natl Cancer Inst 91:1869–1876
56. Johnson MA, Hernandez I, Wei Y, Greenberg N 2000 Isolation and characterization of mouse probasin: an androgen-regulated protein specifically expressed in the differentiated prostate. Prostate 43:255–262
57. Loda M, Cukor B, Tam SW, Lavin P, Fiorentino M, Draetta GF, Jessup JM, Pagano M 1997 Increased proteasome-dependent degradation of the cyclin-dependent kinase inhibitor p27 in aggressive colorectal carcinomas. Nat Med 3:231–234
58. Maki CG, Howley PM 1997 Ubiquitination of p53 and p21 is differentially affected by ionizing and UV radiation. Mol Cell Biol 17:355–363
59. Maki CG, Huibregtse JM, Howley PM 1996 *In vivo* ubiquitination and proteasome-mediated degradation of p53. Cancer Res 56:2649–2654
60. Yu ZK, Gervais JL, Zhang H 1998 Human CUL-1 associates with the SKP1/SKP2 complex and regulates p21(CIP1/WAF1) and cyclin D proteins. Proc Natl Acad Sci USA 95:11324–11329
61. Blagosklonny MV, Wu GS, Omura S, el-Deiry WS 1996 Proteosome-dependent regulation of p21/CIP1 expression. Biochem Biophys Res Commun 227:564–569
62. Chung LWK, Coffey DS 1971 Biochemical characterization of prostatic nuclei. II. Relationship between DNA synthesis and protein synthesis. Biochim Biophys Acta 247:584
63. Furuya Y, Lin XS, Walsh JC, Nelson WG, Isaacs JT 1995 Androgen ablation-induced programmed death of prostatic glandular cells does not involve recruitment into a defective cell cycle or p53 induction. Endocrinology 136: 1898–1906
64. Evans GS, Chandler JA 1987 Cell proliferation studies in the rat prostate. II. The effects of castration and androgen-induced regeneration upon basal and secretory cell proliferation. Prostate 11:339–352
65. Guo Y, Sklar GN, Borkowski A, Kyprianou N 1997 Loss of the cyclin-dependent kinase inhibitor p27(kip1) protein in human prostate cancer correlates with tumor grade. Clin Cancer Res 3:2269–2274
66. Durand B, Gao FB, Raff M 1997 Accumulation of the p27/KIP1 cyclin-dependent kinase inhibitor and the timing of oligodendrocyte differentiation. EMBO J 16: 306–317
67. Hiromura K, Fero ML, Roberts JM, Shankland SJ 1999 Modulation of apoptosis by the cyclin-dependent kinase inhibitor p27. J Clin Invest 103:597–604
68. Ophascharoensuk V, Fero ML, Hughes J, Roberts JM, Shankland SJ 1998 The cyclin dependent kinase inhibitor p27 safeguards against inflammatory injury. Nat Med 4:575–580
69. Eymin B, Haugg M, Droin N, Sordet O, Dimanche-Boitrel M-T, Solary E 1999 p27 induces drug resistance by preventing apoptosis upstream of cytochrome c release and procaspase-3 activation in leukemic cells. Oncogene 18: 1411–1418
70. Minami S, Ohtani-Fujita N, Igata E, Tamaki T, Sakai T 1997 Molecular cloning and characterization of the human p27 gene promoter. FEBS Lett 411:1–6
71. Sutterluty H, Chatelain E, Marti A, Wirbelauer C, Senften M, Muller U, Krek W 1999 skp2 promotes p27 degradation and induces S phase in quiescent cells. Nat Cell Biol 1:207–14
72. Wirbelauer C, Sutterluty H, Blondel M, Gstaiger M, Peter M, Reymond F, Krek W 2000 The F-box protein skp2 is a ubiquitylation target of a Cul1-based core ubiquitin ligase complex: evidence for a role of cul1 in the suppression of skp2 expression in quiescent fibroblasts. EMBO J 19:5362–75
73. Zhang H, Kobayashi R, Galaktionov K, Beach D 1995 p19Skp1 and p45Skp2 are essential elements of the cyclin A-CDK2 S phase kinase. Cell 82:915–925
74. Lu S, Liu M, Epner DE, Tsai SY, Tsai MJ 1999 Androgen regulation of the cyclin-dependent kinase inhibitor p21 gene through an androgen response element in the proximal promoter. Mol Endocrinol 13:376–384
75. Chiarle R, Budel LM, Skolnik J, Frizzera G, Chilosi M, Corato A, Pizzolo G, Magidson J, Montagnoli A, Pagano M, Maes B, De Wolf-Peeters C, Inghirami G 2000 Increased proteasome degradation of cyclin-dependent kinase inhibitor p27 is associated with a decreased overall survival in mantle cell lymphoma. Blood 95:619–626
76. Fink L, Seeger W, Ermert L, Hanze J, Stahl U, Grimminger F, Kummer W, Bohle RM 1998 Real-time quantitative RT-PCR after laser-assisted cell picking. Nat Med 4:1329–1333
77. Thomas GV, Szigeti K, Murphy M, Draetta G, Pagano M, Loda M 1998 Down-regulation of p27 is associated with development of colorectal adenocarcinoma metastases. Am J Pathol 153:681–687
78. Signoretti S, Waltregny D, Dilks J, Isaac B, Lin D, Garraway L, Yang A, McKeon F, Loda M 2000 p63 is a prostate basal cell marker and is required for prostate development. Am J Pathol 157:1769–75

Her-2-neu Expression and Progression Toward Androgen Independence in Human Prostate Cancer

Sabina Signoretti, Rodolfo Montironi, Judith Manola, Annalisa Altimari, Carmen Tam, Glenn Bubley, Steven Balk, George Thomas, Irving Kaplan, Lynn Hlatky, Philip Hahnfeldt, Philip Kantoff, Massimo Loda

Background: **Human prostate cancers are initially androgen dependent but ultimately become androgen independent. Overexpression of the Her-2-neu receptor tyrosine kinase has been associated with the progression to androgen independence in prostate cancer cells. We examined the expression of Her-2-neu in normal and cancerous prostate tissues to assess its role in the progression to androgen independence.** ***Methods:*** **Prostate cancer tissue sections were obtained from 67 patients treated by surgery alone (UNT tumors), 34 patients treated with total androgen ablation therapy before surgery (TAA tumors), and 18 patients in whom total androgen ablation therapy failed and who developed bone metastases (androgen-independent [AI] disease). The sections were immunostained for Her-2-neu, androgen receptor (AR), prostate-specific antigen (PSA), and Ki-67 (a marker of cell proliferation) protein expression. Messenger RNA (mRNA) levels and gene amplification of Her-2-neu were examined by RNA *in situ* hybridization and fluorescent *in situ* hybridization(FISH), respectively, in a subset of 27 tumors (nine UNT, 11 TAA, and seven AI). All statistical tests were two-sided.** ***Results:*** **Her-2-neu protein expression was statistically significantly higher in TAA tumors than in UNT tumors with the use of two different scoring methods (P = .008 and P = .002). The proportion of Her-2-neu-positive tumors increased from the UNT group (17 of 67) to the TAA group (20 of 34) to the AI group (14 of 18) (P<.001). When compared with UNT tumors, tumor cell proliferation was higher in AI tumors (P = .014) and lower in TAA tumors (P<.001). All tumors expressed AR and PSA proteins. Although Her-2-neu mRNA expression was high in TAA and AI tumors, no Her-2-neu gene amplification was detected by FISH in any of the tumor types.** ***Conclusions:*** **Her-2-neu expression appears to increase with progression to androgen independence. Thus, therapeutic targeting of this tyrosine kinase in prostate cancer may be warranted.** **[J Natl Cancer Inst 2000;92:1918–25]**

Her-2-neu is a receptor tyrosine kinase that belongs to the epidermal growth factor receptor family. Her-2-neu overexpression, which is seen in 20%–30% of breast and ovarian cancers, results from gene amplification and is associated with poor prognosis *(1–4)*. Recently, Her-2-neu has become a therapeutic target in breast cancer with the advent of antibodies generated against its extracellular domain *(5)*. In breast cancer clinical trials, one such antibody, trastuzumab (Herceptin; Genentech Inc., South San Francisco, CA), has been shown to be effective when coadministered with other chemotherapeutic agents *(6,7)*

In prostate cancer, the assessment of Her-2-neu overexpression has been more problematic, and the results are controversial *(8–19)*. The controversy is due both to procedural differences, including variability of tissue fixation protocols and use of antibodies from different sources, and to biologic differences, including the heterogeneity of prostate cancers. Also, contradictory results about whether the gene is amplified have been reported from fluorescent *in situ* hybridization (FISH) analysis of the Her-2-neu locus in both primary and metastatic prostate cancers *(20–25)*.

Although unequivocal evidence of Her-2-neu overexpression in human prostate cancer has not been available, evidence suggests that Her-2-neu may be important in prostate cancer progression. First, in the severe combined immunodeficient (SCID) mouse human prostate cancer xenograft LAPC (i.e., Los Angeles Prostate Cancer), Her-2-neu is overexpressed in androgen-independent sublines (i.e., grown in castrated hosts) compared with parental (androgen-dependent) LAPC cells *(26)*. Second, induced overexpression of Her-2-neu in androgen-dependent prostate cancer cells activates the androgen receptor (AR) in a ligand-independent fashion, conferring androgen-independent growth to these cells *(26)*. Because of these observations and the availability of U.S. Food and Drug Administration (FDA) approval to use therapeutic anti-Her-2-neu antibodies for breast cancer therapy, nonrandomized clinical trials of Herceptin have been started in prostate cancer.

We undertook this study with the following aims: 1) to determine whether Her-2-neu protein is expressed in human prostate cancers; 2) to assess whether Her-2-neu protein expression increases with progression toward androgen independence using two scoring methods; and 3) to address the mechanism of Her-2-neu overexpression by analyzing, in a subset of human prostate tumors, genomic copy number by FISH and messenger RNA (mRNA) levels by *in situ* hybridization (ISH).

Patients and Methods

Patient Population

This study was performed after approval by the Institutional Review Board of the Dana-Farber Cancer Institute and Brigham and Women's Hospital, Boston, MA. Archival paraffin-embedded tissue blocks of prostate cancer from patients treated during the period from 1991 through 1996 were retrieved from the Departments of Pathology from Beth Israel Deaconess Medical Center, Boston, from the University of Ancona, Italy, and from the Uni-

Affiliations of authors: S. Signoretti, M. Loda, Department of Adult Oncology, Dana-Farber Cancer Institute, and Department of Pathology, Brigham and Women's Hospital, Harvard Medical School, Boston, MA; R. Montironi, University of Ancona, Italy; J. Manola (Department of Biostatistics), A. Altimari, C. Tam, L. Hlatky, P. Hahnfeldt, P. Kantoff (Department of Adult Oncology), Dana-Farber Cancer Institute; G. Bubley, S. Balk, I. Kaplan, Departments of Medicine and Radiation Therapy, Beth Israel Deaconess Medical Center, Boston; G. Thomas, Department of Pathology, University of California at Los Angeles.

Correspondence to: Massimo Loda, M.D., Department of Adult Oncology, Dana-Farber Cancer Institute, Dana 740B, 44 Binney St., Boston, MA 02215 (e-mail: massimo_loda@dfci.harvard.edu).

See "Notes" following "References."

versity of California, Los Angeles. Prostate cancer tissue sections were analyzed from three groups of patients: 1) patients who did not receive any treatment before surgery (UNT tumors, from 67 patients), 2) patients who were treated with total androgen ablation for 3 months before surgery (goserelin [Zoladex] depot every 28 days plus bicalutamide [Casodex] at a dose of 50 mg/day for 12 weeks) (TAA tumors, from 34 patients), and 3) patients who developed bone metastases after hormonal therapy failure (androgen-independent [AI] tumors, from 18 patients). Stage *(27)* and Gleason grade *(28)* were available for all primary prostate cancers. Times to prostate-specific antigen (PSA) recurrence and survival times were available for 69 prostatectomy cases (38 UNT and 31 TAA). The median follow-up was 3 years.

Immunohistochemistry

Methodology. Immunostaining was performed on all tissue sections with the use of the following primary antibodies: Her-2-neu (AO485; Dako Corp., Carpinteria, CA) at a 1 : 200 dilution, AR (Upstate Biotechnology, Lake Placid, NY) at a 1 : 50 dilution, PSA (BioGenex, San Ramon, CA) at a 1 : 50 dilution, and Ki-67 (Immunotech, Westbrook, ME) at a 1 : 50 dilution. To accurately identify prostate basal cells, we used the 4A4 antibody, directed against the p63 basal cell marker *(29,30)*, at a 1 : 50 dilution. All antibodies were diluted in phosphate-buffered saline (PBS). The anti-Her-2-neu antibody used in this study is the same as the one that is included in the HercepTest kit (Dako, Inc.) approved by the FDA for the evaluation of Her-2-neu expression in breast carcinomas.

Sections (5 μm thick) were placed on slides, deparaffinized, rehydrated, and microwaved in 10 m*M* citrate buffer (pH 6.0) (BioGenex, San Ramon, CA) at 750 W for 15 minutes for Ki-67 and p63 immunostaining and for 30 minutes for AR immunostaining. For Her-2-neu immunostaining, sections were microwaved at 750 W for 5 minutes and at 375 W for an additional 15 minutes. Slides were cooled at room temperature for 30 minutes. Sections were then incubated for 10 minutes with 10% normal goat serum (Vector Laboratories, Inc., Burlingame, CA) diluted in PBS. The primary antibody was applied at room temperature in an automated stainer (Optimax Plus 2.0 bc; BioGenex). Staining was detected with the use of the MultiLink-HRP kit (BioGenex). Standardized 3,3-diaminobenzidine (DAB) development times allowed accurate comparison of all samples. For p63 immunostaining, nickel chloride was added to the DAB to obtain a black stain. Slides were counterstained with either Meyer's hematoxylin or methyl green.

Paraffin sections of the LNCaP and PC3 prostate cancer cell lines (American Type Culture Collection, Manassas, VA) and of the androgen-independent subline of the LAPC4 xenograft *(26)* (gift of Charles L. Sawyers, University of California, Los Angeles) were used for immunostaining controls and to standardize the Her-2-neu staining expression level (*see below*). Omission of the primary antibody with PBS served as a negative staining control.

Scoring methods. Two pathologists (S. Signoretti and M. Loda) read and scored the slides independently. Scoring was performed by two different methods, a relative scoring system and an absolute scoring system.

In the relative scoring system, the staining intensity of the tumor cells was evaluated in comparison to the staining intensity of the basal cells of the adjacent normal glands (internal positive control). The internal control was used to overcome the potential variability of immunoreactivity among the different tissue specimens. Her-2-neu expression in tumor cells was scored as equal to, higher than, or less than the expression in adjacent basal cells. Only tumor cells expressing Her-2-neu at a level equal to or higher than that in basal cells were scored as positive. The percentage of positive cells was assessed in each tumor section and was used as a continuous variable in the statistical analysis. In addition, a cutoff of 50% Her-2-neu-positive cells was applied to separate high (≥50%) and low (<50%) expressors. Maximally selected chi-square methodology *(31)* was used to demonstrate that 50% was a good cutoff point (data not shown).

Before analyzing the entire series of tumors, we confirmed the validity of the relative scoring system by image analysis in a subset of 20 prostate cancer tissue samples (10 high and 10 low Her-2-neu expressors). Overall, nine were UNT, and 11 were TAA. Densitometric quantitation of antibody staining per cell was done as described previously *(32)*. Selected areas that included both tumor cells and adjacent normal basal cells were acquired with the use of imaging software provided with a Quantimet Q570 computerized imaging/microscopy system (Leica, Northvale, NJ). Because Her-2-neu staining was heterogeneous in each tumor sample, tumor cells analyzed were representative of the predominant population (i.e., expressing more or less Her-2-neu than adjacent basal cells). The staining densities in the tumor and normal areas were calculated for each tumor or normal field by dividing the total integrated optical density (i.e., total staining) in the field by the area of the mask, which is a computer-generated region that precisely demarcates the target cells to be quantified in the field. To confirm that basal cells represented an adequate internal control, we observed no statistical difference in the staining intensity of basal cells in UNT and TAA tumors (Student's t test, $P = .15$). Specifically, the mean staining density for basal cells was 1.35 (95% confidence interval [CI] = 1.17–1.53) in the UNT tumors and 1.19 (95% CI = 1.06–1.33) in the TAA tumors. Subsequently, to assess Her-2-neu expression levels in the tumors, we calculated a staining density ratio between tumor and normal cells for each specimen. There was a statistically significant difference in the staining density ratio distribution between the high and low Her-2-neu expressors ($P<.001$). The staining density ratio ranged from 0.31 to 1.56. To specify a cutoff, we selected a point *a priori* that was two standard deviations above the mean for low expressors (staining density ratio = 0.793). The rationale for selecting this cutoff point was to avoid false negatives; if the low expression levels were normally distributed, only 2.5% of low expressors would have levels higher than this cutpoint. With the use of this cutoff point and the image analysis method, the relative scoring system resulted in one false positive and no false negatives (sensitivity of 100% and specificity of 92%), thus validating the use of this scoring methodology in the analysis of the entire series of tumors.

The absolute scoring method was used to evaluate Her-2-neu expression in tissue sections that lacked the internal basal cell controls, such as bone metastases. Immunostains were evaluated according to the scoring method used for Her-2-neu expression in breast cancer *(33)*. Briefly, tumor sections were considered Her-2-neu positive only if complete weak to moderate (2+) or strong (3+) membrane staining was observed in at least 10% of the tumor cells. We used the cell lines PC3 (2+ in <10% of cells; negative standard) and LNCaP (2+ in >90% of cells; positive standard, weak to moderate intensity) and the xenograft LAPC4 (3+ in >90% of cells; positive standard, strong intensity) as reference standards for the evaluation of Her-2-neu expression in the human tumors (Fig. 1, A).

Scoring AR, PSA, and Ki-67 immunostains. Sections stained for PSA and AR were scored as either positive or negative for PSA and AR expression, respectively. The rates of tumor cell proliferation were calculated as the percentage of nuclei in each section that stained positive for Ki-67. For statistical analyses, the proliferation rate was analyzed as a continuous variable, and a proliferation rate of less than 1% was scored as nonproliferating.

In Situ Hybridization

The subset of 20 tumors previously analyzed by image analysis and seven additional AI metastatic tumor samples were analyzed by ISH to detect Her-2-neu mRNA. To generate the complementary RNA (cRNA) probe for ISH, we used a 5′ 329-base-pair segment of Her-2-neu complementary DNA as template for *in vitro* transcription. ^{35}S-labeled (New England Nuclear, Boston, MA) antisense and sense cRNA probes were *in vitro* transcribed with T7 and T3 RNA polymerase (Promega Corp., Madison, WI), respectively. ISH was performed as described previously *(34)*.

The tumor sections were scored for Her-2-neu mRNA expression in a manner similar to the relative scoring system for immunohistochemistry. Specifically, we determined the number of autoradiographic grains in both normal and tumor cells by counting 100 cells in each subset and obtaining an average number of grains per cell. Her-2-neu mRNA expression in tumor cells was scored as equal to, higher than, or less than Her-2-neu mRNA expression in adjacent basal cells. The percentage of tumor cells expressing Her-2-neu at a level equal to or higher than that in basal cells was assessed for each tumor. High-expressing tumors were defined as those in which more than 50% of the tumor cells expressed Her-2-neu at a level equal to or higher than that in basal cells. Her-2-neu mRNA in AI tumors was simply scored as present or absent.

Fluorescent *In Situ* Hybridization

FISH was performed on the same subset of 27 tumors analyzed by ISH and on the LAPC4 xenograft. Paraffin-embedded tissue sections were deparaffinized and digested with proteinase K to remove proteins that might block access to the DNA target. Target DNA in the tissue sections and the biotinylated DNA HER-2-neu probe (Ventana Medical Systems, Inc., Tucson, AZ) were codenatured at 90 °C for 12 minutes and then hybridized with the probe overnight at 37 °C. Tissue sections were washed with 0.5× standard saline citrate to remove unhybridized probe. The hybridized probe was detected by incubation with fluorescein-labeled avidin

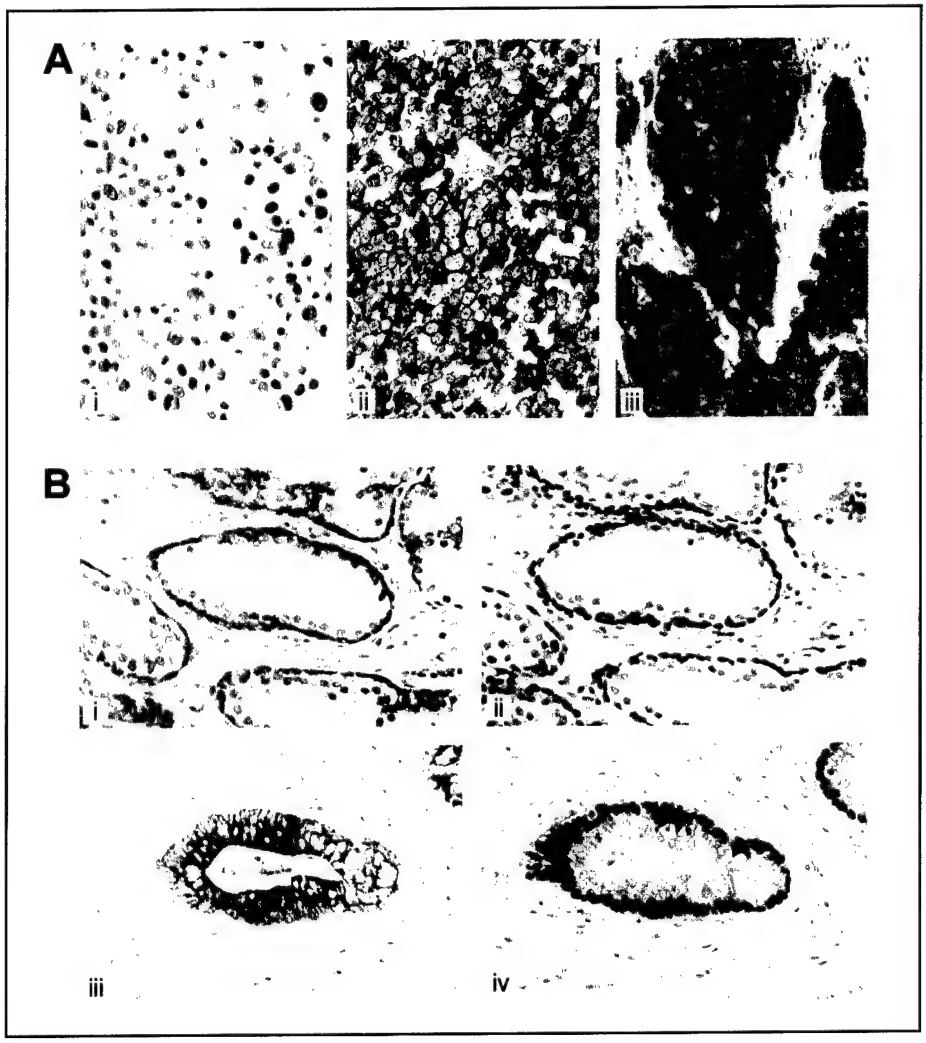

Fig. 1. A) Her-2-neu standards for immunohistochemistry scoring. **i:** Formalin-fixed, paraffin-embedded PC3 prostate carcinoma cells showing complete membrane staining in less than 10% of cells (negative standard) (3,3-diaminobenzidine [DAB] detection with hematoxylin counterstain). Original magnification x400. **ii:** LNCaP prostate carcinoma cells showing crisp 2+ membrane staining in the majority of cells (DAB detection with hematoxylin counterstain). Original magnification x400. **iii:** LAPC4 prostate carcinoma xenograft showing strong (3+) membrane staining in all cells (DAB detection with hematoxylin counterstain). Original magnification x400. **B)** Immunohistochemical staining of normal prostate and prostate from a patient treated by total androgen ablation therapy. **i:** Her-2-neu is expressed in the basal cells of the normal prostate (DAB detection with hematoxylin counterstain). Original magnification x400. **ii:** In a serial section of that analyzed in **i,** basal cells are identified by p63 nuclear staining (DAB-nickel chloride detection with methyl green counterstain). Original magnification x400. **iii:** Her-2-neu is expressed in the basal and secretory cells in the prostate from a patient treated by total androgen ablation therapy (DAB detection with hematoxylin counterstain). Original magnification x400. **iv:** In a serial section of that analyzed in **iii,** basal cells are identified by p63 nuclear staining (DAB-nickel chloride detection with methyl green counterstain). Original magnification x400.

(Ventana Medical Systems, Inc.). Nuclei were counterstained with the DNA-binding dye 2-(4-amidinophenyl)-6-indolecarbamidinedihydrochloride (DAPI) (Ventana Medical Systems, Inc.). Paraffin-embedded breast cancers with and without known Her-2-neu gene amplification were used as positive and negative controls in each experiment.

Sections were examined with an epifluorescence microscope equipped with dual and single filters to detect the fluorescein and DAPI fluorochromes. Two fields of 20 tumor nuclei were evaluated, and the number of HER-2 signals per nucleus was determined. A tumor was considered to be positive for HER-2/neu gene amplification if the average number of signals per nucleus was greater than four.

Statistical Analysis

Student's *t* test was used to compare the percentage of Her-2-neu-positive tumor cells as a continuous variable between TAA and UNT tumors and to compare the staining densities of the basal cells in the two groups of tumors. To validate the relative scoring system using image analysis, we first generated descriptive statistics for the 20 tumors in the validation set. The Wilcoxon rank sum test *(35)* was used to verify differences in staining density ratio obtained in a blinded fashion among cases previously categorized as low and high Her-2-neu expressors. Fisher's exact test *(36)* was used to test for an association between Her-2-neu expression levels (using the 50% cutoff to define low and high expressors) and the treatment status of the tumors (TAA versus UNT) using the relative scoring system. To determine if there were differences in Her-2-neu expression among the three types of tumors (UNT, TAA, and AI) using the absolute scoring system, we compared Her-2-neu expression levels (positive versus negative) in UNT tumors with those in both TAA and AI tumors with the use of Fisher's exact test. Because the same control group was used for both comparisons, a Bonferroni adjustment *(37)* was applied. Thus, a P value of .025 was used to denote statistical significance. Fisher's exact test was also used to test for an association between Her-2-neu expression levels and clinical tumor stage (II versus III or IV). The Jonckheere–Terpstra test *(38)* was used to test for a linear trend for Her-2-neu positivity in the groups of UNT, TAA, and AI tumors. The Wilcoxon rank sum test was used to test for differences in PSA levels between TAA and UNT tumors and to test for differences in Ki-67 immunostaining among UNT, TAA, and AI tumors. Again, the Bonferroni adjustment was applied. The exact test for ordered categorical data described by Mehta et al. *(39)* was used to test for an association between Her-2-neu expression and Gleason grade (Gleason score 4–6 versus 7 versus 8–10) in TAA and UNT tumors. The same test was also used to test for differences in the distribution of clinical tumor stage and Gleason grade between TAA and UNT tumors. Logistic regression was used to test for an association between Her-2-neu positivity and treatment categories (UNT and TAA) controlling for both Gleason grade (4–6 versus 7 versus 8–10) and stage (stage II versus stage III or IV) *(36)*. All statistical tests were two-sided, and a P value of .05 was considered to be statistically significant.

Results

Her-2-neu Protein Expression in Normal and Neoplastic Human Prostates

We first analyzed the expression of Her-2-neu protein in normal prostate tissue adjacent to tumor in the same sections. Her-2-neu expression was universally detected by immunohistochemistry in the basal cells from both UNT and TAA specimens. Thus, we used basal cell Her-2-neu expression as an internal control for the analysis of Her-2-neu expression in the tumor cells. Her-2-neu expression was not detected in secretory cells from UNT tumors. In contrast, Her-2-neu expression, as characterized by diffuse membrane staining, was detected in secretory cells from TAA tumors (Fig. 1, B).

All of the primary prostate cancers expressed Her-2-neu in at least 1% of cells. Variability in Her-2-neu expression was observed both in the intensity of immunostaining and in the percentage of positive tumor cells. With the use of both the relative and the absolute scoring methods, Her-2-neu expression was statistically

significantly higher in TAA than in UNT primary prostate cancers. Specifically, with the use of the relative scoring method, there was a statistically significant difference in the percentage of Her-2-neu-positive cells (continuous variable) between TAA and UNT tumors (P = .008). When the cutoff of 50% was used to categorize high and low expressors, 34 (51%) of 67 UNT cases versus 27 (79%) of 34 TAA cases expressed high Her-2-neu levels (P = .011). With the use of the absolute scoring method, 17 (25%) of 67 UNT cases versus 20 (59%) of 34 TAA cases (P = .002) were scored as positive (Table 1, A and B; Fig. 2).

Because AI tumors lack basal cells in the metastases, we used the absolute scoring method to assess Her-2-neu expression in these tumors. There was a statistically significant higher percentage of Her-2-neu-positive cases (14 [78%] of 18) in AI tumors than in UNT tumors (P<.001) (Table 1, B). Finally, the percentage of Her-2-neu-positive cases showed a statistically significant increase from UNT to TAA to AI tumors (P<.001) (Table 1, B; Fig. 2).

Although Gleason grade is usually overestimated following androgen ablation treatment *(40)*, both UNT and TAA tumors were assigned a Gleason grade to determine if there was an association between Her-2-neu expression and tumor

Table 1. Her-2-neu expression*

A) Relative scoring method

	UNT (n = 67)	TAA (n = 34)	P
Mean percentage of Her-2-neu-positive cells (95% confidence interval)	50.1 (42.3–57.9)	67.7 (57.8–77.5)	Student's t test: P = .008
Percentage of Her-2-neu high expressors, applying a 50% cutoff (95% confidence interval)	51 (39–64)	79 (62–91)	Fisher's exact test: P = .011

B) Absolute scoring method†

	UNT (n = 67)	TAA (n = 34)	AI (n = 18)
Percentage of Her-2-neu-positive cases (95% confidence interval)	25 (16–37)	59 (41–75)	78 (52–94)

*UNT = tumors from patients not treated with total androgen ablation therapy; TAA = tumors from patients treated with total androgen ablation therapy; AI = tumors from patients that failed to respond to total androgen ablation therapy and developed androgen-independent disease metastatic to the bone.

†Fisher's exact test: UNT versus TAA, P = .002; UNT versus AI, P<.001; TAA versus AI, P = .227.

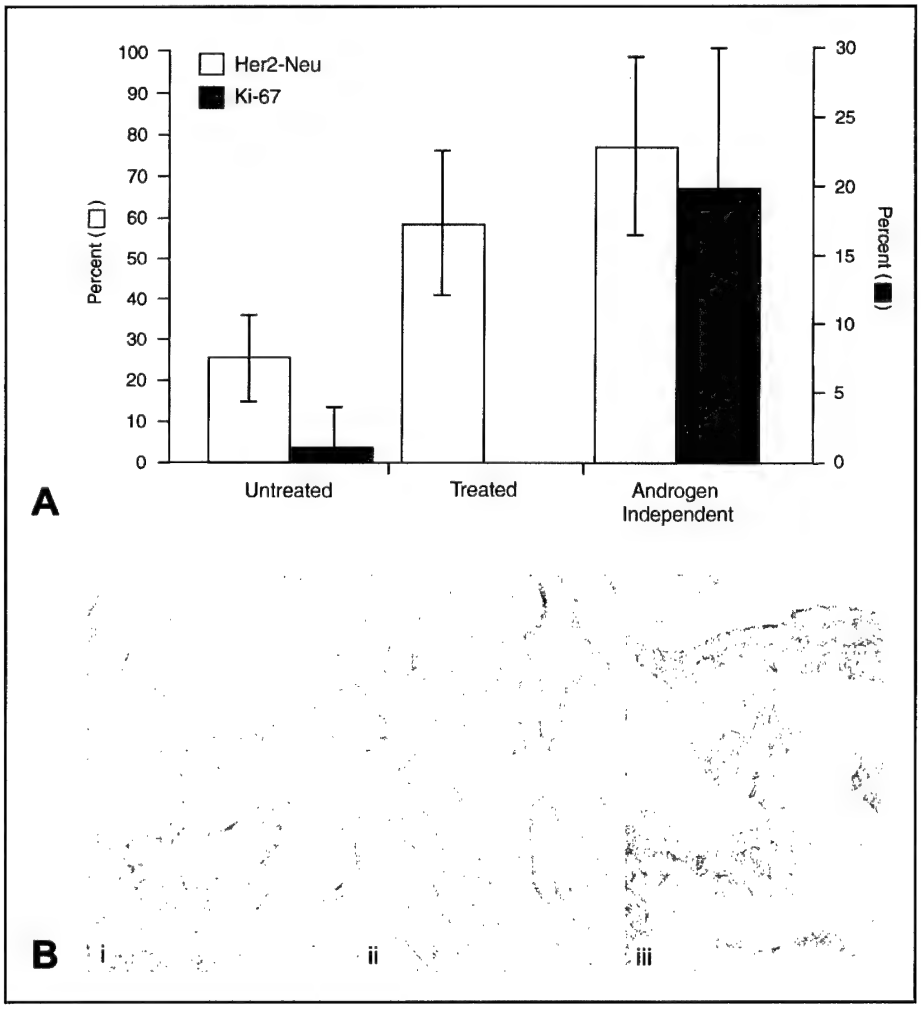

Fig. 2. A) Her-2-neu expression in tumors from patients who were not treated with total androgen ablation therapy (UNT tumors), who received total androgen ablation therapy (TAA tumors), and who had metastatic prostate cancer (androgen-independent [AI] tumors) and its relationship to proliferation rate as assessed by Ki-67 immunostaining. Her-2-neu expression was quantified by the absolute scoring method. Data are expressed as mean percentage of positive cases, with 95% confidence intervals (**open bars, left scale**). Percentage positive Ki-67 staining is expressed as median percentage of positive cases, with interquartile ranges (**solid bars, right scale**). **B**) Her-2-neu immunohistochemical staining in UNT, TAA, and AI prostate cancers. **i:** Her-2-neu negative UNT prostate cancer. Adjacent normal gland shows positive Her-2-neu expression in the basal cells (3,3-diaminobenzidine [DAB] detection with hematoxylin counterstain). Original magnification x200. **ii:** Prostate cancer from a patient treated with total androgen ablation therapy shows moderate to complete Her-2-neu membrane staining in the tumor cells. Adjacent normal gland shows positive Her-2-neu expression in both the basal and the secretory cells (DAB detection with hematoxylin counterstain). Original magnification x200. **iii:** AI prostate cancer metastatic to the bone shows strong complete membrane staining for Her-2-neu in the tumor cells (DAB detection with hematoxylin counterstain). Original magnification x200.

differentiation. Positive Her-2-neu expression, as assessed by the absolute scoring method, was associated with higher Gleason grade in primary prostate cancers considered as one group ($P = .007$). When TAA and UNT patients were analyzed separately, the association with Gleason grade was still statistically significant for the UNT patients but not for the TAA patients ($P = .002$ and $P = .42$, respectively).

No significant difference in either Gleason grade or tumor stage distribution was found between TAA and UNT tumors ($P = .97$ and $P = .80$, respectively). However, to ensure that the association between Her-2-neu expression and treatment categories (UNT versus TAA) was independent of both Gleason grade and tumor stage, we used a logistic regression model. This association remained statistically significant after controlling for Gleason grade and stage ($P = .004$).

No association was observed between Her-2-neu expression (absolute scoring method) and tumor stage in primary prostate cancers ($P = .081$) or between Her-2-neu expression and the time to PSA recurrence or survival.

Overexpression of Her-2-neu confers androgen-independent growth to the LNCaP prostate cancer cell line *in vitro* through the activation of the AR in a ligand-independent fashion *(26)*. Therefore, to determine if increased expression of Her-2-neu in human prostate cancers was associated with expression and activation of the AR, we assessed the expression of the AR and of its known downstream target, PSA, in all of the tumors. All of the tumors were positive for both AR and PSA, as detected by immunohistochemistry (Fig. 3, ii and iii), except for three AI metastatic tumors, which expressed AR but not PSA. The lack of PSA expression in these three tumors may be a result of the scant fragments of tumor tissue available for analysis.

Both the biologic and clinical progression of prostate cancer to androgen-independent disease following androgen ablation therapy can be broken down into two distinct phases. The tumor initially escapes dependence on androgen for survival, and it subsequently escapes dependence on androgen for growth *(41)*. To determine whether prostate cancers of the TAA and AI types belonged to the survival or growth stage, we assessed the proliferation rate in the tumor sections by Ki-67 immunostaining. The proliferation rate was statistically significantly lower in TAA tumors than in UNT tumors ($P<.001$), whereas Her-2-neu expression was higher in TAA tumors than in UNT tumors. In contrast, the proliferation rate of AI metastatic prostate cancers was statistically significantly higher than in both UNT ($P = .014$) and TAA ($P<.001$) tumors (Fig 2, A).

Genomic and mRNA Analysis of Her-2-neu

With the use of ISH, Her-2-neu mRNA was detected in 17 of 20 prostatectomy specimens, both in tumor cells and in the adjacent normal prostate glands. The other three tumors appeared to lack Her-2-neu mRNA, most likely because the RNA had degraded. Of the 17 positive tumors, 12 were found to express high levels of Her-2-neu mRNA (Fig. 3, iv). Seven of these 12 tumors also expressed high levels of Her-2-neu protein. Five tumors that expressed low levels of Her-2-neu mRNA also expressed low levels of Her-2-neu protein. Six of seven AI metastatic tumors tested by ISH expressed Her-2-neu mRNA. All of these tumors expressed high Her-2-neu protein levels. Thus, there was concordance between Her-2-neu protein and mRNA expression. No hybridization signal was detected with the control sense probe (Fig. 3, v).

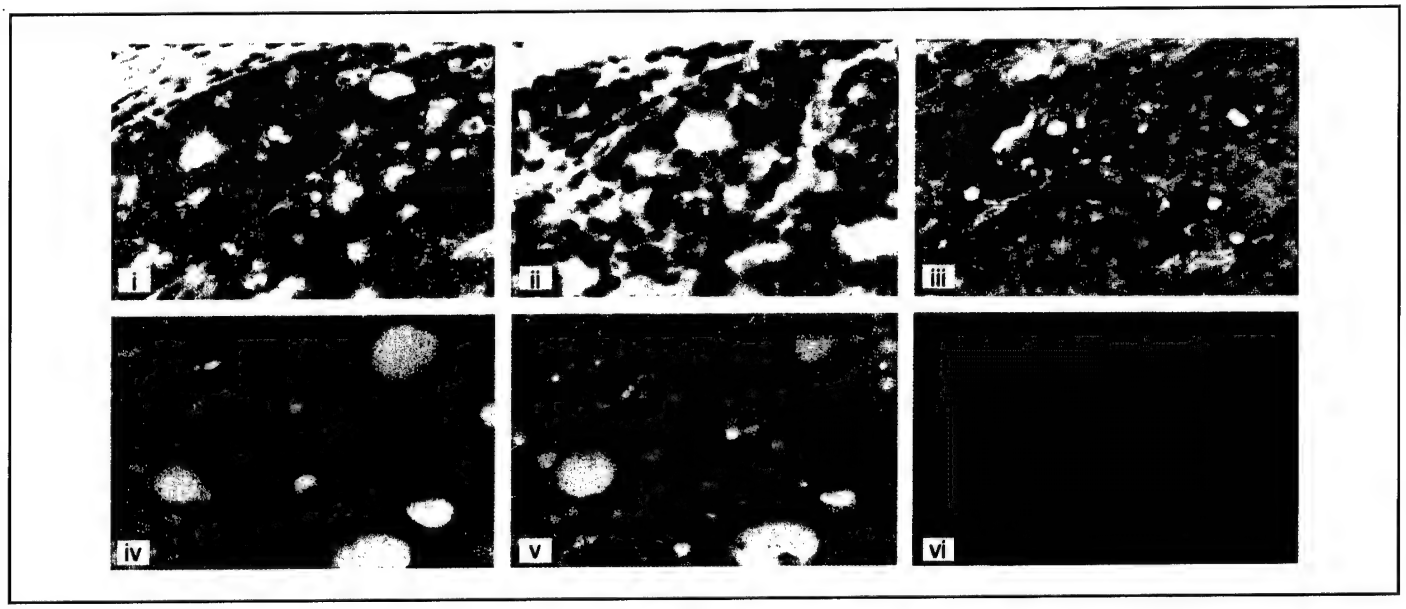

Fig. 3. Serial sections from a TAA prostate cancer (i.e., cancer from a patient who received total androgen ablation therapy) analyzed by immunohistochemistry for Her-2-neu, androgen receptor, and prostate-specific antigen (PSA) protein expression, by *in situ* hybridization (ISH) for Her-2-neu messenger RNA expression, and by fluorescent *in situ* hybridization (FISH) for analysis of the Her-2-neu locus. **i:** Complete membrane staining for Her-2-neu in the tumor cells (3,3-diaminobenzidine [DAB] detection with hematoxylin counterstain). Original magnification ×400. **ii:** Nuclear immunostaining for the androgen receptor (DAB detection with hematoxylin counterstain). Original magnification ×400. **iii:** Positive cytoplasmic immunostaining for PSA (DAB detection with hematoxylin counterstain). Original magnification ×400. **iv:** ISH with the antisense ^{35}S-labeled Her-2-neu probe generates a specific signal in neoplastic cells (hematoxylin–eosin counterstain). Original magnification ×400. **v:** ISH with the sense ^{35}S-labeled Her-2-neu probe. No specific signal is detected (hematoxylin–eosin counterstain). Original magnification ×400. **vi:** FISH for the Her-2-neu locus shows no gene amplification [2-(4-amidinophenyl)-6-indolecarbamidinedihydrochloride counterstain]. Original magnification x1000.

We also analyzed the same subset of tumors for evidence of genomic amplification. Of the 28 tumor samples analyzed by FISH, seven (five primary carcinomas and two metastases) did not produce an adequate result because of either tissue overdigestion or high background. Genomic amplification of the HER-2-neu locus was not detected in any of the prostate tumors or in the LAPC4 xenograft. All scorable tumor samples (n = 21), including the LAPC4 xenograft, had a Her-2-neu FISH score of less than 4 (Fig. 3, vi). The breast carcinoma used as the positive control showed amplification of the Her-2-neu locus (FISH score >10), while the one used as the negative control showed no amplification.

Discussion

Tumor progression to androgen-independent growth eventually occurs in prostate cancer patients treated with androgen ablation therapy. No modes of therapy are currently available for AI tumors. Molecular characterization of the progression of prostate cancer to androgen independence is of paramount importance in understanding the biologic mechanisms underlying this process.

The majority of AI prostate tumors express both AR *(32,42)* and androgen-dependent genes, indicating that the AR-signaling pathway is functional in the absence of androgen. However, the mechanism by which the pathway is activated in the absence of androgen is unknown. AR mutations *(43–48)* or AR gene amplification *(49)* and alterations in kinases *(50–55),* growth factors *(52,56),* and nuclear receptor coactivators *(57)* have all been proposed to modulate AR signaling and may, therefore, play key roles in the mechanism of androgen independence in prostate cancer.

One possible player in the development of androgen independence is Her-2-neu. Craft et al. *(26)* demonstrated that overexpression of Her-2-neu confers androgen-independent growth to the androgen-dependent LNCaP prostate cancer cell line. Furthermore, in the absence of androgen, overexpression of Her-2-neu activates the transcription of PSA. It is interesting that, unlike other kinases that are able to activate the AR pathway in the absence of the ligand *(50),* Her-2-neu-mediated PSA activation requires the AR but is not inhibited by the antiandrogen drug Casodex. Thus, Her-2-neu overexpression in prostate cancer cells activates the AR pathway in the absence of the ligand, simulating androgen independence of prostate cancer *in vivo.*

Further evidence that Her-2-neu may play an important role in the progression to AI prostate cancer is our observation of a progressive increase in Her-2-neu expression in UNT, TAA, and AI prostate cancers. In addition, primary prostate carcinomas treated with TAA and AI metastases coexpressed AR and PSA, which is important because coexpression of Her-2-neu with AR and PSA is consistent with activation of the AR pathway by Her-2-neu in a ligand-independent fashion.

During the natural history of prostate cancer progression, both human and experimental, there is a latent, relatively quiescent period when tumor cells survive but do not proliferate in an environment devoid of androgen *(40,41,58).* Subsequently, a second period ensues during which highly proliferating tumor cells expand and metastasize. Our data show that, although there was an increase in Her-2-neu expression in primary tumors treated by androgen ablation, there was a decrease in proliferation rates relative to those of untreated prostate tumors. In contrast, there was a dramatic increase in the proliferation rates of androgen-independent bone metastases. A possible explanation for the differences in proliferation rates is that Her-2-neu initially confers survival to tumor cells by activating the AR pathway in an androgen-independent fashion. These same cells, however, may still require androgens for proliferation. This hypothesis is supported by the observation that, although the majority of secretory cells undergo apoptosis upon androgen withdrawal *(59,60),* residual secretory cells present in the treated prostate express high levels of Her-2-neu protein. Increased expression of Her-2-neu may, therefore, be a prostate-specific rather than a tumor-specific mechanism for cell survival in an androgen-depleted environment.

Although genomic amplification of the HER-2-neu locus is responsible for Her-2-neu protein overexpression in breast and ovarian carcinomas *(2),* the mechanism for Her-2-neu overexpression in prostate cancer is unknown, and, in fact, overexpression itself in the prostate is still controversial. Our findings show that the Her-2-neu protein is expressed at statistically significantly higher levels in prostate cancers treated by androgen deprivation (TAA and AI) than in untreated cancers ($P<.005$) and that high protein expression is accompanied by high mRNA expression but is not accompanied by HER-2-neu gene amplification. Thus, steady-state Her-2-neu transcripts (and, consequently, Her-2-neu protein) may be progressively increased by androgen ablation. Alternatively, tumor cells with initial high levels of Her-2-neu may be selected for during androgen deprivation through the elimination of the androgen-sensitive, low-Her-2-neu-expressing tumor cell subpopulation. Indeed, in untreated primary prostate carcinomas, positive immunostaining for Her-2-neu was associated with decreased tumor cell differentiation, i.e., a higher Gleason grade ($P = .007$). The response to androgen therapy appears to be inversely related to Gleason grade *(40).* Thus, the Her-2-neu-expressing tumor component with high Gleason grade may not be responsive to androgen ablation therapy and might, therefore, be selected for survival. However, our data indicate that the increased Her-2-neu expression in treated tumors relative to untreated tumors is independent of Gleason grade. Thus, increased Her-2-neu expression may be a necessary mechanism for prostate tumor cells to survive in an androgen-depleted environment, independent of the differentiation status of tumor cells.

There is evidence that determining the functional status of Her-2-neu may not be a requirement in order to target the molecule therapeutically. Protein levels of Her-2-neu do not necessarily reflect its functional activity. However, in a human xenograft model of prostate cancer, Herceptin dramatically inhibited growth in androgen-dependent tumors that had been characterized purely on the basis of immunohistochemical overexpression of Her-2-neu. Herceptin was also effective against AI tumors when it was used in combination with the chemotherapy agent paclitaxel *(61).* In addition, as a single agent, a different anti-Her-2-neu antibody that is directed against a more proximal epitope of the extracellular domain of the Her-2-neu protein strongly inhibited Her-2-neu-positive, AI xenograft tumors *(62).* Taken together, these data support the approach of therapeutic targeting of Her-2-neu in both androgen-dependent and androgen-independent stages of prostate cancer on the basis of protein expression alone.

The demonstration that a population of Her-2-neu-positive tumor cells gradually

increases with progression toward AI prostate cancer further justifies targeting Her-2-neu in androgen-independent disease. In addition, because Her-2-neu-positive tumor cells are present in untreated tumors and increase in relative number during the early phases of androgen deprivation, combining hormonal ablation with Her-2-neu targeting may help eradicate those tumor cells that are able to survive in an androgen-depleted environment and are destined to become androgen independent for growth.

Finally, it has recently been shown that PEA3, a member of the ets family of transcription factors, specifically targets a DNA sequence on the Her-2-neu promoter, repressing its activity *(63)*. Because we have shown that the levels of Her-2-neu mRNA parallel protein expression in prostate carcinomas, future development of transcriptional inhibitors of Her-2-neu may also represent a valid therapeutic option.

In summary, we have shown that progression of prostate cancer toward androgen independence is characterized by a gradual increase in Her-2-neu expression by the tumor cells. We propose that Her-2-neu may function by initially permitting prostate cancer cell survival in an androgen-depleted environment. We also speculate that, over time, reactivation of proliferation occurs in Her-2-neu-positive cells, probably in association with additional genetic events. Her-2-neu targeting in advanced AI prostate cancers is, therefore, justified. More important, our data suggest that the combination of androgen ablation and Her-2-neu targeting could be effective in androgen-dependent tumors.

References

(1) Slamon DJ, Clark GM, Wong SG, Levin WJ, Ullrich A, McGuire WL. Human breast cancer: correlation of relapse and survival with amplification of the HER-2/neu oncogene. Science 1987;235:177–82.

(2) Slamon DJ, Godolphin W, Jones LA, Holt JA, Wong SG, Keith DE, et al. Studies of the HER-2/neu proto-oncogene in human breast and ovarian cancer. Science 1989;244:707–12.

(3) Naber SP, Tsutsumi Y, Yin S, Zolnay SA, Mobtaker H, Marks PJ, et al. Strategies for the analysis of oncogene overexpression. Studies of the neu oncogene in breast carcinoma. Am J Clin Pathol 1990;94:125–36.

(4) Berchuck A, Kamel A, Whitaker R, Kerns B, Olt G, Kinney R, et al. Overexpression of HER-2/neu is associated with poor survival in advanced epithelial ovarian cancer. Cancer Res 1990;50:4087–91.

(5) Shepard HM, Lewis GD, Sarup JC, Fendly BM, Maneval D, Mordenti J, et al. Monoclonal antibody therapy of human cancer: taking the HER2 protooncogene to the clinic. J Clin Immunol 1991;11:117–27.

(6) Pegram M, Hsu S, Lewis G, Pietras R, Beryt M, Sliwkowski M, et al. Inhibitory effects of combinations of HER-2/neu antibody and chemotherapeutic agents used for treatment of human breast cancers. Oncogene 1999;18: 2241–51.

(7) Pegram MD, Slamon DJ. Combination therapy with trastuzumab (Herceptin) and cisplatin for chemoresistant metastatic breast cancer: evidence for receptor-enhanced chemosensitivity. Semin Oncol 1999;26(4 Suppl 12):89–95.

(8) Visakorpi T, Kallioniemi OP, Koivula T, Harvey J, Isola J. Expression of epidermal growth factor receptor and ERBB2 (HER-2/Neu) oncoprotein in prostatic carcinomas. Mod Pathol 1992;5:643–8.

(9) Sadasivan R, Morgan R, Jennings S, Austenfeld M, Van Veldhuizen P, Stephens R, et al. Overexpression of Her-2/neu may be an indicator of poor prognosis in prostate cancer. J Urol 1993;150:126–31.

(10) Schwartz S Jr, Caceres C, Morote J, De Torres I, Rodriguez-Vallejo JM, Gonzalez J, et al. Over-expression of epidermal growth factor receptor and c-erbB2/neu but not of int-2 genes in benign prostatic hyperplasia by means of semi-quantitative PCR. Int J Cancer 1998;76: 464–7.

(11) Kuhn EJ, Kurnot RA, Sesterhenn IA, Chang EH, Moul JW. Expression of the c-erbB-2 (HER-2/neu) oncoprotein in human prostatic carcinoma. J Urol 1993;150:1427–33.

(12) Fox SB, Persad RA, Coleman N, Day CA, Silcocks PB, Collins CC. Prognostic value of c-erbB-2 and epidermal growth factor receptor in stage A1 (T1a) prostatic adenocarcinoma. Br J Urol 1994;74:214–20.

(13) Giri DK, Wadhwa SN, Upadhaya SN, Talwar GP. Expression of NEU/HER-2 oncoprotein (p185neu) in prostate tumors: an immunohistochemical study. Prostate 1993;23:329–36.

(14) Gu K, Mes-Masson AM, Gauthier J, Saad F. Overexpression of her-2/neu in human prostate cancer and benign hyperplasia. Cancer Lett 1996;99:185–9.

(15) Lyne JC, Melhem MF, Finley GG, Wen D, Liu N, Deng DH, et al. Tissue expression of neu differentiation factor/heregulin and its receptor complex in prostate cancer and its biologic effects on prostate cancer cells *in vitro*. Cancer J Sci Am 1997;3:21–30.

(16) Morote J, de Torres I, Caceres C, Vallejo C, Schwartz S Jr, Reventos J. Prognostic value of immunohistochemical expression of the c-erbB-2 oncoprotein in metastatic prostate cancer. Int J Cancer 1999;84:421–5.

(17) Mydlo JH, Kral JG, Volpe M, Axotis C, Macchia RJ, Pertschuk LP. An analysis of microvessel density, androgen receptor, p53 and HER-2/neu expression and Gleason score in prostate cancer: preliminary results and therapeutic implications. Eur Urol 1998;34:426–32.

(18) Myers RB, Srivastava S, Oelschlager DK, Grizzle WE. Expression of p160erbB-3 and p185erbB-2 in prostatic intraepithelial neoplasia and prostatic adenocarcinoma. J Natl Cancer Inst 1994;86:1140–5.

(19) Visakorpi T. New pieces to the prostate cancer puzzle [news]. Nat Med 1999;5:264–5.

(20) Ross JS, Sheehan C, Hayner-Buchan AM, Ambros RA, Kallakury BV, Kaufman R, et al. HER-2/neu gene amplification status in prostate cancer by fluorescence *in situ* hybridization. Hum Pathol 1997;28:827–33.

(21) Ross JS, Sheehan CE, Hayner-Buchan AM, Ambros RA, Kallakury BV, Kaufman RP Jr, et al. Prognostic significance of HER-2/neu gene amplification status by fluorescence *in situ* hybridization of prostate carcinoma. Cancer 1997;79:2162–70.

(22) Kallakury BV, Sheehan CE, Ambros RA, Fisher HA, Kaufman RP Jr, Muraca PJ, et al. Correlation of p34cdc2 cyclin-dependent kinase overexpression, CD44s downregulation, and HER-2/neu oncogene amplification with recurrence in prostatic adenocarcinomas. J Clin Oncol 1998;16:1302–9.

(23) Bubendorf L, Kononen J, Koivisto P, Schraml P, Moch H, Gasser TC, et al. Survey of gene amplifications during prostate cancer progression by high-throughout fluorescence *in situ* hybridization on tissue microarrays. Cancer Res 1999;59:803–6.

(24) Mark HF, Feldman D, Das S, Kye H, Mark S, Sun CL, et al. Fluorescence *in situ* hybridization study of HER-2/neu oncogene amplification in prostate cancer. Exp Mol Pathol 1999; 66:170–8.

(25) Schwartz S Jr, Caceres C, Morote J, De Torres I, Rodriguez-Vallejo JM, Gonzalez J, et al. Gains of the relative genomic content of erbB-1 and erbB-2 in prostate carcinoma and their association with metastasis. Int J Oncol 1999;14:367–71.

(26) Craft N, Shostak Y, Carey M, Sawyers CL. A mechanism for hormone-independent prostate cancer through modulation of androgen receptor signaling by the HER-2/neu tyrosine kinase. Nat Med 1999;5:280–5.

(27) Faming ID, Cooper JS, Henson DE, Hutter RV, Kennedy BJ, Murphy BJ, et al, eds. AJCC cancer staging manual. 5th ed. Philadelphia (PA) and New York (NY): Lippincott-Raven Publishers; 1997. p 219–24.

(28) Gleason DF. Histologic grading of prostate cancer: a prospective. Hum Pathol 1992;23: 273–9.

(29) Yang A, Kaghad M, Wang Y, Gillett E, Fleming MD, Dotsch V, et al. p63, a p53 homolog at 3q27–29, encodes multiple products with transactivating, death-inducing, and dominant-negative activities. Mol Cell 1998;2:305–16.

(30) Signoretti S, Waltregny D, Dilks J, Isaac B, Lin D, Garraway L, et al. p63 is a prostate basal cell marker and is required for prostate development. Am J Pathol. In press 2000.

(31) Miller R, Siegmund D. Maximally selected chi square statistics. Biometrics 1982;38:1011–6.

(32) Magi-Galluzzi C, Xu X, Hlatky L, Hahnfeldt P, Kaplan I, Hsiao P, et al. Heterogeneity of androgen receptor content in advanced prostate cancer. Mod Pathol 1997;10:839–45.

(33) Jacobs TW, Gown AM, Yaziji H, Barnes MJ, Schnitt SJ. Specificity of HercepTest in deter-

mining HER-2/neu status of breast cancers using the United States Food and Drug Administration-approved scoring system. J Clin Oncol 1999;17:1983–7.

(34) Gu L, Tseng S, Horner RM, Tam C, Loda M, Rollins BJ. Control of TH2 polarization by the chemokine monocyte chemoattractant protein-1. Nature 2000;404:407–11.

(35) Wilcoxon F. Individual comparisons by ranking methods. Biometrics 1945;1:80–3.

(36) Cox DR. Analysis of binary data. London (U.K.): Methuen and Co.; 1970.

(37) Bland JM, Altman DG. Multiple significance tests: the Bonferroni method. BMJ 1995;310: 170.

(38) Jonckheere AR. A distribution-free k-sample test against ordered alternatives. Biometrika 1954;41:133–45.

(39) Mehta CR, Patel NR, Tsiatis AA. Exact significance testing to establish treatment equivalence with ordered categorical data. Biometrics 1984;40:819–25.

(40) Montironi R, Schulman CC. Pathological changes in prostate lesions after androgen manipulation. J Clin Pathol 1998;51:5–12.

(41) Craft N, Chhor C, Tran C, Belldegrun A, DeKernion J, Witte ON, et al. Evidence for clonal outgrowth of androgen-independent prostate cancer cells from androgen-dependent tumors through a two-step process. Cancer Res 1999;59:5030–6.

(42) Culig Z, Hobisch A, Hittmair A, Peterziel H, Cato AC, Bartsch G, et al. Expression, structure, and function of androgen receptor in advanced prostatic carcinoma. Prostate 1998;35: 63–70.

(43) Veldscholte J, Berrevoets CA, Ris-Stalpers C, Kuiper GG, Jenster G, Trapman J, et al. The androgen receptor in LNCaP cells contains a mutation in the ligand binding domain which affects steroid binding characteristics and response to antiandrogens. J Steroid Biochem Mol Biol 1992;41:665–9.

(44) van der Kwast TH, Schalken J, Ruizeveld de Winter JA, van Vroonhoven CC, Mulder E, Boersma W, et al. Androgen receptors in endocrine-therapy-resistant human prostate cancer. Int J Cancer 1991;48:189–93.

(45) Newmark JR, Hardy DO, Tonb DC, Carter BS, Epstein JI, Isaacs WB, et al. Androgen receptor gene mutations in human prostate cancer. Proc Natl Acad Sci U S A 1992;89:6319–23.

(46) Culig Z, Hobisch A, Cronauer MV, Cato AC, Hittmair A, Radmayr C, et al. Mutant androgen receptor detected in an advanced-stage prostatic carcinoma is activated by adrenal androgens and progesterone. Mol Endocrinol 1993;7: 1541–50.

(47) Elo JP, Kvist L, Leinonen K, Isomaa V, Henttu P, Lukkarinen O, et al. Mutated human androgen receptor gene detected in a prostatic cancer patient is also activated by estradiol. J Clin Endocrinol Metab 1995;80:3494–500.

(48) Evans BA, Harper ME, Daniells CE, Watts CE, Matenhelia S, Green J, et al. Low incidence of androgen receptor gene mutations in human prostatic tumors using single strand conformation polymorphism analysis. Prostate 1996;28:162–71.

(49) Koivisto P, Kononen J, Palmberg C, Tammela T, Hyytinen E, Isola J, et al. Androgen receptor gene amplification: a possible molecular mechanism for androgen deprivation therapy failure in prostate cancer. Cancer Res 1997;57: 314–9.

(50) Culig Z, Hobisch A, Cronauer MV, Radmayr C, Trapman J, Hittmair A, et al. Androgen receptor activation in prostatic tumor cell lines by insulin-like growth factor-I, keratinocyte growth factor, and epidermal growth factor. Cancer Res 1994;54:5474–8.

(51) Nazareth LV, Weigel NL. Activation of the human androgen receptor through a protein kinase A signaling pathway. J Biol Chem 1996; 271:19900–7.

(52) Hobisch A, Eder IE, Putz T, Horninger W, Bartsch G, Klocker H, et al. Interleukin-6 regulates prostate-specific protein expression in prostate carcinoma cells by activation of the androgen receptor. Cancer Res 1998;58:4640–5.

(53) Gioeli D, Mandell JW, Petroni GR, Frierson HF Jr, Weber MJ. Activation of mitogen-activated protein kinase associated with prostate cancer progression. Cancer Res 1999;59: 279–84.

(54) Abreu-Martin MT, Chari A, Palladino AA, Craft NA, Sawyers CL. Mitogen-activated protein kinase kinase kinase 1 activates androgen receptor-dependent transcription and apoptosis in prostate cancer. Mol Cell Biol 1999;19: 5143–54.

(55) Sadar MD. Androgen-independent induction of prostate-specific antigen gene expression via cross-talk between the androgen receptor and protein kinase A signal transduction pathways. J Biol Chem 1999;274:7777–83.

(56) Sherwood ER, Van Dongen JL, Wood CG, Liao S, Kozlowski JM, Lee C. Epidermal growth factor receptor activation in androgen-independent but not androgen-stimulated growth of human prostatic carcinoma cells. Br J Cancer 1998;77:855–61.

(57) Miyamoto H, Yeh S, Wilding G, Chang C. Promotion of agonist activity of antiandrogens by the androgen receptor coactivator, ARA70, in human prostate cancer DU145 cells. Proc Natl Acad Sci U S A 1998;95:7379–84.

(58) Westin P, Stattin P, Damber JE, Bergh A. Castration therapy rapidly induces apoptosis in a minority and decreases cell proliferation in a majority of human prostatic tumors. Am J Pathol 1995;146:1368–75.

(59) English HF, Kyprianou N, Isaacs JT. Relationship between DNA fragmentation and apoptosis in the programmed cell death in the rat prostate following castration. Prostate 1989;15: 233–50.

(60) Colombel MC, Buttyan R. Hormonal control of apoptosis: the rat prostate gland as a model system. Methods Cell Biol 1995;46:369–85.

(61) Agus DB, Scher HI, Higgins B, Fox WD, Heller G, Fazzari M, et al. Response of prostate cancer to anti-Her-2/neu antibody in androgen-dependent and -independent human xenograft models. Cancer Res 1999;59:4761–4.

(62) Agus DB, Scher HI, Fox WD, Higgins B, Maiese KM, Akita RA, et al. Differential antitumor effects of targeting distinct epitopes of the Her-2/neu extracellular domain in xenograft models of prostate cancers [abstract]. Proc Am Assoc Cancer Res 2000;41:719.

(63) Xing X, Wang SC, Xia W, Zou Y, Shao R, Kwong KY, et al. The ets protein PEA3 suppresses HER-2/neu overexpression and inhibits tumorigenesis. Nat Med 2000;6:189–95.

NOTES

Supported by Public Health Service grant 5R01CA81755–03 from the National Cancer Institute, National Institutes of Health, Department of Health and Human Services; and by grant DOD DAMD #17 98–8574 from the Department of Defense.

We thank William Sellers, Myles Brown, and David Waltregny for critical review of the manuscript, Jane Hayward for assistance with photography, and Marty Olesiak for assistance with image analysis.

American Journal of Pathology, Vol. 157, No. 6, December 2000

Short Communication

p63 Is a Prostate Basal Cell Marker and Is Required for Prostate Development

Sabina Signoretti,*† David Waltregny,* James Dilks,* Beth Isaac,* Douglas Lin,* Levi Garraway,* Annie Yang,‡ Rodolfo Montironi,§ Frank McKeon,‡ and Massimo Loda*†

From the Department of Adult Oncology, Dana-Farber Cancer Institute, Boston, Massachusetts; the Department of Pathology,† Brigham and Women's Hospital, Boston, Massachusetts; and the Department of Cell Biology,‡ Harvard Medical School, Boston, Massachusetts; and the Department of Pathology,§ University of Ancona, Ancona, Italy*

The *p53* homologue *p63* encodes for different isotypes able to either transactivate *p53* reporter genes (*TAp63*) or act as *p53*-dominant-negatives (*ΔNp63*). p63 is expressed in the basal cells of many epithelial organs and its germline inactivation in the mouse results in agenesis of organs such as skin appendages and the breast. Here, we show that prostate basal cells, but not secretory or neuroendocrine cells, express p63. In addition, prostate basal cells in culture predominantly express the ΔNp63α isotype. In contrast, p63 protein is not detected in human prostate adenocarcinomas. Finally, and most importantly, *p63*(−/−) mice do not develop the prostate. These results indicate that p63 is required for prostate development and support the hypothesis that basal cells represent and/or include prostate stem cells. Furthermore, our results show that p63 immunohistochemistry may be a valuable tool in the differential diagnosis of benign *versus* malignant prostatic lesions. *(Am J Pathol 2000, 157:1769–1775)*

p63 is a recently cloned homologue of the *p53* tumor suppressor gene.[1–4] In contrast to *p53*, the *p63* gene encodes for at least six major isotypes.[4] Three isotypes (*TAp63α*, *TAp63β*, and *TAp63γ*) contain the transactivating (TA) domain and are able to transactivate *p53* reporter genes and induce apoptosis. In contrast, the other three isotypes (*ΔNp63α*, *ΔNp63β*, and *ΔNp63γ*) are transcribed from an internal promoter localized within intron 3, lack the TA domain, and act as dominant-negatives to suppress transactivation by both *p53* and *TAp63* isotypes. *p63* is selectively expressed in the basal cell compartment of a variety of epithelial tissues.[4,5] Further, *p63*-deficient mice show severe defects in the development of epithelial organs that express p63 protein, namely agenesis of squamous epithelia, mammary, salivary, and lachrymal glands.[6,7] Altogether, these results suggest that p63 may be essential for the maintenance of a stem cell population in various epithelial tissues.

Knowledge of the molecular events underlying prostate development is limited. Normal prostate epithelium consists of three different types of cells: secretory, basal, and neuroendocrine. A subset of cells that is morphologically and immunophenotypically intermediate between basal and secretory cells has also been identified within the normal prostate epithelium.[8–11] This observation has lead to the hypothesis that basal cells represent the precursors of secretory cells. In contrast to this hypothesis, cell kinetic studies in the rat prostate suggest that basal and secretory cells are independent lineages with self-renewal capacities.[12,13] Therefore, the existence of a prostate stem cell able to give rise to both basal and secretory cells remains highly controversial.

We have previously shown that both human and mouse prostate basal cells express p63 protein (see Yang et al[4] and data not shown). This result suggests that p63 may play a critical role in prostate development by maintaining a prostate stem cell population. However, because the mouse prostate starts to develop only during the last few days of gestation[14,15] and *p63*(−/−) mice die at birth, assessment of prostate development in these mice requires a very accurate morphological analysis and no data are currently available in the literature.

In the present study, we first confirmed that p63 represents a selective marker of basal cells within the prostatic epithelium by analyzing p63 expression in a series of normal prostates and in normal, basal PrEC prostate cells. Second, because it has been demonstrated that prostate cancers express markers of secretory cells and

Supported by grants from CaPCURE, National Cancer Institute (CA, 81755–03), and Department of Defense (DAMD 17 98-8574).

Accepted for publication August 22, 2000.

Address reprint requests to Massimo Loda, Department of Adult Oncology, Dana Farber Cancer Institute, Dana 740B, 44 Binney St., Boston, MA 02215. E-mail: massimo_loda@dfci.harvard.edu.

are usually negative for basal cell markers,[16,17] we analyzed p63 expression in a series of 130 prostatic carcinomas and in prostate cancer cell lines. Finally, to assess the role of p63 in prostate development we histologically analyzed the periurethral region in day 1, *p63*(−/−) male mice.

Our results show that p63 is a reliable prostate basal cell marker and that the ΔNp63α isotype is the most abundantly represented in normal prostate basal (PrEC) cells. Because p63 protein is consistently undetectable in prostate cancers, we propose that p63 expression may be used in the differential diagnosis between benign and malignant lesions of the prostate. Finally and most importantly, our results indicate that p63 expression is necessary for the normal development of the mouse prostate, suggesting that p63-positive basal cells may represent/include prostate stem cells.

Materials and Methods

Prostatectomy Specimens and Prostate Cell Lines

This study was performed after approval by the Institutional Review Board of the Dana Farber Cancer Institute and Brigham and Women's Hospital.

One hundred thirty prostate cancer specimens, were retrieved from the files of the departments of Pathology of the Brigham and Women's Hospital, the Beth Israel Deaconess Medical Center, Boston, MA, and the University of Ancona, Italy, and used in immunohistochemistry experiments. The prostate cancer patients analyzed included 29 patients treated with total androgen ablation therapy for 3 months before surgery (Zoladex depot every 28 days plus Casodex 50 mg/day for 12 weeks) and 101 patients who did not receive any treatment before surgery.

Normal basaloid PrEC prostate cells (Clonetics, Walkersville, MD) and LNCaP, PC3, and DU145 prostate cancer cell lines (ATCC, Rockville, MD) were used in immunohistochemistry, immunoblotting, and real-time polymerase chain reaction (PCR) experiments. PC3 cells were also used for transfection experiments. Normal stromal PrSC prostate cells (Clonetics) were used in immunoblotting experiments.

Immunohistochemistry

Immunostaining was performed in all tissue specimens and paraffin-embedded cell lines using the 4A4 anti-p63 antibody, which recognizes all six p63 isotypes.[4] A subset of 58 samples was double-immunostained for p63 and HMWCK (34βE12; DAKO, Carpinteria, CA). Double-immunostaining for p63 and chromogranin A (Novocastra Laboratories Ltd., Newcastle on Tyne, UK) was performed in 10 samples.

For p63 immunostaining, 5-μm sections were deparaffinized, rehydrated, and subjected to microwaving in 10 mmol/L citrate buffer, pH 6.0 (BioGenex, San Ramon, CA) in a 750 W oven for 15 minutes. Slides were allowed to cool at room temperature for 30 minutes. The 4A4 antibody (1:50 dilution) was applied at room temperature for 2 hours in an automated stainer (Optimax Plus 2.0 bc; BioGenex, San Ramon, CA). Detection steps were performed by the instrument using the MultiLink-HRP kit (BioGenex). Peroxidase activity was localized using 3,3-diaminobenzidine or 3,3-diaminobenzidine-nickel chloride. Standardized development time periods allowed accurate comparison of all samples.

For double-immunostaining experiments, tissue sections were subsequently incubated with the second antibody (anti-HMWCK or anti-chromogranin A) at 1:50 dilution for 30 minutes. Detection was performed using alkaline-phosphatase-conjugated streptavidin and new fuchsin (BioGenex).

Substitution of the primary antibody with phosphate-buffered saline (PBS) served as negative-staining control.

Immunoblot Analysis

PrEC, PrSC, LNCaP, PC3, and DU145 cells were lysed in 200 μl of lysis buffer (50 mmol/L Tris, pH 7.5, 250 mol/L NaCl, 0.1% Triton X-100, 1 mmol/L ethylenediaminetetraacetic acid, 50 mmol/L NaF, 0.1 mmol/L Na_3VO_4) containing 1 mmol/L dithiothreitol, 1 mmol/L phenylmethyl sulfonyl fluoride, and protease inhibitor cocktail (Boehringer Mannheim, Indianapolis, IN). Immunoblotting was performed as previously described[18] using the 4A4 anti-p63 antibody at 1:250 dilution.

Cell Transfection

PC3 cells were maintained in F-12 nutrient mixture medium supplemented with 8% fetal bovine serum (Life Technologies, Inc., Gaithersburg, MD). A pCDNA3 vector encoding myc epitope-tagged *ΔNp63α* isotype[4] was transfected in PC3 cells using FuGENE 6 transfection reagent (Boehringer Mannheim) according to the manufacturer's direction. Briefly, PC3 cells were incubated at 37°C in a 250-ml flask with a solution consisting of 20 μg of DNA, 30 μl of FuGENE 6 transfection reagent, and F-12 nutrient mixture medium supplemented with 8% fetal bovine serum. Cells were harvested 24 hours after transfection.

Real-Time Quantitative PCR (Taqman PCR)

RNA Extraction and Reverse Transcription (RT)

Total RNA was extracted from PrEC, LNCaP, PC3, and DU145 cells with the use of the RNeasy mini kit (Qiagen, Chatsworth, CA), according to manufacturer's directions. For cDNA synthesis, 1 μg of total RNA was reverse-transcribed in a 20-μl reaction mixture containing 250 μmol/L of each dNTP, 20 U of RNase inhibitor, 50 U of MuLV reverse transcriptase, 2.5 μmol/L random hexamers, and 1× buffer (1.5 mmol/L $MgCl_2$) (all reagents were purchased from PE Applied Biosystems, Foster City, CA). The reaction mix was incubated at 42°C for 45 minutes and then denatured at 99°C for 5 minutes. For each sample, a control reaction not containing the reverse transcriptase enzyme was also performed.

Oligonucleotide name	Sequence	Exon
TAp63 amplicon size: 126 bp		
TAp63 forward primer	TGTATCCGCATGCAGGACT	e3
TAp63 reverse primer	CTGTGTTATAGGGACTGGTGGAC	e4
TAp63 hybridization probe	ACCTGAGTGACCCCATGTGGCC	e3-e4
ΔNp63 amplicon size: 125 bp		
ΔNp63 forward primer	GAAAACAATGCCCAGACTCAA	e3'
ΔNp63 reverse primer	TGCGCGTGGTCTGTGTTA	e4
ΔNp63 hybridization probe	TGAGCCACAGTACACGAACCTGGG	e3'-e4

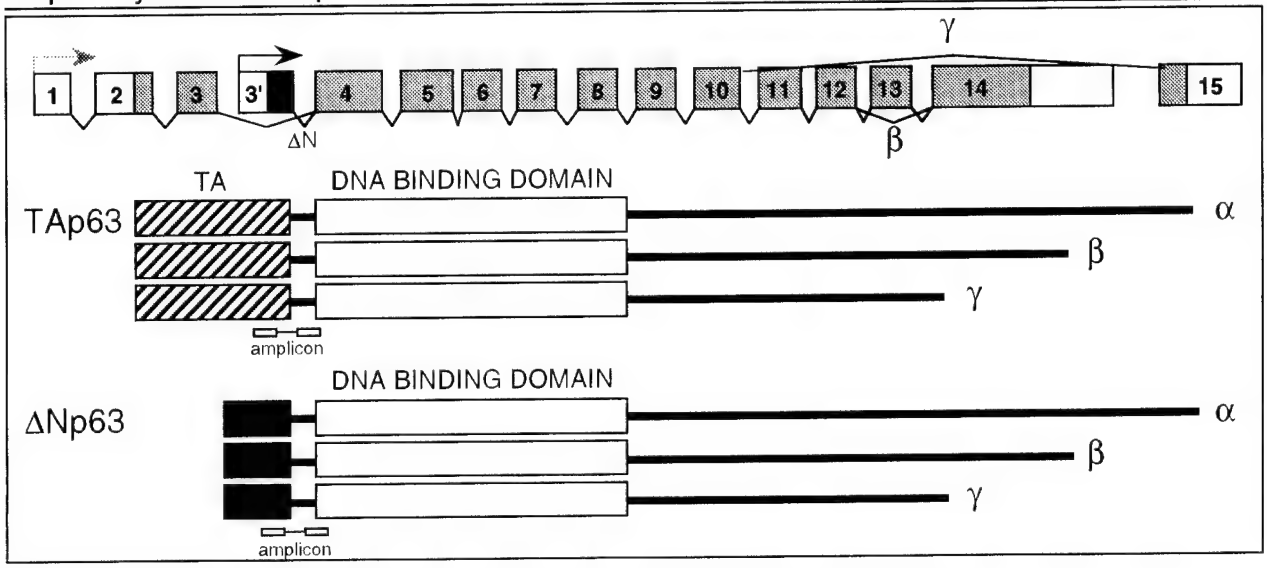

Figure 1. Sequences, amplicon sizes, and exon localizations of primers and probes used for Taqman® PCR experiment.

Real-Time PCR

Specific primers and probe sets for *TAp63* and *ΔNp63* isotypes (Figure 1) were designed from sequences in the GenBank database using the Primer Express 1.0 Software (PE Applied Biosystems). The primers and hybridization probes spanned an intron to exclude annealing to genomic DNA. The housekeeping glyceraldehyde-3-phosphate dehydrogenase (GAPDH) gene was used as endogenous control to standardize the amount of RNA in each reaction (Taqman GAPDH control reagents). All primers and probes were synthesized by PE Applied Biosystems. PCR was performed on the cDNA samples using an ABI PRISM 7700 Sequence Detector (PE Applied Biosystems). The Taqman PCR Core Reagent Kit (PE Applied Biosystems) was used according to the manufacturer's protocol with the following modifications: dUTP was replaced by dTTP and incubation with AmpErase was omitted. For each sample tested, PCR reaction was performed in a 50 μl volume containing 2 μl of cDNA reaction (equivalent to 100 ng of template RNA) and 2.5 U of AmpliTaq Gold. Oligonucleotide primers and fluorogenic probes were added to a final concentration of 100 nmol/L each. The amplification step consisted of 60 cycles of 94°C for 45 seconds, 54°C for 45 seconds, and 64°C for 1 minute.

In each experiment, additional reactions with seven serial twofold dilutions of PrEC cDNA as template were performed with each set of primers and probes (*TAp63*, *ΔNp63*, and GAPDH) on the same 96-well plate to generate standard curves, which related the threshold cycle (C_T) to the log input amount of template. All samples were amplified in triplicates. The relative amount of each p63 transcript in each cell line was determined by using the standard curve method and by normalizing for GAPDH mRNA expression levels, as described in detail in the ABI PRISM Sequence Detection System User Bulletin No. 2 (PE Applied Biosystems) and elsewhere.[19] The amplification efficiencies for ΔNp63 and TAp63 transcripts were also calculated. Because they were approximately similar (TA/ΔN relative efficiency curve had a slope value of 0.91), ΔNp63 and TAp63 transcripts levels could be compared with reasonable accuracy.

Prostate Analysis of p63(−/−) and Wild-Type Newborn Mice

p63(−/−) mice were generated as previously described.[6] The periurethral region of newborn *p63*(−/−) male mice and of newborn wild-type B57Bl/6 male mice (controls) was analyzed. Specifically, the caudal portion

Figure 2. a: Normal prostate gland showing selective p63 nuclear expression in basal cells. **b:** Double-immunostaining for p63 (black nuclear staining) and chromogranin A (red cytoplasmic staining): neuroendocrine cells do not express p63. **c:** Double-immunostaining for p63 (black nuclear staining) and HMWCK (red cytoplasmic staining): the majority of basal cells co-express p63 and HMWCK. A subset of basal cells expresses p63 only. **d:** Prostate gland with basal cell hyperplasia double-immunostained for p63 (brown nuclear staining) and HMWCK (red cytoplasmic staining): a subset of p63-positive and HMWCK-negative basal cells is identified. **e:** Dysplastic cells from high-grade prostatic intraepithelial neoplasia glands are negative for p63 expression whereas a rim of residual p63-positive basal cells can be identified. **f:** Prostate cancer cells do not express p63 (**left**) whereas an adjacent normal prostate gland (**right**) shows p63 expression in basal cells.

of each animal was sectioned along a coronal plane, fixed in 10% buffered formalin, and embedded in paraffin. Histological examination was performed on paraffin sections stained with hematoxylin and eosin. Coronal sections of the entire length of the urethra were examined. In addition, the periurethral region of both newborn *p63*(−/−) and wild-type male mice was immunostained for p63 as described in the Immunohistochemistry section.

Results

p63 Protein Is Selectively Expressed in the Nuclei of Basal Cells of Normal Prostate Glands

Prostatectomy Specimens

We first determined the expression of p63 protein in normal prostate tissue. All prostatectomy specimens showed universal p63 immunostaining of basal cell nuclei, whereas secretory cells were consistently negative (Figure 2a).

To assess p63 expression in neuroendocrine cells and to test for p63 and HMWCK co-expression in basal cells, double-immunostaining for p63/chromogranin A and p63/HMWCK, respectively, was performed. Neuroendocrine cells did not express p63 protein (Figure 2b). Double-immunostaining for p63 and HMWCK showed co-localization of the two antigens in the majority of basal cells. However, a minority (~1 to 5%) of p63-positive/HMWCK-negative basal cells was identified (Figure 2, c and d).

Normal Prostate Cells (PrEC and PrSC)

PrEC and PrSC cells are commercially available, normal prostate basal and stromal cells, respectively. We

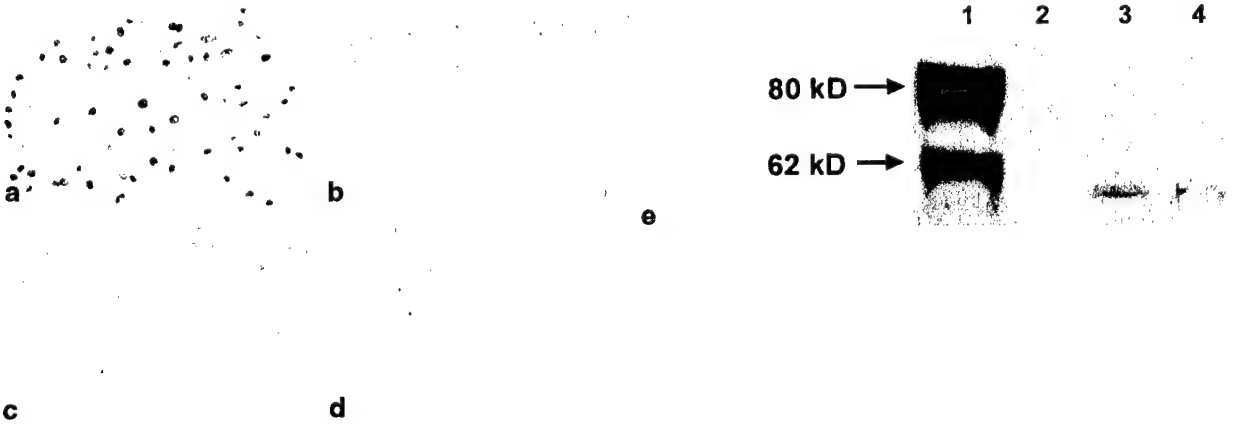

Figure 3. a: p63 protein is expressed in the nuclei of ~80% of normal basal prostate PrEC cells by immunohistochemistry. LNCaP (**b**), PC3 (**c**), and DU145 (**d**) cells do not express p63 protein. **e:** Immunoblotting of PrEC cell lysate (**lane 1**) with anti-p63 antibody shows a major band at ~80 kd and a fainter band at ~60 kd. LNCaP (**lane 2**), PC3 (**lane 3**) and DU145 (**lane 4**) cells are negative for p63 protein expression by immunoblotting.

confirmed by immunohistochemistry the basal cell phenotype of PrEC cells (positivity for HMWCK and negativity for androgen receptor and prostate-specific antigen) (Signoretti and Loda, unpublished data).

By immunohistochemistry, 80% of PrEC cells expressed p63 protein in the nuclei (Figure 3a). Immunoblot analysis of PrEC cell lysate with anti-p63 antibody showed a major band at ~80 kd and a fainter band at ~60 kd (Figure 3e). In contrast, PrSC cells were negative for p63 expression by immunoblotting (not shown). Immunoblotting of PC3 cells transfected with a mammalian expression vector encoding myc epitope-tagged ΔNp63α isotype generated a band that migrated slightly slower than the 80 kd band obtained with PrEC cells (not shown). These results are consistent with our previous data obtained in primary human foreskin keratinocytes.[4] Taken together our results suggest that ΔNp63α is the predominant p63 isotype in PrEC cells.

p63 Protein Is Not Expressed in Prostatic Intraepithelial Neoplasia and Invasive Prostate Cancer

Prostatectomy Specimens

We next examined p63 protein expression in 130 human prostate cancers. HMWCK expression was concomitantly analyzed in a subset of 58 cases by double-immunostaining.

High-grade prostatic intraepithelial neoplasia was detected in 48 of 130 prostatectomy specimens. In all prostatic intraepithelial neoplasia cases, dysplastic cells were negative for both p63 and HMWCK, but a rim of residual p63-positive basal cells could be identified (Figure 2e).

One hundred twenty-six of 130 (97%) invasive prostate cancers were negative for p63 (Figure 2f), whereas in four cases, <1% of cells were positive for both p63 and HMWCK (not shown). In contrast, in three cases a minority of cells (<5%) was positive for HMWCK but negative for p63 (not shown).

Prostate Cancer Cell Lines (LNCaP, PC3, DU145)

By both immunoblot and immunohistochemical analysis LNCaP, PC3, and DU145 cells were negative for p63 protein expression (Figure 3, b–e).

ΔNp63 Is the Most Abundant p63 Isotype in PrEC Cells

Immunoblot analysis showed that ΔNp63α likely represents the most abundant p63 protein in PrEC cells whereas prostate tumor cell lines are negative for p63 expression. To investigate the relative abundance of p63 isotypes at the RNA level, ΔNp63 and TAp63 transcripts levels were compared in PrEC, LNCaP, PC3, and DU145 cells by real-time relative quantitative PCR (TaqMan-PCR). As compared to PrEC cells and after normalization for GAPDH mRNA levels, ΔNp63 mRNA levels were at least 2,000 times lower in PC3 cells and were undetectable in LNCaP and DU145 cells. TAp63 mRNA levels were similar in PrEC and PC3 cells (ratio PC3/PrEC = 1.3) and were significantly lower in LNCaP and DU145 cells with 14-fold and sevenfold decreases, respectively. Reactions in which the reverse transcriptase enzyme was omitted did not yield significant amplification (data not shown). These results indicate that ΔNp63 transcripts are virtually absent in prostate cancer cell lines, whereas TAp63 mRNA levels are detectable in varying amounts in all three cancer cell lines tested.

In PrEC cells, the threshold cycle (C_T) for *ΔNp63* amplification was significantly lower as compared to the C_T for *TAp63* (23 *versus* 30 when 100 ng of RNA were used as template) (not shown), indicating that ΔNp63 transcripts are expressed at significantly higher levels than TAp63 transcripts in these cells.

p63 Is Essential for Normal Prostate Development in the Mouse

Histological examination of the entire length of the urethra in newborn *p63*(−/−) male mice revealed absence of the prostate. Specifically, no ducts or epithelial budding structures could be identified either in the ventral or in the dorsolateral region of the periurethral mesenchyma (Figure 4b). Conversely, in control mice, epithelial structures were present in both the ventral and dorsolateral portions of the periurethral region (Figure 4a). The epithelial structures consisted of both solid buds and small glands. By immunohistochemistry, both urothelial and prostatic basal cells of wild-type mice expressed p63 protein (Figure 4a, inset). In contrast, p63 expression could not be detected in either epithelial or stromal cells of *p63*(−/−) mice (Figure 4b, inset).

Discussion

As previously demonstrated in the hematopoietic system, cancers arise from cells arrested at various stages of differentiation.[20] As a result, the identification of stem cells and subsequent stages of differentiation in normal tissues is an essential step in understanding the mechanisms involved in neoplastic transformation.

In normal prostate epithelium, the lineage relationships between secretory, basal, and neuroendocrine cells, and the existence of a common precursor, are still matters of debate. The vast majority of prostate cancers express markers of secretory cells such as androgen receptor and prostate-specific antigen, and are negative for basal cell markers.[16,17] Consequently, it has been generally accepted that prostate cancer arises from malignant transformation of secretory cells. However, prostate carcinomas may also express genes characteristic of basal cells.[17,21–25] Thus, the cell from which prostate cancer arises is still unknown.

The *p63* gene is expressed exclusively in the basal cells of several epithelial organs and has been suggested to play a major role in the maintenance of the stem cell compartment in these organs.[4,6,7] Here, in a large

Figure 4. a: A coronal section of the periurethral region of a wild-type mouse shows the presence of prostatic buds (**arrowheads**) in both the ventral (**V**) and dorsolateral periurethral region. **Arrows** indicate ejaculatory ducts. By immunohistochemistry, basal urothelial and prostatic cells express p63 (**inset**). **b:** A coronal section of the periurethral region of a p63(−/−) mouse shows complete absence of prostatic ducts or budding structures in both the ventral (**V**) and dorsolateral region of the periurethral mesenchyma. p63 expression could not be detected in either epithelial or stromal cells by immunohistochemistry (**inset**). Ejaculatory ducts (**arrows**) are present in the posterior periurethral region. Detached urothelial cells are present within the urethral lumen.

series of prostate specimens, we confirm that the p63 protein is selectively expressed in the nuclei of basal cells of normal prostate glands. In addition, we show that homozygous inactivation of this gene in the mouse results in prostate agenesis.

Because p63 is selectively expressed in adult prostate basal cells and it is undetectable in adult prostate stromal cells both *in vivo* and *in vitro*, the defect in prostate development in *p63*(−/−) mice is likely ascribed to the epithelial component. However, p63 may be essential for either maintaining a prostate epithelial stem cell population or sustaining a basal cell population, which does not represent a stem cell compartment *per se* but is essential for prostate development (eg, signaling to the surrounding mesenchyma).

The *p63*(−/−) mouse is the first engineered animal model demonstrating prostate agenesis. Further manipulation of this animal model will certainly provide a unique tool to study prostate development, differentiation, and neoplastic transformation.

In prostate basal cells grown *in vitro*, the predominantly expressed p63 isotype is the ΔNp63α that lacks the transactivating domain. This isotype has been shown to act as a dominant-negative on the transactivation by both *TAp63* and *p53*.[4] We have previously shown that keratinocytes differentiation *in vitro* is associated with down-regulation of the ΔNp63 transcripts.[5] Because secretory cells do not express p63, we speculate that down-regulation of the ΔNp63α isotype may be required for differentiation of basal cells into secretory cells. These findings are interesting inasmuch as p53-mediated transcriptional activity increases in a variety of differentiating cells including muscle cells and keratinocytes, despite unchanged[26] or decreased p53 protein levels.[27] In addition, transfection of mutant *p53*[27] or dominant-negative *p53*[26] results in a lack of *p53*-dependent transactivation and differentiation, suggesting that transcription of *p53*-regulated genes is necessary for differentiation. However, because terminal differentiation occurs in *p53*(−/−) cells, *p53* homologues, including *TAp63*, may have overlapping functions to those of p53 in differentiation. Altogether, these data suggest that relief of the dominant-negative function of ΔNp63 in basal cells may be necessary for activating the *p53*-dependent gene transcription machinery required for the differentiation of these cells into secretory cells.

We have demonstrated that p63 is not expressed in prostate carcinomas. This finding supports the hypothesis that prostatic carcinomas have a secretory phenotype. Because we have shown that p63 is expressed in

virtually all basal cells, including a cell subset negative for HMWCK, p63 immunohistochemistry may be a valuable tool for the differential diagnosis of benign *versus* malignant prostatic lesions.

In conclusion, the basal cell marker p63 is essential for prostate development in the mouse suggesting that prostate basal cells may represent and/or include prostate stem cells. In addition, because of the universal expression of p63 by basal cells, p63 immunohistochemistry may be a useful adjunct to morphological analysis in the prostate surgical pathology setting.

References

1. Osada M, Ohba M, Kawahara C, Ishioka C, Kanamaru R, Katoh I, Ikawa Y, Nimura Y, Nakagawara A, Obinata M, Ikawa S: Cloning and functional analysis of human p51, which structurally and functionally resembles p53. Nat Med 1998, 4:839–843
2. Senoo M, Seki N, Ohira M, Sugano S, Watanabe M, Inuzuka S, Okamoto T, Tachibana M, Tanaka T, Shinkai Y, Kato H: A second p53-related protein, p73L, with high homology to p73. Biochem Biophys Res Commun 1998, 248:603–607
3. Trink B, Okami K, Wu L, Sriuranpong V, Jen J, Sidransky D: A new human p53 homologue. Nat Med 1998, 4:747–748
4. Yang A, Kaghad M, Wang Y, Gillett E, Fleming MD, Dotsch V, Andrews NC, Caput D, McKeon F: p63, a p53 homolog at 3q27-29, encodes multiple products with transactivating, death-inducing, and dominant-negative activities. Mol Cell 1998, 2:305–316
5. Parsa R, Yang A, McKeon F, Green H: Association of p63 with proliferative potential in normal and neoplastic human keratinocytes. J Invest Dermatol 1999, 113:1099–1105
6. Yang A, Schweitzer R, Sun D, Kaghad M, Walker N, Bronson RT, Tabin C, Sharpe A, Caput D, Crum C, McKeon F: p63 is essential for regenerative proliferation in limb, craniofacial and epithelial development. Nature 1999, 398:714–718
7. Mills AA, Zheng B, Wang XJ, Vogel H, Roop DR, Bradley A: p63 is a p53 homologue required for limb and epidermal morphogenesis. Nature 1999, 398:708–713
8. Verhagen AP, Aalders TW, Ramaekers FC, Debruyne FM, Schalken JA: Differential expression of keratins in the basal and luminal compartments of rat prostatic epithelium during degeneration and regeneration. Prostate 1988, 13:25–38
9. Jones EG, Harper ME: Studies on the proliferation, secretory activities, and epidermal growth factor receptor expression in benign prostatic hyperplasia explant cultures. Prostate 1992, 20:133–149
10. Peehl DM, Leung GK, Wong ST: Keratin expression: a measure of phenotypic modulation of human prostatic epithelial cells by growth inhibitory factors. Cell Tissue Res 1994, 277:11–18
11. Robinson EJ, Neal DE, Collins AT: Basal cells are progenitors of luminal cells in primary cultures of differentiating human prostatic epithelium. Prostate 1998, 37:149–160
12. English HF, Santen RJ, Isaacs JT: Response of glandular versus basal rat ventral prostatic epithelial cells to androgen withdrawal and replacement. Prostate 1987, 11:229–242
13. Evans GS, Chandler JA: Cell proliferation studies in the rat prostate: II. The effects of castration and androgen-induced regeneration upon basal and secretory cell proliferation. Prostate 1987, 11:339–351
14. Cunha GR, Donjacour AA, Cooke PS, Mee S, Bigsby RM, Higgins SJ, Sugimura Y: The endocrinology and developmental biology of the prostate. Endocr Rev 1987, 8:338–362
15. Bhatia-Gaur R, Donjacour AA, Sciavolino PJ, Kim M, Desai N, Young P, Norton CR, Gridley T, Cardiff RD, Cunha GR, Abate-Shen C, Shen MM: Roles for Nkx3.1 in prostate development and cancer. Genes Dev 1999, 13:966–977
16. Nagle RB, Ahmann FR, McDaniel KM, Paquin ML, Clark VA, Celniker A: Cytokeratin characterization of human prostatic carcinoma and its derived cell lines. Cancer Res 1987, 47:281–286
17. Liu AY, True LD, LaTray L, Nelson PS, Ellis WJ, Vessella RL, Lange PH, Hood L, van den Engh G: Cell-cell interaction in prostate gene regulation and cytodifferentiation. Proc Natl Acad Sci USA 1997, 94:10705–10710
18. Pagano M, Tam SW, Theodoras AM, Beer-Romero P, Del Sal G, Chau V, Yew PR, Draetta GF, Rolfe M: Role of the ubiquitin-proteasome pathway in regulating abundance of the cyclin-dependent kinase inhibitor p27. Science 1995, 269:682–685
19. Fink L, Seeger W, Ermert L, Hanze J, Stahl U, Grimminger F, Kummer W, Bohle RM: Real-time quantitative RT-PCR after laser-assisted cell picking. Nat Med 1998, 4:1329–1333
20. Sawyers CL, Denny CT, Witte ON: Leukemia and the disruption of normal hematopoiesis. Cell 1991, 64:337–350
21. McDonnell TJ, Troncoso P, Brisbay SM, Logothetis C, Chung LW, Hsieh JT, Tu SM, Campbell ML: Expression of the protooncogene bcl-2 in the prostate and its association with emergence of androgen-independent prostate cancer. Cancer Res 1992, 52:6940–6944
22. Colombel M, Symmans F, Gil S, O'Toole KM, Chopin D, Benson M, Olsson CA, Korsmeyer S, Buttyan R: Detection of the apoptosis-suppressing oncoprotein bc1–2 in hormone-refractory human prostate cancers. Am J Pathol 1993, 143:390–400
23. Pisters LL, Troncoso P, Zhau HE, Li W, von Eschenbach AC, Chung LW: c-met proto-oncogene expression in benign and malignant human prostate tissues. J Urol 1995, 154:293–298
24. Reiter RE, Gu Z, Watabe T, Thomas G, Szigeti K, Davis E, Wahl M, Nisitani S, Yamashiro J, Le Beau MM, Loda M, Witte ON: Prostate stem cell antigen: a cell surface marker overexpressed in prostate cancer. Proc Natl Acad Sci USA 1998, 95:1735–1740
25. Gu Z, Thomas G, Yamashiro J, Shintaku IP, Dorey F, Raitano A, Witte ON, Said JW, Loda M, Reiter RE: Prostate stem cell antigen (PSCA) expression increases with high Gleason score, advanced stage and bone metastasis in prostate cancer. Oncogene 2000, 19:1288–1296
26. Tamir Y, Bengal E: p53 protein is activated during muscle differentiation and participates with MyoD in the transcription of muscle creatine kinase gene. Oncogene 1998, 17:347–356
27. Weinberg WC, Azzoli CG, Chapman K, Levine AJ, Yuspa SH: p53-mediated transcriptional activity increases in differentiating epidermal keratinocytes in association with decreased p53 protein. Oncogene 1995, 10:2271–2279

0022-5347/98/1593-0941$03.00/0
THE JOURNAL OF UROLOGY
Copyright © 1998 by AMERICAN UROLOGICAL ASSOCIATION, INC.

Vol. 159, 941–945, March 1998
Printed in U.S.A.

LOW P27 EXPRESSION PREDICTS POOR DISEASE-FREE SURVIVAL IN PATIENTS WITH PROSTATE CANCER

RONALD M. YANG, JOHN NAITOH, MICHAEL MURPHY, HE-JING WANG, JULIA PHILLIPSON, JEAN B. DEKERNION, MASSIMO LODA AND ROBERT E. REITER*

From the Departments of Urology, Pathology and Biomathematics, UCLA School of Medicine, Los Angeles, California, and Department of Pathology, Beth Israel Deaconess Medical Center, West Campus, Harvard Medical School, Boston, Massachusetts

ABSTRACT

Purpose: p27 is an inhibitor of the cell cycle with potential tumor suppressor function. Decreased levels of p27 protein expression have been correlated with poor prognosis in patients with breast and colorectal carcinomas. Although as many as a third of patients with clinically localized prostate cancer will have relapse after radical prostatectomy, predicting who will have recurrence remains enigmatic. We examined the ability of p27 protein levels to predict outcome in patients with clinically localized disease who underwent radical prostatectomy.

Materials and Methods: p27 protein expression was evaluated in 86 patients with clinical stage T1-2 prostate cancer who were treated with radical prostatectomy. Archived paraffin embedded specimens were sectioned and immunostained with p27 antibody, and scored by 2 independent observers in a blinded fashion. The absence or presence of p27 protein was then correlated with biochemical relapse in univariate and multivariate analyses.

Results: In a multivariate analysis that included age, preoperative prostate specific antigen, Gleason score and pathological stage p27 was a strong independent predictor of disease-free survival ($p = 0.0184$, risk ratio 3.04), second only to pathological stage ($p = 0.0001$, risk ratio 6.73). Even more strikingly, multivariate analysis demonstrated that p27 was the strongest predictor of biochemical recurrence ($p = 0.0081$, risk ratio 4.99) among factors studied in patients with pathological T2a-T3b disease.

Conclusions: Absent or low levels of p27 protein expression appear to be an adverse prognostic factor in patients with clinically organ confined disease treated by radical prostatectomy. This marker appears to be especially useful in those patients in whom surgery is believed to be potentially curative, that is patients with pathological T2-T3b disease. Patients with low or absent p27 protein expression may be candidates for novel adjuvant therapies.

KEY WORDS: prostatic neoplasms; gene products, rex; tumor markers

p27 is a candidate tumor suppressor gene that belongs to the Cip/Kip family of cyclin dependent kinase inhibitors.[1] It regulates progression of the cell cycle from the G1 to S phase by binding to and inhibiting the cyclin E/cdk2 complex.[2] Recent publications have suggested that p27 has an important role in normal cell cycle regulation and cancer.[3]

Although mutations of the p27 gene appear to be rare in human tumors,[4] alterations in the posttranslational processing of p27 leading to decreased amounts of p27 protein have been detected in a variety of cancers. Low levels of p27 protein presumably interfere with the ability of cancer cells to halt cell cycling and lead to the accumulation of additional genetic alterations and more malignant growth.[5] p27 has also been suggested to have a role in adhesion dependent cell growth, as loss of p27 may alter intercellular adhesion and facilitate metastasis.[6] Consistent with these hypotheses, immunohistochemical analysis of p27 protein expression in breast,[7,8] colorectal[9] and gastric[10] carcinomas has demonstrated a relationship between reduced levels of p27 protein and poor clinical outcome. In particular, low levels of p27 expression independently predict cancer recurrence following definitive local therapy for all 3 cancers.

To our knowledge no studies of p27 protein expression in prostate cancer have been reported. The study of p27 expression in prostate is particularly attractive, since there are still few reliable independent prognostic markers for this disease. We examined the expression of p27 protein in 86 patients with clinically organ confined disease who underwent radical prostatectomy. The relationship of p27 protein expression and biochemical disease relapse was studied to determine whether p27 has prognostic value in patients with clinically localized prostate cancer. We also evaluated whether p27 could provide information independent of conventional criteria, such as pathological stage. We found that p27 expression level was an independent predictor of biochemical relapse among the entire cohort studied. Remarkably, p27 is the strongest predictor of outcome in patients with pathological T2-T3b prostate cancer.

MATERIALS AND METHODS

Specimens. Formalin fixed, paraffin embedded tissue blocks were recovered from 86 patients who underwent radical prostatectomy for adenocarcinoma of the prostate. The cases were identified from the 385 consecutive radical prostatectomies performed by a single urological surgeon (J. B. D.) between 1987 and 1995. All cases that fit the inclusion and exclusion criteria were evaluated, and all attempts were made to avoid bias in the selection of cases.

All pathological specimens were processed in a uniform manner, with the margins inked and serial step sections of the prostate taken at 0.5 cm. intervals. All patients in the

Accepted for publication October 31, 1997.
Supported in part by grants from the UCLA Carolan Foundation and the STOP Cancer Foundation.
* Requests for reprints: Department of Urology, 66-134 Center for the Health Sciences, Box 951738, Los Angeles, California 90095-1738.

study had a clinical T1 or T2 tumor, at least 2 years of clinical and biochemical followup, and adequate pathological tissue for immunohistochemical analysis. Patients were excluded from the study if tissue blocks with histologically confirmed prostate cancer could not be found, any neoadjuvant or adjuvant endocrine therapy had been administered or a patient had received adjuvant radiotherapy. All histopathological features of the tumors were rereviewed and confirmed by a single pathologist (J. P.) using the standard Gleason grading and TNM pathological staging systems. The Gleason grade of the tumors was further confirmed by a second pathologist (M. L.).

Patients were examined at followup every 3 months in year 1 following surgery, every 6 months during year 2 and annually thereafter. Patients were evaluated with a digital rectal examination and serum prostate specific antigen (PSA) level. Median followup of the study population was 40 months (range 24 to 115). Cancer recurrence was defined as a PSA value greater than 0.4 ng./dl. (Hybritech assay). Information about preoperative PSA level, Gleason score of the pathological specimen, pathological stage and postoperative PSA levels was obtained from the UCLA prostate cancer data base.

Immunohistochemistry. Archival specimen blocks containing the primary tumor were identified. Formalin fixed, paraffin embedded 5 μm. sections were mounted on charged glass slides, deparaffinized and rehydrated through graded alcohol rinses. Immunohistochemistry was then performed in an automated processor. Slides were immersed in 10 mmol./l. citrate buffer, pH 6.0, and microwaved in a 750 W. oven inside a pressure cooker for a 30-minute period. The slides were cooled at room temperature for 30 minutes, after which a 1:200 dilution of p27 mouse monoclonal antibody was applied to the specimens for 24 minutes at 37C in the automated stainer. Steps performed by the automated instrument included the application of goat/horse serum blocking antibodies, application of the secondary antibody conjugated to an avidin-biotin peroxidase complex and selection of the bound antibody complex using 3,3-diaminobenzidine as the substrate. The processed slides were then counterstained with hematoxylin and cover slips were applied.

Antibodies with no known human recognition site were used as negative controls. Normal prostate basal cells served as negative internal controls for p27 antibody (fig. 1, *A*). Preserved antigenicity of the formalin fixed, paraffin tissue was verified by looking for p27 immunostaining of lymphocytes in each section examined. Prostate secretory epithelium and infiltrating lymphocytes served as internal positive controls for p27 staining (fig. 1, *C*).

p27 Scoring. Each specimen was scored by 2 independent investigators (R. M. Y. and J. P.) for p27 expression. Scoring was done blinded, with neither observer having knowledge of clinical history, pathological stage or disease status postoperatively. The area of highest Gleason grade was scored for each specimen. Approximately 500 cells from the selected area were counted, and the number and percentage of cells with nuclear p27 staining were noted. Cells that had either weak or strong nuclear staining were considered to be positive for p27 protein expression (fig. 1, *B* and *C*). Cells without nuclear staining were considered negative (fig. 1, *D*). The percentage of cells expressing p27 was recorded as the ratio of positive cells-to-the total number of cells counted. Based on prior reports of p27 expression in breast cancer, cases were classified as being high or low p27 expressers.[7,8] Patients with low p27 expression had less than 30% of the nuclei in

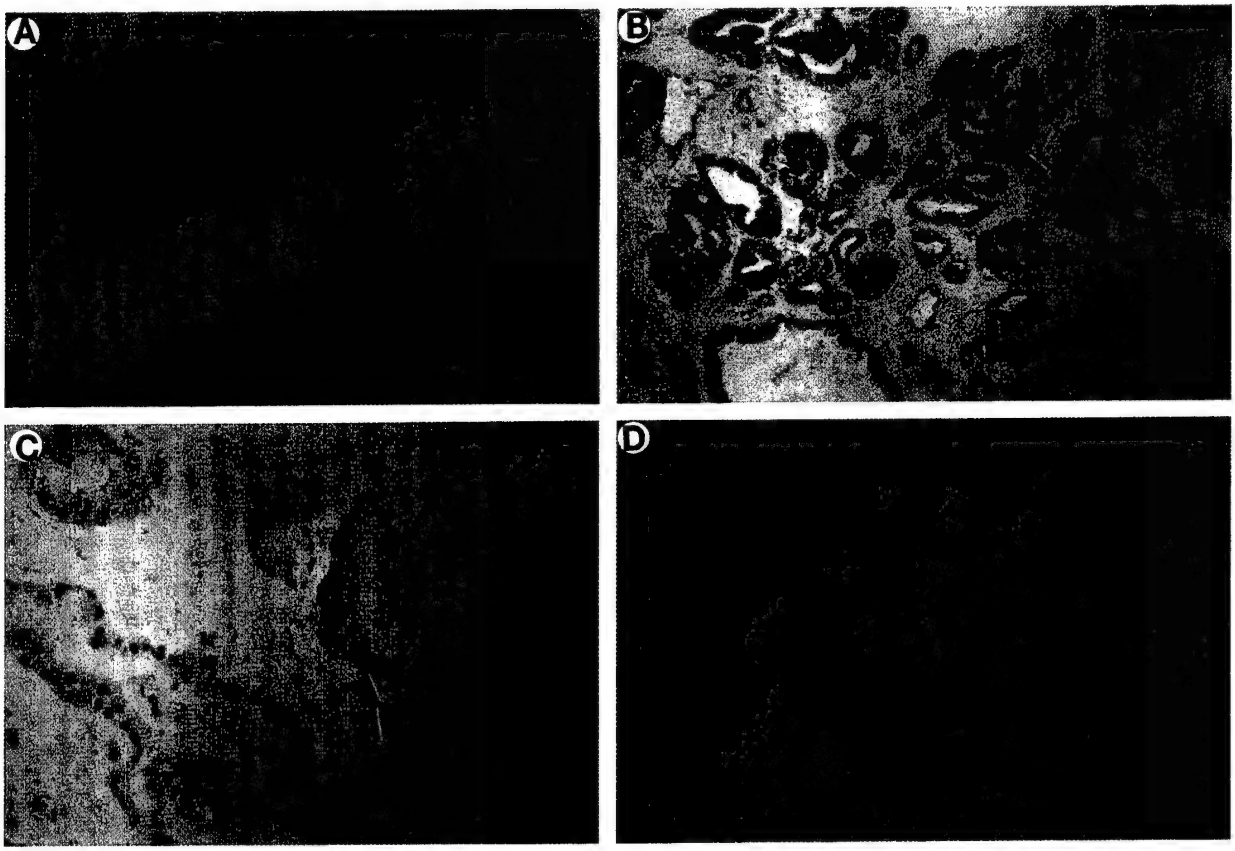

FIG. 1. Immunoreactivity for p27. *A*, p27 staining in normal prostate demonstrates strong positivity of secretory epithelium (large arrow) and absent staining of underlying basal cell epithelium (small arrow). Reduced from ×78. *B*, prostatic adenocarcinoma (arrow) shows strong immunoreactivity for p27 in almost all of neoplastic cells. Reduced from ×31. *C*, weakly positive p27 staining (arrow) in majority of cancer cells. Reduced from ×78. *D*, absent p27 staining in cancer (arrowhead) with internal positive controls, including lymphocytes (small arrow) and normal secretory epithelium (large arrow). Reduced from ×31.

the specimen staining positive, while those with high levels of p27 expression had more than 30% of the nuclei staining for the bound antibody.

Of the specimens 25% were randomly chosen and rescored to determine the degree of interobserver and intraobserver concordance. We obtained a greater than 95% interobserver and intraobserver concordance. Furthermore, there were no instances in which the difference in the first and second review resulted in changing a case from 1 summary category to another.

Statistical methods. Univariate associations between p27 and age, preoperative PSA, Gleason score and pathological stage were calculated using Spearman's rank or Pearson's correlation coefficients, depending on the characteristics of the variables. Dichotomized data were also created and separately analyzed using the chi-square test. Disease-free survival curves based on p27 and the other covariates were created using the Kaplan-Meier method. The Cox proportional hazards model was used to determine the relative contributions of p27 and the other covariates to the risk of biochemical recurrence. All calculations were performed using statistical software.

RESULTS

Patient characteristics. Mean patient age at radical prostatectomy was 63.1 years (range 48 to 77, table 1). All patients had clinically localized disease (T1 or T2) and were followed postoperatively for a minimum of 2 years, with a mean followup of 39.81 months and median followup of 40 months. Of the specimens 48 (55.8%) were pathological stage T2a-c, 19 (22.1%) T3a-b, 10 (11.6%) T3c, 7 (8.1%) T4 and 2 (2.3%) stage N1/N2 (both in patients who had either pathological T3C or T4 tumors). Taking into account only the highest tumor grade in each radical prostatectomy specimen, 16 tumors (18.6%) had a Gleason score of 5, 25 (29.1%) Gleason score of 4, 42 (48.8%) Gleason score of 3 and 3 (3.5%) Gleason score of 2. Overall 26.7% of patients (23) had a PSA defined biochemical recurrence during followup.

Univariate analysis. The relationship between p27 expression and biochemical relapse was examined initially in an univariate analysis (table 2). Based on a prior report of p27 expression in breast cancer, cases were classified as being high or low p27 expressors. Patients with low p27 expression (less than 30% positive staining) tended to have a higher risk of PSA recurrence than those with high levels of p27 expression (30% or greater), although this difference did not reach statistical significance in a univariate analysis ($p = 0.082$). Of the other covariates examined only pathological stage correlated significantly with biochemical relapse ($p = 0.0001$), while Gleason grade and preoperative PSA did not reach statistical significance ($p = 0.096$ and $p = 0.146$, respectively).

We also studied the relationship between p27 and the covariates of age, PSA, Gleason grade and pathological stage (table 3). There was a significant inverse relationship between p27 staining and Gleason grade, with low p27 staining correlating with higher Gleason scores (Spearman's rank correlation coefficient -0.221, $p = 0.041$). There was no relationship between p27 staining and age, preoperative PSA or pathological stage.

Multivariate analysis. A Cox proportional hazards model was constructed to assess the contributions of p27 and other covariates to the risk of biochemical relapse. Among factors studied only low p27 protein expression and high pathological stage (T3c, T4, N1-2) predicted for PSA recurrence after radical prostatectomy for clinically localized disease ($p = 0.0184$ and $p = 0.0001$, respectively, table 4). The relative risk of PSA recurrence for patients expressing low amounts of p27 compared with those expressing high amounts of PSA was 3.04. Likewise, the relative risk of disease relapse for patients with higher pathological stage (T3c, T4, N1-2) compared with lower pathological stage (T2a-c, T3a-b) was 6.73.

Although the univariate analysis revealed no correlation between p27 and pathological stage, suggesting that p27 is not a surrogate marker for pathological stage, we wanted to test whether p27 could predict recurrence when the 67 patients with pathologically stage T2a-T3b tumors were separated from the 19 with T3c-N2 tumors. Cases of T3c-N2 tumors virtually all recur with time, while there is currently no accurate way to predict which cases with T2a-3b disease will relapse. Multivariate analysis revealed a highly significant correlation between low p27 expression and risk of PSA recurrence among patients with pathological T2a-3b disease, with a relative risk of 4.99 ($p = 0.0081$, table 4). This result is depicted in a Kaplan-Meier survival plot in figure 2. This correlation was also present among patients with high stage

TABLE 1. *Patient demographics and tumor characteristics*

Pt. Characteristics	No Recurrence	Recurrence	Overall
Total No. pts. (%)	63 (73.3)	23 (26.7)	86
Mean age ± SD	62.5 ± 7.2	64.9 ± 6.7	63.1 ± 7.1
No. pathological stage (%):			
T2a-c	41 (85.4)	7 (14.6)	48 (55.8)
T3a-b	15 (78.9)	4 (21.1)	19 (22.1)
T3c	3 (30.0)	7 (70.0)	10 (11.6)
T4	4 (57.1)	3 (42.9)	7 (8.1)
N1,2	0 (0)	2 (100)	2 (2.3)
Mean preop. PSA ± SD (ng./dl.)*	10.8 ± 10.2	14.3 ± 17.8	11.8 ± 12.6
No. postop. Gleason grade (%):†			
1	0	0	0
2	3 (100)	0 (0)	3 (3.5)
3	33 (78.6)	9 (21.4)	42 (48.8)
4	17 (68.0)	8 (32.0)	25 (29.1)
5	10 (62.5)	6 (37.5)	16 (18.6)
No. p27 Staining (%):			
Low expressors‡	7 (50.0)	7 (50.0)	14 (16.3)
High expressors§	56 (77.8)	16 (22.2)	72 (83.7)

* Three patients did not have preoperative PSA values.

† Areas of tumor that represented the highest Gleason grade were identified and scored in each immunostained specimen.

‡ Specimens with less than 30% cells staining overall for p27.

§ Specimens with 30% or greater cells staining overall for p27.

TABLE 2. *Univariate analysis of clinicopathological factors and recurrence*

Clinicopathological Factors	Parameter Estimate	Wald Test p Value	Risk Ratio (95% CI)
Pathological stage *	1.732	0.0001	5.65 (2.46–13.01)
Gleason grade†	0.420	0.096	1.52 (0.93–2.50)
p27 Staining‡	0.789	0.082	2.20 (0.91–5.36)
Preop. PSA§	0.630	0.146	1.88 (0.80–4.40)
Age	0.019	0.550	1.02 (0.96–1.08)

Cox proportional hazard regression analysis was used to assess the relationship of each of the clinicopathological factors with biochemical relapse, including p27 staining, preoperative PSA, Gleason grade and pathological stage.

* Dichotomized as lower pathological stage (T2a-c/T3a-b) and higher pathological stage (T3c/T4/N1,2).

† The highest Gleason grade in each specimen was used for analysis.

‡ Dichotomized as low p27 expression (less than 30% staining) and high p27 expression (30% or greater staining).

§ Dichotomized as lower preoperative PSA (less than 10 ng./dl.) and higher preoperative PSA (10 ng./dl. or greater). The cutoff was based on the median of all preoperative PSA values.

TABLE 3. *Univariate analysis of p27 staining and clinicopathological factors*

Type of Analysis	Correlation Coefficient	p Value
p27 Staining and Gleason grade	−0.221 Spearman	0.041
p27 Staining and pathological stage	−0.025 Spearman	0.818
p27 Staining and preop. PSA	−0.11 Pearson	0.319
p27 Staining and age	−0.086 Pearson	0.432

Spearman's rank and Pearson's correlation coefficients were used to assess the relationship between p27 staining and clinicopathological factors of Gleason grade, pathological stage, preoperative PSA and age.

TABLE 4. *Multivariate analysis of the association among p27, pathological stage and recurrence*

Covariates Selected	Parameter Estimate	Wald Test p Value	Risk Ratio (95% CI)
All pts.:			
p27 Staining	1.11	0.0184	3.04* (1.21–7.64)
Pathological stage	1.91	0.0001	6.73† (2.83–16.01)
Pts. with T2a-c/T3a-b pathologically staged tumors:			
p27 Staining	1.61	0.0081	4.99* (1.52–16.39)

Cox proportional hazard regression model was used to study the association between different clinicopathological factors. Analysis was performed on all patients and a subset of patients with pathologically staged T2a-c/T3a-b tumors. Age, p27 staining, preoperative PSA, Gleason grade, and pathological stage were included as covariates for the first analysis. Stepwise procedure selected pathological stage and p27 staining as the most significant prognostic factors. Pathological stage was dichotomized as T2a-c/T3a-b versus T3c/T4/N1-2. Age, p27 staining, preoperative PSA and Gleason grade were included as covariates for the latter analysis. Stepwise procedure selected p27 staining as the sole significant prognostic factor.

* Comparing the prognosis of low p27 expression to high p27 staining.

† Comparing the prognosis of high pathological stage to low pathological stage.

prostate cancer, although the small sample size (19) precluded this from reaching statistical significance (data not shown).

DISCUSSION

The pathological stage and Gleason grade of the tumor are powerful predictors of prognosis among patients with prostate cancer treated by radical prostatectomy. Patients with a pathological stage T3c or higher tumor have a 75% probability of cancer recurrence within 5 years of surgery.[11] In contrast, patients with lower stage tumors (pathological stage T2a-c, T3a-b) have a 10 to 20% risk of PSA recurrence within 5 years of treatment.[12] At this time no independent prognostic factor better than preoperative PSA and Gleason score has been found that can predict which T2a-c/T3a-b tumors will recur following radical prostatectomy.

While there was a trend for the preoperative PSA to predict the later occurrence of biochemical relapse, this trend did not reach statistical significance in either the univariate or multivariate analysis. While other authors have found a stronger correlation between preoperative PSA and outcome following radical prostatectomy,[13,14] our study revealed a weaker relationship possibly due to differences in patient selection. All patients evaluated in this study had clinically organ confined tumors and relatively low preoperative PSA levels (average PSA 11.8). Starting with a group that had a narrower range of PSA levels may have limited the ability of the preoperative PSA to predict tumor recurrence following surgery.

Multivariate analysis demonstrated a statistically significant inverse relationship between p27 expression and the risk of PSA recurrence ($p = 0.0184$). More strikingly and usefully, low p27 expression was able to separate a group of cases at high risk to recur despite otherwise favorable pathological features. Among patients with pathological T2a-T3b tumors, those with tumors expressing low levels of p27 had a significantly higher chance of cancer relapse during a 5-year period ($p = 0.0081$) than those with high levels of p27 expression. These results are comparable to those recently reported for breast and colorectal cancers. In colorectal cancer, in particular, it was found that p27 expression significantly improved the prediction of recurrence among patients with stage II disease, a group in many ways analogous to the group with T2-T3b prostate cancer.[9] In addition, given that the mean followup of this study population is only 36 months, it is certainly possible that the correlation between p27 and biochemical relapse will become even stronger with longer followup.

In a recent editorial about p27 Steeg and Abrams argued that novel biological markers needed to pass 3 hurdles before entering clinical use: 1) a new marker must provide information independent of conventional pathological markers, 2) this marker should provide information that can alter treatment decisions and 3) studies with a new marker should be reproducible.[15] As a novel marker for prostate cancer, p27 appears able to meet the first 2 criteria. The level of p27 expression provides independent information about prognosis among patients treated with radical prostatectomy and, in particular, is the only predictor of disease recurrence

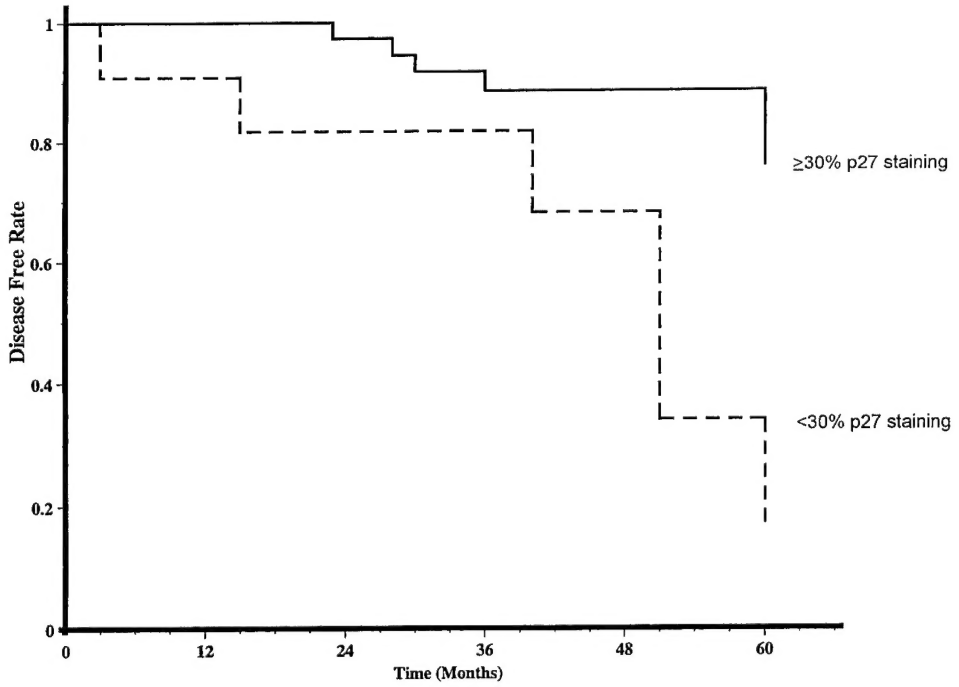

FIG. 2. Overall disease specific survival in patients with pathologically staged T2a-c/T3a-b tumors. Kaplan-Meier method was used to estimate survival function and plot data for all patients whose status at followup was known ($p = 0.0081$, risk ratio 4.99).

among patients with T2-T3b cancers in our study. Identification of cases likely to fail surgical monotherapy has the potential to alter treatment decisions by selecting those that may benefit from adjuvant systemic therapy, although the benefit of adjuvant therapy in prostate cancer has not been established. Clearly, additional studies replicating these results will be necessary to establish a role for p27 in the clinic, which has already been done for breast cancer.[16] p27 also needs to be assessed as a preoperative marker by prospectively analyzing prostate biopsies before prostatectomy.

From a biological standpoint, these data suggest that p27 may have an important role in either the initiation or progression of prostate cancer. The expression of p27 in normal prostate by secretory cells, which are terminally differentiated, and not basal cells, which are actively dividing, suggests that p27 may have an important role in the regulation of normal prostatic growth. Whether p27 functions in prostate cancer as a cell cycle inhibitor or whether it has alternative functions, such as a regulator of cell adhesion, remains to be defined. Regardless, restoration of normal p27 gene expression by interfering with posttranslational p27 degradation may represent an attractive approach for prostate cancer therapy in the future.

CONCLUSIONS

Absent or decreased p27 protein expression appears to be an adverse prognostic factor in patients with clinically localized prostate cancer treated with radical prostatectomy. The presence or relative absence of p27 protein expression was able to discriminate between patients at high and low risk of recurrence, particularly among those with pathological T2a-c/T3a-b tumors. In so doing p27 has the potential to select patients who may benefit from adjuvant systemic therapy. Furthermore, since p27 appears to have a role in normal prostate cell cycle regulation, restoration of normal p27 protein expression may be a potential route by which prostate cancer may be manipulated therapeutically.

REFERENCES

1. Koff, A., Cross, F., Fisher, A., Schumacher, J., Leguellec, K., Philippe, M. and Roberts, J. M.: Human cyclin E, a new cyclin that interacts with two members of the CDC2 gene family. Cell, **66:** 1217, 1991.
2. Dulic, V., Lees, E. and Reed, S. I.: Association of human cyclin E with a periodic G1-S phase protein kinase. Science, **257:** 1958, 1992.
3. Polyak, K., Kato, J. Y., Solomon, M. J., Sherr, C. J., Massague, J., Roberts, J. M. and Koff, A.: p27Kip1, a cyclin-Cdk inhibitor, links transforming growth factor-β and contact inhibition to cell cycle arrest. Gene Dev., **8:** 9, 1994.
4. Ferrando, A. A., Balbin, M., Pendas, A. M., Vizoso, F., Velasco, G. and Lopez-Otin, C. F.: Mutational analysis of the human-cyclin dependent kinase inhibitor p27Kip1 in primary breast carcinomas. Hum. Genet., **97:** 91, 1996.
5. Coats, S., Flanagan, W. M., Nourse, J. and Roberts, J. M.: Requirement of p27Kip1 for restriction point control of the fibroblast cell cycle. Science, **272:** 877, 1996.
6. St Croix, B., Florenes, V. A., Rak, J. W., Flanagan, M., Bhattacharya, N., Slingerland, J. M. and Kerbel, R. S.: Impact of the cyclin-dependent kinase inhibitor p27Kip1 on resistance of tumor cells to anticancer agents. Nat. Med., **2:** 1204, 1996.
7. Catzavelos, C., Bhattacharya, N., Ung, Y. C., Wilson, J. A., Roncari, L., Sandhu, C., Shaw, P., Yeger, H., Morava-Protzner, I., Kapusta, L., Franssen, E., Pritchard, K. I. and Slingerland, J. M.: Decreased levels of the cell-cycle inhibitor p27Kip1 protein: prognostic implications in primary breast cancer. Nat. Med., **3:** 227, 1997.
8. Porter, P. L., Malone, K. E., Heagerty, P. J., Alexander, G. M., Gatti, L. A., Firpo, E. J., Daling, J. R. and Roberts, J. M.: Expression of cell-cycle regulators p27Kip1 and cyclin E, alone and in combination, correlates with survival in young breast cancer patients. Nat. Med., **3:** 222, 1997.
9. Loda, M., Cukor, B., Tam, S. W., Lavin, P., Fiorentino, M., Draetta, G. F., Jessup, J. M. and Pagano, M.: Increased proteasome-dependent degradation of the cyclin-dependent kinase inhibitor p27 in aggressive colorectal carcinomas. Nat. Med., **3:** 231, 1997.
10. Mori, M., Mimori, K., Shiraishi, T., Tanaka, S., Ueo, H., Sugimachi, K. and Akiyoshi, T.: p27 expression and gastric carcinoma. Nat. Med., **3:** 593, 1997.
11. Epstein, J. I., Carmichael, M. and Walsh, P. C.: Adenocarcinoma of the prostate invading the seminal vesicle: definition and relation of tumor volume, grade and margins of resection to prognosis. J. Urol., **149:** 1040, 1993.
12. Catalona, W. J. and Smith, D. S.: 5-year tumor recurrence rates after anatomical radical retropubic prostatectomy for prostate cancer. J. Urol., **152:** 1837, 1994.
13. Kupelian, P. A., Katcher, J., Levin, H. S. and Klein, E. A.: Stage T1–2 Prostate Cancer: a multivariate analysis of factors affecting biochemical and clinical failures after radical prostatectomy. Int. J. Rad. Oncol., Biol. Phys., **37:** 1043, 1997.
14. Lerner, S. E., Blute, M. L. and Zincke, H.: Risk factors for progression in patients with prostate cancer treated with radical prostatectomy. Sem. Urol. Oncol., **14:** 12, 1996.
15. Steeg, P. S. and Abrams, J. S.: Cancer prognostics: past, present and p27. Nat. Med., **3:** 152, 1997.
16. Tan, P., Cady, B., Wanner, M., Worland, P., Cukor, B., Magi-Galluzzi, C., Lairn, P., Draetta, G., Pagano, M. and Loda, M.: The cell cycle inhibitor p27 is an independent prognostic marker in small (T1a,b) invasive breast carcinomas. Cancer Res., **57:** 1259, 1997.

545 DOWN-REGULATION OF P27 IN ADENOCARCINOMA OF PROSTATE AFTER ANDROGEN ABLATION

Y.C. Cai, M. McMenamin, C. Magi-Galluzzi, E. Macri, R. Montironi, M. Loda
Departments of Pathology, Brigham and Women's Hospital, and Adult Oncology, Dana Farber Cancer Institute, Harvard Medical School, Boston, MA, Ospedale Civile di Belluno, and University of Ancona, Italy

Background: p27 is a negative regulator of the cell cycle. Low expression has been associated with poor prognosis in patients with organ-confined adenocarcinoma of prostate. Low p27 expression in patients treated with total androgen ablation (TAA) was found to be a powerful predictor of poor outcome in a limited database. In addition, castration is known to down-regulate p27 in rat prostates.

Design: Routinely processed tissue sections of either transurethral resections or radical prostatectomies of 156 patients with prostatic adenocarcinoma, including 88 untreated and 68 treated with TAA for a minimum of 3 months, were immunohistochemically stained with anti-p27 antibody. Tumors with ≥50% cells with strong nuclear p27 staining were regarded as positive.

Results: p27 expression decreased in patients previously treated with TAA, compared to untreated tumors.

	Untreated (n=88)	Treated (n=68)	
p27 + (≥50%)	44 (50%)	23 (34%)	p= 0.043 (Chi-Square)

Conclusions: p27 is down-regulated in residual prostatic adenocarcinoma after 3 months of TAA. TAA may select for p27 negative tumor cells.

546 PROGNOSTIC SIGNIFICANCE OF GLEASON SCORE 3+4 VERSUS GLEASON SCORE 4+3 TUMOR AT RADICAL PROSTATECTOMY.

TY Chan, AL Partin, PC Walsh, JI Epstein. The Johns Hopkins Hospital, Baltimore, MD.

Background: The clinical significance of Gleason scores 3+4 vs. 4+3 tumor at radical prostatectomy (RRP) has not been well defined. **Design:** Of 2390 men who underwent RRP, 570 had Gleason score 7 tumors with no lymph node metastases, seminal vesicle invasion or tertiary Gleason pattern 5. Cases were evaluated for biochemical recurrence (PSA progression) and distant metastases. **Results:** 80% of patients had Gleason score 3+4, while 20% had Gleason score 4+3. The rates of established extraprostatic extension at RRP for Gleason scores 3+4 and 4+3 tumors were 35% and 53%, respectively (P=0.008). With a mean follow-up of 4.6 years for men without progression, Gleason score 4+3 tumors had an increased risk of progression independent of stage and margin status (P<0.001). The 5 year actuarial risks of progression were 15% and 40% for Gleason scores 3+4 and 4+3 tumors, respectively. Mean time to progression was 4.4 years for Gleason score 3+4 tumors and 3.2 years for Gleason score 4+3 tumors. We stratified cases into 4 prognostic groups based on organ-confined status, margin status, and Gleason score 3+4 vs. 4+3. Their 5 year actuarial risks of progression were 10%, 35%, 45%, and 61% with 10 year progression rates of 29%, 42%, 69%, and 84%. 18 patients with Gleason score 3+4 and 12 with Gleason score 4+3 tumors developed metastatic disease at a mean of 5.7 and 5.6 years, respectively. Gleason score 3+4 vs. 4+3 was predictive of metastatic disease (P=0.002), but not local recurrence. **Conclusion**: Gleason score 7 tumors are heterogeneous in their biologic behavior. There are significant differences in prognosis in tumors with Gleason scores 3+4and 4+3 at RRP. Whereas the assessment of percent pattern 4 at RRP is not likely to be reproducible, the distinction of Gleason score 3+4 vs. 4+3 should be easier for pathologists to perform.

547 Biopsy Results and Percent Free PSA Levels in Patients with Elevated Total PSA Levels between 4.0 and 10.0 ng/ml

Chand EM, Stewart CT, Lee JR. Medical College of Georgia & VAMC, Augusta, GA

Background: Prostatic specific antigen (PSA) is considered to be the most useful parameter in the detection of prostate cancer. Elevated PSA levels greater than 10 ng/ml are seen in prostatic adenocarcinoma. PSA levels less than 4 ng/ml have been reported with benign pathology. Therefore, a gray zone exists between 4 and 10 ng/ml, which causes the clinician to question the need for a biopsy. The evaluation of the percent free PSA is reported to improve the sensitivity of the PSA within this gray zone.

Design: A retrospective study was performed looking at patients with free and total serum PSA levels, particularly in the subset with a total PSA levels between 4.0 and 10.0 ng/ml. The biopsy result, free PSA, and percent free PSA in these patients were reviewed, along with the digital rectal exam, prostate volume, and PSA density.

Results: Between June 1998 and July 1999, 200 patients had a total and free PSA level performed. Of these, 54 patients had biopsies evaluated. The target subset of total PSA levels between 4.0 and 10.0 ng/ml included 42 patients. The biopsy results revealed chronic inflammation in 30 of the 42 patients (71%), with the mean % free PSA 17.7, Std Dev =5.21, and a range of 5 to 30. Prostatic adenocarcinoma was seen in 11 biopsies (26%) with the mean of the % free PSA 13.64, Std Dev =4.78, with a range of 8 to 23. The differences between the means of the % free PSA in the patients with chronic inflammation and prostatic adenocarcinoma were statistically significant (T test =0.028). The lone biopsy with no pathology had a PSA level of 7.3 with a % free PSA level of 10.

Conclusions: Within the gray zone, a high (>25) % free PSA level implies a low risk of cancer. Our study shows that the mechanism that binds the PSA with adenocarcinoma also binds the PSA with chronic inflammation to a slightly higher level. The threshold for % free PSA should possibly be lowered from 25 to 20, decreasing the number of biopsies in benign conditions. In our study, 10 of the 30 (33%) patients with inflammation had % free PSA levels greater than 20. Only 1 carcinoma patient had a level greater than 20.

548 CORRELATION BETWEEN BIOPSY AND RADICAL CYSTECTOMY IN GRADING AND INVASION ACCESSMENT OF BLADDER UROTHELIAL CARCINOMA.

B.S.Chang, X.J.Yang. The University of Chicago, Chicago, IL.

Background: Muscular propria (MP) invasion by bladder urothelial carcinoma (UC) on biopsy has traditionally been the indicator for radical cystectomy (RC). The purpose of this study was to evaluate the effectiveness of this indicator.

Design: Ninety-three RCs with corresponding biopsies (Bx) including transurethral resections were selected from 118 RCs performed between 1992 and 1999. Histologic grades and invasiveness of UC from Bx and RC were compared.

Results: For histologic grading, there was a complete agreement between Bx and RC in 53 of 79 cases (67%); down-grading in 13% cases; up-grading in 15% case from biopsy, or not available in 5%. All variations are within one grade. Invasion was categorized by assessment of deepest degree of penetration, either as not specified (NS) or no evidence of tumor (NET), carcinoma in situ (CIS), lamina propria (LP), muscular propria (MP), or extravesicular fat (EV). Metastasis (MT) was defined as tumor involvement of pelvic lymph nodes.

Bx \ RC	NS	NET	CIS	LP	MP	EV	MT	Total
NS	1	2	1	0	0	1	0	5
CIS	0	1	4	1	0	0	1	7
LP	0	3	5	5	1	1	7	22
MP	1	7	1	2	13	11	24	59
Total	2	13	11	8	14	13	32	93

Conclusion: There is a good correlation between biopsy and RC in histologic grades. The presence of MP invasion on bladder biopsy failed to demonstrate tumor invasion beyond MP in 59% of cases including metastases. The presence of LP invasion on biopsy failed to reveal invasion beyond LP in 41% of cases. A better indicator for RC should be investigated. Earlier treatment of high grade invasive UC of the bladder may be appropriate.

549 BILATERAL TESTICULAR GERM CELL TUMORS (GCT): 20-YEAR EXPERIENCE AT A CANCER CENTER.

M Che, P Tamboli, RJ Amato, JY Ro, AG Ayala. The University of Texas MD Anderson Cancer Center, Houston TX.

Background: Bilateral primary testicular GCT (BTGCT) are uncommon. Incidence of 2 to 5% is reported in the literature, with seminoma being the most common synchronous and metachronous GCT in both testes.

Design: This is a clinico-pathologic study of 23 patients (pts) with BTGCT. These represent 1% of 2256 pts treated at our institution from 1978 to 1999.

Results: Pts' mean age: 28 years (range: 17 to 46). 3/23 (13%) pts had synchronous tumors, while 20/23 (87%) had metachronous tumors. Of 3 pts with synchronous tumors, 2 had seminoma on both sides, and 1 had seminoma on one side and nonseminomatous GCT (NSGCT) on the other side. In the metachronous group (20 pts), the first tumor was a seminoma in 9 and NSGCT in 11. The second tumors were 10 seminomas and 10 NSGCT, which developed after a median interval of 42 months (range: 14 to 180). Of the 9 pts with seminoma as the first tumor, 7 developed seminoma in the opposite testis and 2 developed NSGCT. Of the 11 pts with NSGCT, 8 developed NSGCT in the opposite testis and 3 developed seminoma. Median follow-up after the second tumor was 34 months (range: 2 to 245). All pts were alive without evidence of disease following the second GCT.

Conclusion: Our incidence of BTGCT, diagnosed over the past 20 years, is 1% of all testicular GCT; this is less than 2 to 5% reported in the literature. Furthermore, in contrast to the literature, only 50% of our patients developed seminoma on the contralateral side (up to 75% in the literature). These findings may have potentially important implications for patient management.

550 Risk of Prostate Cancer Death in Patients with Lymph Node Metastasis

L Cheng[1,2], H Zincke[3], ML Blute[3], EJ Bergstralh[4], DG Bostwick[6]. Depts. of Pathology[1] and Urology[2]. IU School of Medicine, Indianapolis, IN; Dept. of Urology[3], Biostatistics[4], and the Department of Pathology[5], Mayo Clinic, Rochester, MN; Bostwick Laboratories[6], Richmond, VA.

Background: The presence of lymph node metastasis is a poor prognostic sign for prostate cancer patients. **Design:** We analyzed 3463 consecutive Mayo Clinic patients who were treated by radical prostatectomy and bilateral pelvic lymphadenectomy for prostate cancer between 1987-1993. Of these patients, 322 had lymph node metastasis at the time of surgery, and 297 node-positive patients also received adjuvant hormonal therapy within 90 days of surgery. Mean follow-up was 6.3 years. Progression was defined by elevation of serum prostate-specific antigen (PSA) after surgery, development of local recurrence or distant metastasis. **Results:** Five-year and 10-year cancer-specific survival for patients with lymph node metastatsis were 94% and 83%, respectively. Among patients with single lymph node metastasis, 5-year and 10-year cancer specific-survival was 99% and 94%, respectively. After adjustment for extraprostatic extension, seminal vesicle invasion, Gleason grade, surgical margins, DNA ploidy, preoperative PSA concentration, and adjuvant therapy, hazard ratio for prostate cancer death among patients with single lymph node metastasis, in comparison to those without lymph node metastasis, was 1.5 (95% confidence interval, 0.5-5.0; p=0.478). There was no significant difference in progression-free survival among patients with or without lymph node metastasis in multivariate analysis after controlling for all relevant variables including treatments (hazard ratio,1.0; 95% CI, 0.7-1.3; p=0.90). **Conclusions:** Prostate carcinoma patients with regional lymph node metastasis had increased risk of cancer death, whereas patients with single lymph node involvement appear to have a favorable prognosis after radical prostatectomy and immediate adjuvant hormonal therapy. Excellent local cancer control was achieved by combined surgery and adjuvant hormonal therapy in lymph node-positive patients.